Technical Report WF/89/14

MRP Report 102

Geophysical and geochemical investigations of the manganese deposits of Rhiw, western Llŷn, North Wales

M J Brown and A D Evans

BRITISH GEOLOGICAL SURVEY

Technical Report WF/89/14

Mineral Resources Series

Geophysical and geochemical investigations of the manganese deposits of Rhiw, western Llŷn, North Wales

Geochemistry

M J Brown, BSc

Geophysics

A D Evans, BSc

Cover illustration

A banded carbonate/sphalerite/marcasite/galena vein from the Gwynfynydd Gold Mine, near Dolgellau in North Wales

This report was prepared for the Department of Trade and Industry

Bibliographical reference

Brown, M J, and Evans, A D. 1989. Geophysical and geochemical investigations of the manganese deposits of Rhiw, western Llŷn, North Wales. *British Geological Survey Technical Report* WF/89/14 (*BGS Mineral Reconnaissance Programme Report* 102).

Mineral Reconnaissance Programme Report 102

Keyworth, Nottingham 1989

BRITISH GEOLOGICAL SURVEY

The full range of Survey publications is available through the Sales Desks at Keyworth and Murchison House, Edinburgh. Selected items can be bought at the BGS London Information Office, and orders are accepted here for all publications. The adjacent Geological Museum bookshop stocks the more popular books for sale over the counter. Most BGS books and reports are listed in HMSO's Sectional List 45, and can be bought from HMSO and through HMSO agents and retailers. Maps are listed in the BGS Map Catalogue and the Ordnance Survey's Trade Catalogue, and can be bought from Ordnance Survey agents as well as from BGS.

The British Geological Survey carries out the geological survey of Great Britain and Northern Ireland (the latter as an agency service for the government of Northern Ireland), and of the surrounding continental shelf, as well as its basic research projects. It also undertakes programmes of British technical aid in geology in developing countries as arranged by the Overseas Development Administration.

The British Geological Survey is a component body of the Natural Environment Research Council.

Keyworth, Nottingham NG12 5GG
☎ Plumtree (060 77) 6111 Telex 378173 BGSKEY G
Fax ☎ 060 77–6602

Murchison House, West Mains Road, Edinburgh EH9 3LA
☎ 031–667 1000 Telex 727343 SEISED G
Fax ☎ 031–668 2683

London Information Office at the Geological Museum, Exhibition Road, South Kensington, London SW7 2DE
☎ 01–589 4090 Fax ☎ 01–584 8270
☎ 01–938 9056/57

64 Gray's Inn Road, London WC1X 8NG
☎ 01–242 4531 Telex 262199 BGSCLR G
Fax ☎ 01-242 0835

19 Grange Terrace, Edinburgh EH9 2LF
☎ 031–667 1000 Telex 727343 SEISED G

St Just, 30 Pennsylvania Road, Exeter EX4 6BX
☎ Exeter (0392) 78312

Bryn Eithyn Hall, Llanfarian, Aberystwyth, Dyfed SY23 4BY
☎ Aberystwyth (0970) 611038

Windsor Court, Windsor Terrace, Newcastle upon Tyne NE2 4HB
☎ 091-281 7078 Fax ☎ 091-281 9016

Geological Survey of Northern Ireland, 20 College Gardens, Belfast BT9 6BS
☎ Belfast (0232) 666595

Maclean Building, Crowmarsh Gifford, Wallingford, Oxfordshire OX10 8BB
☎ Wallingford (0491) 38800 Telex 849365 HYDROL G
Fax ☎ 0491-25338

Parent Body

Natural Environment Research Council

Polaris House, North Star Avenue, Swindon, Wiltshire SN2 1EU
☎ Swindon (0793) 411500 Telex 444293 ENVRE G
Fax ☎ 0793-411501

This report relates to work carried out by the British Geological Survey on behalf of the Department of Trade and Industry. The information contained herein must not be published without reference to the Director, British Geological Survey.

Dr D J Fettes
Programme Manager
British Geological Survey
Murchison House
West Mains Road
Edinburgh EH9 3LA

CONTENTS

APPENDICES

ILLUSTRATIONS

TABLES

SUMMARY

Detailed magnetic surveys have been carried out near Rhiw, in western Llŷn, North Wales. These surveys covered ground south-west from the old Benallt manganese mine as far as the old Nant mine, and northwards from Benallt towards Sarn. Rocks within the area are of Arenig and Llanvirn age (Lower Ordovician) and consist of mudstones, siltstones and sandstones with interbedded basic lavas and sills. The manganese deposits occur in a structurally complex setting within sediments of Arenig age. These sediments are confined between a basic sill and a dolerite or basalt lava. That part of the manganese mineralisation which is of ore grade is unique within the British Isles because of its strong magnetisation, caused by the presence of the mineral jacobsite, an iron-manganese oxide analogous to magnetite.

The geophysical survey was supported by the collection of soil samples from across-strike traverses. The soils, which were analysed for a wide range of elements, proved of limited use for exploration purposes, mainly due to the variable depth of drift cover. Both Ti and V proved useful in areas of limited drift cover as an aid to mapping the sub-crop of the basic igneous rocks.

Several very localised magnetic anomalies were identified, and three of these were investigated by drilling. These anomalies were thought likely to be due to discrete bodies of manganese ore. Other more extensive anomalies mark the sub-crop of a basic sill (the Footwall Sill) which occurs below the sediments which host the manganese mineralisation. Two of the anomalies drilled were found to be due to stratabound ironstones of very limited lateral extent, and of particularly high magnetic susceptibility. These ironstones contain up to ~70% Fe_2O_3 and show a marked depletion in manganese when compared to the enclosing sediments and basic igneous rocks.

INTRODUCTION

The mines of Benallt and Nant, near Rhiw (Figure 1), were the single most important souce of manganese ore in the British Isles during their short working life in the first half of this century. Total production amounted to some 150 000 tons. The Nant mine provided about a third of this total, from a single orebody. At Benallt, which Groves (1952, p.303) considered to be 'geologically one of the most complicated of the British metalliferous mines', the orebodies ranged in size from a few tens of tons to 30 000 tons.

Manganese ore was worked from the Nant mine between approximately 1902 and 1925, and from various underground and opencast workings at Benallt* sporadically between 1886 and 1928 (Down, 1980). Detailed descriptions, plans and sections for these old workings are available (Groves, 1952, Figures 38, 39, 41). Both mines were re-examined during the Second World War, as possibly able to meet the need for a domestic source of manganese. The Nant orebody was found, after de-watering the mine, to be largely worked out. But at Benallt, the Ministry of Supply re-opened one of the numerous old shafts, and carried out extensive underground diamond drilling and development. During this wartime phase of activity at Benallt, some 60 000 tons of ore were produced.

Previous Exploration

The magnetic nature of the Benallt ore was first noted by Groves (1947) by its effect on a compass needle, and he also recognised a relationship between the strength of magnetisation and the ore grade. This occurrence of a manganese ore which is strongly magnetic is unique in the British Isles. Occurrences elsewhere are also rare, though Bhimasankaram and Rao (1958) have described an example from southern India. The possibility of thus being able to identify ore reserves ahead of the re-opened mine workings at Benallt led to the first magnetic survey in the area (Groves, 1947).

This magnetic survey covered a 300m strike length of prospective ground immediately west of the village of Rhiw, and south of Benallt. Three orebodies indicated by the magnetic data were subsequently proved by southward extension of the Benallt workings. The equipment employed for the survey was a Watts Vertical Force Variometer, this instrument being quite adequate to resolve the anomalies of a few hundred nanoTesla amplitude which outlined the orebodies. The instrument is briefly described and illustrated by Shaw (1936).

Two years prior to the magnetic survey, drilling had been carried out between the Nant and Benallt mines (Groves, 1952, pp.315-318), and the results provided strong evidence for the persistence south-westwards from Benallt of the manganese-rich sediments, and for the persistence of the confining igneous rocks (a dolerite sill beneath the sediments and a lava flow above). However, the concentrations of manganese ore which were located were of too low a grade to justify more intensive exploration. Cattermole and Romano (1981) note a report of 'a recent borehole' at Ty'n Rhedyn (near the Nant mine), which proved 'large quantities of high grade ore'. However, Cattermole (written communication, May 1984) advises that this information is based on a verbal account, and so cannot be substantiated. With no other evidence of exploration since 1945, it seems most likely that this is in fact a reference to the drilling noted above; one of the boreholes drilled at that time was located within 100m of Ty'n Rhedyn.

---

*In this report, the name Benallt will be used to refer to the group of workings which operated under the individual names of Rhiw, Benallt, Tyddyn Meirion and Ty Canol.

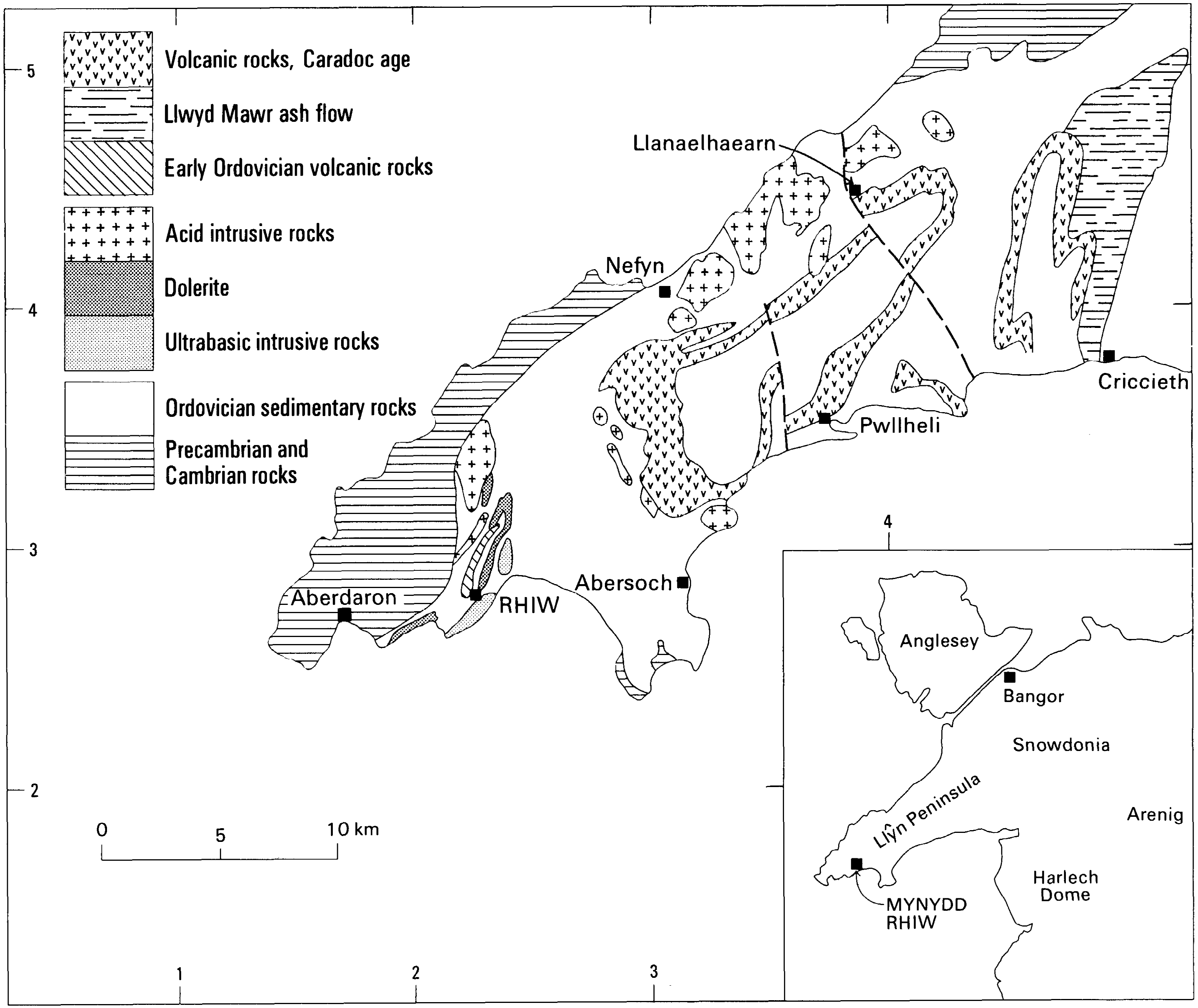

Figure 1 Llŷn: general geology

In 1971, a reconnaissance magnetic survey was carried out over the area between Mynydd Rhiw and the Nant mine, reported by Cornwell (1979). Observations were made along eight traverses, spaced 1000 feet apart. The results indicated that the intrusion underlying the ore-bearing rocks (the Footwall Sill) persists across the area, and that its position differs from that suggested by the mapping of Matley (1932). No evidence of new manganese orebodies was recorded, but this was not unexpected because of the widely spaced traverse lines.

Unrelated to the manganese deposits, but of interest because of its proximity, is the exploration carried out in the early 1970's by Noranda-Kerr Ltd., over the area immediately to the east of the 'manganese belt'. Detailed soil sampling was carried out to investigate the potential of the Mynydd y Graig and Mynydd Rhiw layered intrusives for copper and nickel mineralisation. On Mynydd Rhiw, part of the area sampled falls within the area of the present survey. The results were not sufficiently encouraging to justify more detailed work, or drilling. The data are available for inspection at the British Geological Survey office (National Geosciences Data Centre) at Keyworth, Nottingham.

Present investigations

As part of the Mineral Reconnaissance Key Metals Programme it was decided in 1984 to extend the earlier exploration. This required covering thoroughly the prospective ground between the Benallt and Nant mines (a strike length of some 1.4km) and also examining the ground to the north of Benallt, historically regarded as barren.

This survey, reported here, again made use of the magnetic method, as it was thought unlikely that ore could readily be detected by any other geophysical means; the magnetic method offered the advantages of being able to locate ore, and to map the sub-crop of the Footwall Sill, with detailed coverage of the area being achievable quickly.

The magnetic observations were made along closely spaced traverse lines between the Nant mine and the most southerly of the Benallt workings at Tyddyn Meirion. Additional traverses covered the western and northern flanks of Mynydd Rhiw, from the northern limit of the Benallt workings as far as Coch-y-Moel (Figure 2) some 2.7km to the north. Separate detailed sets of traverses, to investigate strong local anomalies, were measured near the Nant mine; at Tyddyn Meirion; and on Mynydd Rhiw. The magnetic susceptibilities of various exposed rocks were measured at localities from Gallt y Mor in the south-west, to quarry exposures near Ty Engan in the north (Figure 2).

Soil sampling was undertaken in support of the magnetic survey, with samples collected from twelve across-strike traverses (Figure 14). Rock samples were collected from available exposures and analysed for a wide range of elements. Following interpretation of the magnetic and geochemical data, five boreholes were drilled to investigate the cause of some significant magnetic anomalies.

Location

The area covered by the present survey lies within the Ordnance Survey 1:50 000 Sheet 123 (Lleyn Peninsula) and within 1:10 000 sheets SH22NW and SH23SW. The village of Rhiw, 16km south-south-west of Pwllheli (Figure 1), lies approximately at the centre of the area surveyed. The area is dominated by the mountain of Mynydd Rhiw (OD 304m) to the north of the village; farmland for sheep and dairy grazing lies to the south. Minor roads, and tracks on Mynydd Rhiw, provide good vehicle access throughout the area.

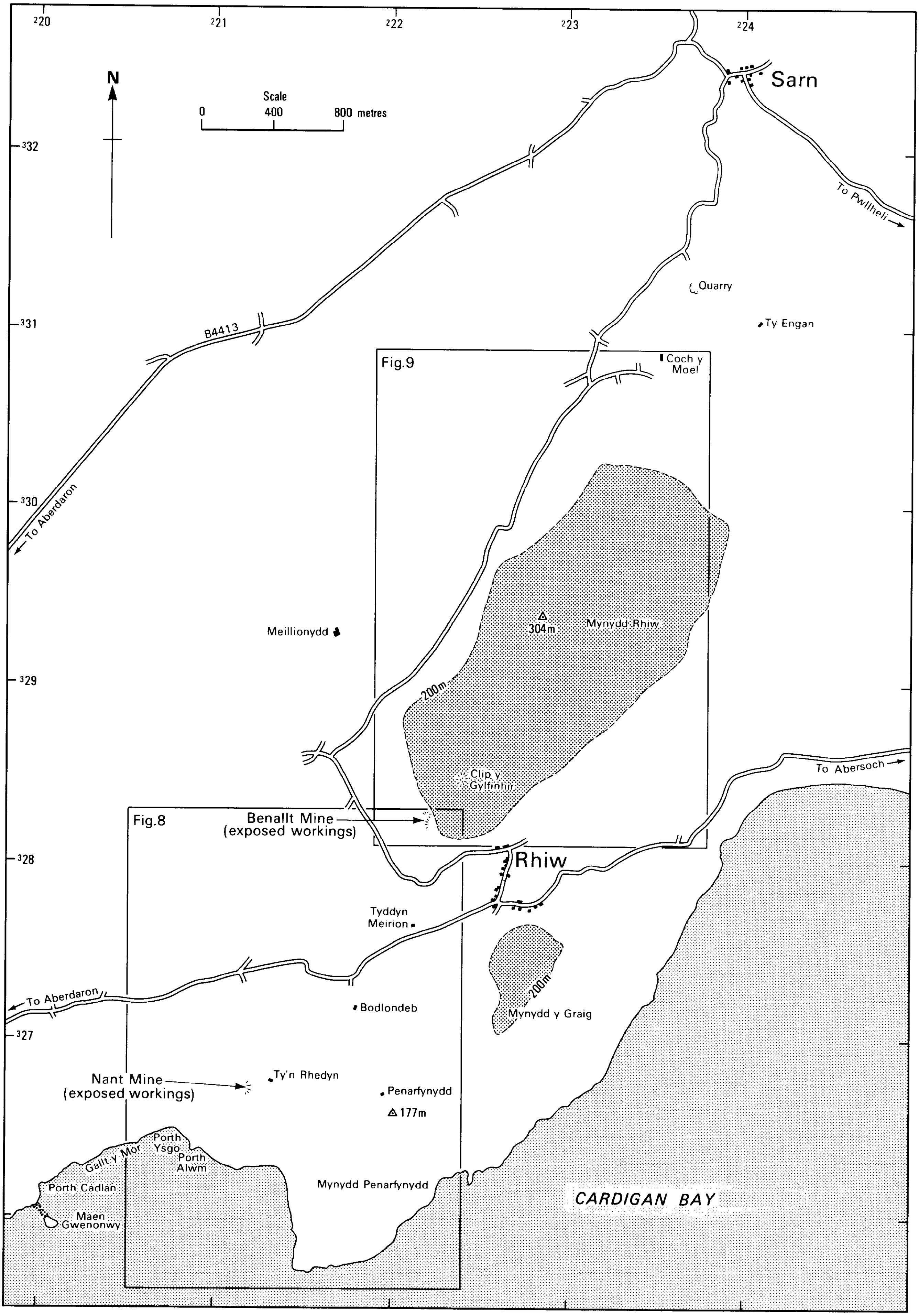

Figure 2 Rhiw/Sarn area—Location map

Data availability

All of the geochemical data (analyses for soil, rock, and drill-core samples) are presented in the Appendices to the present report. The geophysical data are available for inspection by arrangement with the Head, Regional Geophysics Research Group, British Geological Survey, Keyworth, Nottingham, NG12 5GG. The magnetic profile data are also available in digital format. An example of the type of data presentation possible by using digital data (in conjunction with the Regional Geophysics in-house graphics software) is presented as Appendix 10. This is a copy of a coloured relief presentation of the raw field data for the Penarfynydd area, viewed from the east.

GEOLOGY AND MINERALISATION

Previous work

The earliest work undertaken within the area was by Sedgwick (1843, 1852) and the first field map was by Sharpe (1846). The first Geological Survey map and Memoir for the area were produced by Ramsay (1866, 1881) and further re-mapping was undertaken by Harker (1888). Matley (1932) carried out detailed mapping (1:10 560 scale) over Mynydd Rhiw and around Sarn, which formed the basis for the more recent studies of the area. The structure was discussed by Matley (1932) and the interpretation of the structure subsequently revised by Shackleton (1956) and Hawkins (1983).

The Arenig rocks of western Llŷn have been described by Crimes (1970) in terms of sedimentary facies, with particular reference to lithology and biogenic and inorganic sedimentary structures. The Arenig succession has been recently revised by Beckly (1985, 1987) who has also presented a new interpretation based on biostratigraphical correlation (Beckly, 1988) using the three stages defined for the Arenig of South Wales (Fortey and Owens, 1978, 1987). The age and deposition of Ordovician ironstones in North Wales, including those of the Rhiw area, have been discussed by Trythall and others (1987).

The volcanic rocks have been described by Allen (1982) and the intrusive rocks by Le Bas (1982). Geochemical studies of the layered igneous complex to the south-east of the present survey area have been reported by Cattermole (1969, 1976).

Stratigraphy

The geological map of the area presented here (Figure 3) is based on recent work undertaken as part of the revision of the British Geological Survey 1:50 000 map (Bardsey Island, Sheet 133). Ordovician rocks within the area overlie rocks of the Sarn Complex to the west (Figure 3), which consist mainly of granitic to dioritic igneous rocks and granitic gneisses (Gibbons, 1980, 1983). Rb-Sr radiometric dating for the Sarn Complex suggests an age of 540-550Ma (Beckinsale and others, 1984). The boundary between the Ordovician succession and the Sarn Complex was originally considered to be tectonic and was referred to as the 'Boundary Thrust' by Matley (1932). Later Shackleton (1956) described exposures which indicated that the boundary was an unconformity, a view accepted by Crimes (1970) and Hawkins (1983).

Within the area of the present survey, sedimentary and volcanic rocks of Lower Ordovician age (Arenig/Llanvirn) are exposed. The sedimentary rocks consist mainly of dark grey mudstones, laminated siltstones and bioturbated sandstones; ironstone bands provide good marker horizons within the succession (T. Young, personal communication, 1988). Rocks of volcanic origin interbedded with the sedimentary rocks include spilitic and andesitic pillow lavas, chert and crystal tuff. The succession is intruded by sills of albite-augite-dolerite which are associated with the volcanism. The wartime mining operations showed the presence of a basic dyke, named the Ty Canol Dyke (Groves, 1952, p.304) trending WNW-ESE across the strike of the Arenig succession south of Mynydd Rhiw over a distance of at least 150m. This dyke cuts rocks both above and below the manganiferous horizon and is most likely one of the suite of Tertiary dykes, generally NW-SE trending, of Anglesey and Llŷn.

Some of the best exposure is seen on Mynydd Rhiw, where lavas and dolerite sills, interbedded with sediments, trend north to NNE (Figure 3) and generally dip and young to the south-east. Petrographic examination of the lavas from outcrop and drill-core indicates that they were probably not extruded, but intruded into wet sediments below the sea floor (A.J. Reedman, personal communication, 1988). South of Benallt exposure

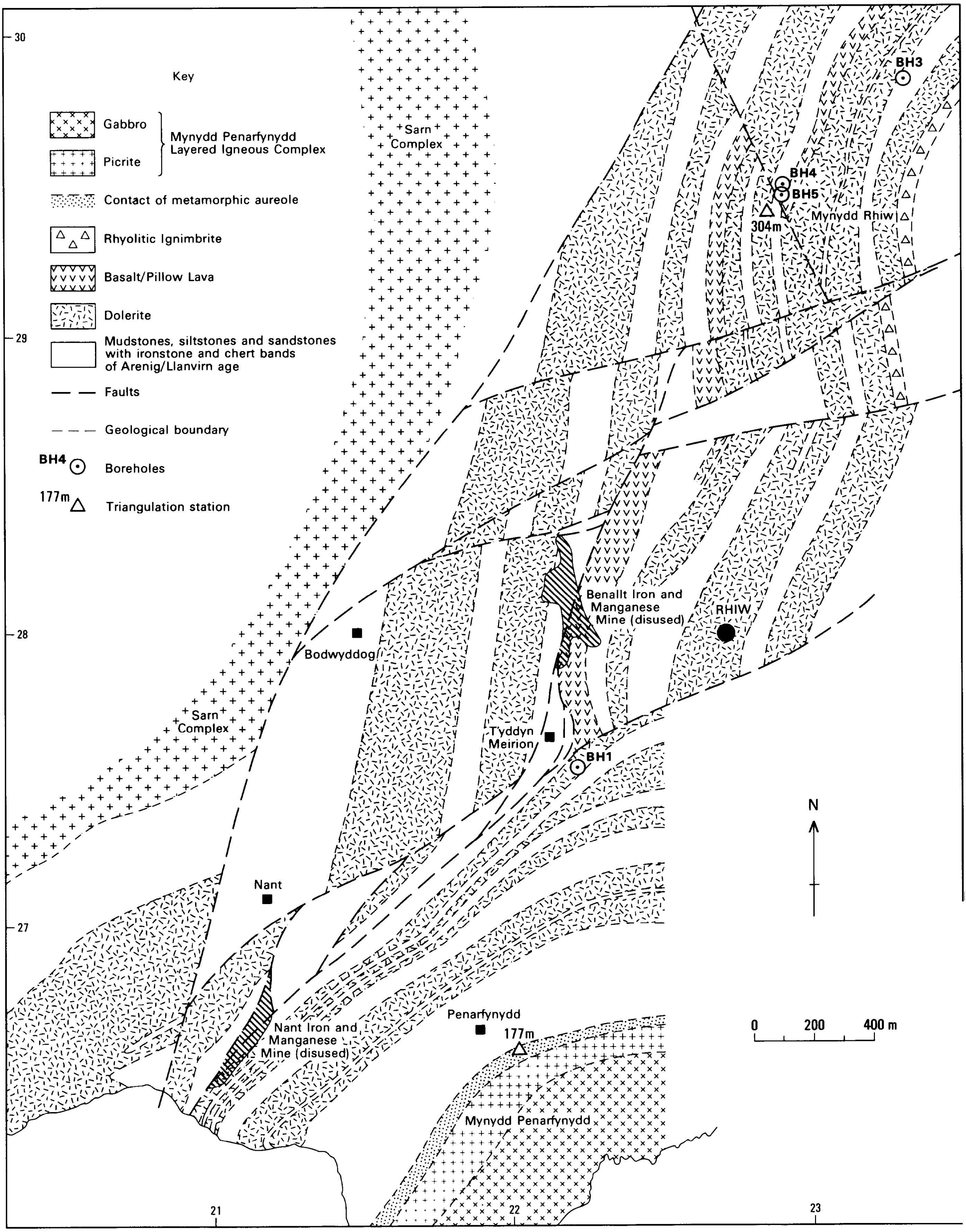

Figure 3 Geology of the Rhiw area, after Gibbons & McCarroll

is poor, with the exception of the mined area of Nant y Gadwen, where the structure and palaeontology are seen to be complex (Beckly, 1988; Gibbons and McCarroll, in preparation).

From recent biostratigraphical studies of the Arenig succession (Beckly, 1988) the area is thought to be unique in North Wales, being the only locality where all three Arenig stages are present. The approximate boundary between the Arenig and Llanvirn is well marked by tuffaceous beds, locally interbedded with sediments, known as the Carw Formation. The revised stratigraphy for the Rhiw area given by Beckly (1988) is shown in Table 1 below.

Llanvirn		
Arenig		Carw Fm.
	Fennian	Aberdaron Fm.
	Whitlandian	
	Moridunian	Wîg Member
		Sarn Fm.

TABLE 1 Proposed lithostratigraphy for the Rhiw area, after Beckly (1988).

Structure

Three phases of deformation have been recognised within the Lower Ordovician sedimentary sequence of the area (Hawkins, 1983). The first deformation phase produced SE-verging mesoscopic folds with steep to moderate-dipping axial surfaces and a sporadic axial-plane cleavage. A weak second deformation followed, producing only a low-dipping crenulation cleavage at a few localities. A third phase gave rise to numerous small buckle folds, an axial-plane cleavage and a suite of quartz veins. These three phases of deformation are similar to those described for other Lower Palaeozoic sequences in North Wales. Beckly (1988) has presented a stratigraphy which suggests greater structural complexity than recognised by earlier workers and has concluded that the present distribution of lithofacies reflects depositional variations rather than subsequent tectonic juxtaposition.

Examination of the best exposures in the Nant y Gadwen valley also demonstrates that the structure within this area is complex (Gibbons and McCarroll, in preparation). The valley can be divided into three structural units, separated by faults. The sediments and the mineralisation exposed within the valley are underlain and overlain by dolerite sills.

Manganese mineralisation

Within Wales significant manganese mineralisation is reported from three areas: the Harlech Dome, the Arenig area, and the Llŷn Peninsula (Figure 1). In the Harlech Dome manganese mineralisation occurs throughout the greywackes and pelites of the Harlech Grit Group (Lower/Middle Cambrian). The mineralisation is most intense at the base of the Hafotty Formation and the manganese bed has been exploited at several localities (Down, 1980). The mineralisation is syngenetic/syndiagenetic and is thought to have been supplied to the basin by exhalative hydrothermal solutions and directly precipitated as an oxide/carbonate sediment or formed by replacement of pre-exsisting carbonate (Bennett, 1987). The Arenig and Llŷn deposits occur in Ordovician rocks. The former consist of mixed carbonate-silicate ore occurring in joints and fissures, occasionally swelling into pockets, in feldspathic ash (Halse, 1892). The manganese deposits of Llŷn comprise a minor bedded deposit worked from adits on the southern flank of Gurn Ddu, near Llanaelhaearn (Figure 1) (Down, 1980), and the important deposits at Benallt and Nant, near Rhiw.

The Benallt and Nant mines (Figure 3) were responsible for the greater part of British manganese ore production over the period 1900-1945. The mineralisation has been described by Dewey and Dines (1923), Groves (1947, 1952) and Woodland (1956), and the mining history by Down (1980). The manganese ore is different in both mode of occurrence and mineralogy from that of the Harlech Dome. The ore occurs as a number of irregular bodies, usually lenticular in shape and elongate parallel to the regional strike, within Ordovician mudstones overlain and underlain by igneous rocks. The orebodies at Benallt were small and numerous, but at Nant the ore comprised a single tabular body larger than any of the individual orebodies at Benallt.

The mineralogy of the ore is complex compared to that of the manganese mineralisation of the Harlech Dome, and there are also local differences between the ores of Benallt and Nant. The poorly manganiferous rocks also appear to be different, as chamositic mudstone is characteristic of Benallt whereas keratophyric tuff occurs at Nant.

The Benallt and Nant ores were at first considered to be principally rhodochrosite (Dewey and Dines, 1923; Groves, 1938, p.31). Woodland (1939) first identified a manganese chlorite as a constituent of the ore; Groves (1952, p.309) subsequently reported that the Benallt ore comprised a complex mixture of manganese silicates (mainly the manganese chlorite, pennantite) with subsidiary manganese and iron oxides, but insignificant carbonate. However, the mineralogical composition varied considerably between different parts of the mine (Groves, 1947); for example, in ore from the Ty Canol incline tephroite was the dominant silicate. The results of the present magnetic surveys and sampling suggest that, for the Nant and Benallt ores of higher manganese content, jacobsite is also a significant constituent.

In addition to the minerals noted above, the following have also been recorded, either as constituents of the ore, or as present in veins : alleghanyite, banalsite, cymrite, ganophyllite, grovesite, pyrochroite, pyrophanite, rhodonite, and spessartite (Groves, 1952, p.309; Woodland, 1956).

The ore at Benallt lies within mudstones below a basalt known as the Lower Clip Lava and above a dolerite sill named the Footwall Sill (Groves, 1947). In detail, the geology of the mined area is complex, the rocks being folded, overfolded, thrusted and faulted, and described by Groves (1947) as of typical imbricate structure. The ore shows stromatolitic, pisolitic and oolitic structures. Groves (1952, p.306) has suggested that the thicker orebodies were built up by the crushing together of the ore bed within limbs of adjacent overfolds, and the squeezing out of the intervening mudstone.

At Nant the orebody is entirely bounded by thrusts, with doleritic rocks in proximity, both above and below. The ore is highly altered and contains manganese and iron oxides with replaced keratophyric fragments consisting of rhodochrosite, sericite, epidote and chlorite (Woodland, 1956). The Nant ore differs from that at Benallt in that rhodochrosite is ubiquitous (Woodland, 1939), though not the most abundant manganese mineral. Stromatolitic and pisolitic structures occur within the matrix, usually made up of haematite or carbonate-quartz-sericite-chlorite intergrowths with or without narrow concentric zones of finely dispersed haematite.

There have been no workings or trials between Benallt and Nant; the most southerly of the Benallt group of workings being east of Tyddyn Meirion [SH 2220 2763] (Figure 2), with the northern end of the Nant ore body being 1.35km south-west of here.

The paragenesis of the ore has been discussed by Woodland (1956) who considered the ore, as did Matley (1932), to have been a single bed, broken by faulting and displaced by a major ENE-WSW fault south of Benallt (Figure 3). Groves (1952) considered the ore at Benallt to have been formed by the metasomatic alteration of chamositic mudstone. The present interpretation is that the ore is likely to have been of exhalative origin, formed subaqueously accompanied by the deposition of mudstones. The differences in chemical composition between the ores at Benallt and Nant may reflect their positions with respect to that of the exhalative centre. Following precipitation, alteration of the ore was probably pene-contemporaneous and caused by the circulation of hydrothermal solutions. In the Nant area the fluids must have carried more CO_2, giving rise to the formation of rhodochrosite.

A classification of major economic manganese deposits has recently been proposed by Machamer (1987). For Type I of this classification, associated rocks include andesitic to basaltic metavolcanics, highly deformed and structurally complex, with thin manganiferous beds often thickened by tectonic duplication. The deposits of Rhiw thus appear to be an example of this type.

GEOPHYSICAL INVESTIGATIONS

The geophysical investigations comprised extensive field measurements of magnetic susceptibility for the manganese ores and other exposed rocks; reconnaissance magnetic surveying of blocks of ground to the south and north of the Benallt mine (the Penarfynydd and Mynydd Rhiw areas respectively - Figure 2); and detailed surveying in four areas where significant magnetic anomalies were recorded. No attempt was made to locate ore in depth beneath the old workings, because of the relatively small dimensions of the typical orebodies and the steep dip of the host sediments. All of the localities referred to in the following account are shown in Figure 2.

Regional setting

The contoured aeromagnetic data for western Llŷn are illustrated in Figure 4. The aeromagnetic survey was flown in 1960 by Canadian Aero Service Ltd., on contract to the Geological Survey. The data were recorded along north-south flight lines, spaced 2km apart, approximately along the even-numbered National Grid whole-kilometre eastings. Control lines were flown east-west along the 320, 330 and 340km grid northings.

A very broad positive magnetic anomaly is observed over the whole of Llŷn, its margins closely following the coast, a few kilometres offshore. Culminations of this broad anomaly are seen in two areas in western Llyn, and these appear to be due to secondary short-wavelength positive anomalies along the line of the maximum of the principal anomaly. Their closures ([2200 2900] and [3200 4000]*) are clearly seen in Figure 4. The former location lies close to the Rhiw survey area, and the axis of the anomaly here trends approximately north-south, immediately to the west of the 'manganese belt'.

The true areal extent of this short-wavelength anomaly is not well defined, because the magnetic gradients here are approximately parallel to the flight line direction; only the east-west control line along the 330km grid northing provides a clear profile across the anomaly. The superposition of the strong short-wavelength 'Rhiw' anomaly on the broader 'Llŷn' anomaly is evident on this profile. Furthermore, superimposed on the eastern flank of the 'Rhiw' anomaly is a much weaker peak, which is located approximately over the interpreted northward extension of the Footwall Sill.

The 'Rhiw' anomaly (represented by the stippled area in Figure 4) has its peak on the control line located approximately at a point [2220 3000]. On the flight record its amplitude is approximately 240nT, as on Figure 4, which has been compiled from data digitised from the flight records. However, the published aeromagnetic map for the area shows the anomaly amplitude as only 60nT, because of smoothing prior to contouring. The anomaly is possibly due to magnetic rocks within the Monian gneisses of the Sarn Complex, exposed a short distance to the west of Mynydd Rhiw, around Meillionydd (Figure 2), and which may underlie the Ordovician rocks on the lower western slopes of Mynydd Rhiw; or possibly to an unrecognised intrusion within the Ordovician, at or close to the contact between the Ordovician rocks and those of the Sarn Complex. It is clear from the detailed magnetic data described in this report that the source of the anomaly lies outside the area covered by the present survey.

---

* Throughout this report, National Grid References are given in square brackets. These refer to 100km square SH, and are given to four figures (10m).

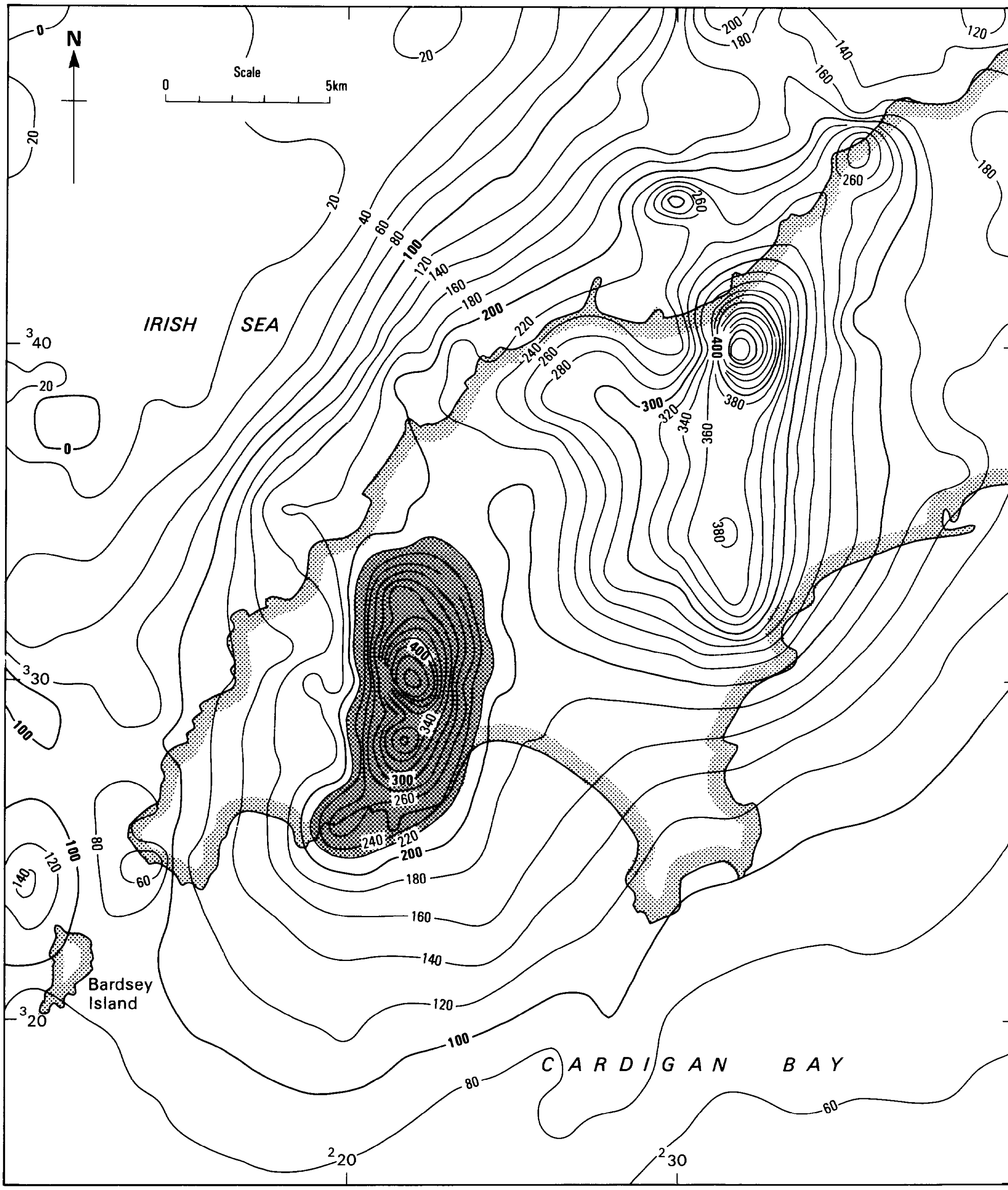

Figure 4 Regional aeromagnetic data for western Llŷn

Rock Physical Properties

Manganese Ore

The magnetic nature of the ore at Benallt was first noted by Groves (1947). The magnetisation was attributed to the manganese mineral jacobsite, which had been identified as being present in the ore by W.Campbell Smith of the British Museum. This has been confirmed more recently by Nancarrow (1987). Jacobsite may be highly magnetic; reports include those by Fermor (1908, 1909), Deb (1939, 1943), Mason (1943) and De Villiers (1945). It is worth noting also that Campbell Smith and others (1946) reported that pennantite (a manganese chlorite) was readily attracted by the electromagnet, and that this mineral was an important constituent of the Benallt ore. (Note that ore from the Nant mine is not referred to in these early reports, although the data presented below support the view that it is, in terms of magnetic susceptibility, comparable to the Benallt ore).

Jacobsite is one of the few minerals which have susceptibilities greater than 0.1 (SI) (others include magnetite and pyrrhotite). Mason (1943) applied the name jacobsite to cover a range of compositions within the system Fe_3O_4-Mn_3O_4, intermediate between magnetite (Fe_3O_4) and vredenburgite (the latter being an intergrowth of jacobsite and hausmannite (Mn_3O_4)). However, Essene and Peacor (1983) considered jacobsite to be a distinct mineral and end-member. Useful summaries covering these manganese minerals (and many others) are provided by Frenzel (1980) and Roy (1981); the former author suggests the more complex composition of $(Mn^{II},Fe^{II},Mg,Zn)(Fe^{III},Mn^{III})_2O_4$ for jacobsite.

A number of authors have provided magnetic property data for jacobsite. Fermor (1908,1909) and Frenzel (1980) describe the mineral as being as magnetic as magnetite, and Povarennykh (1964) places jacobsite in the category of 'very strongly magnetic' minerals (susceptibilities greater than 0.04 (SI)). Deb (1939, 1943) reported a value of 1.16 (SI) for two jacobsite-rich vredenburgites from India, and 1.07 (SI) for a Swedish jacobsite. Mason (1943) illustrated the variation in susceptibility across the Mn_3O_4-Fe_3O_4 system, indicating a minimum susceptibility for jacobsite of around 1.0 (SI), increasing with Fe_3O_4 content. Ore specimens from the Kodur manganese belt, southern India, were examined by Bhimasankaram and Rao (1958), who derived (by extrapolation) a value of 1.9 (SI) for the mass susceptibility of pure $(Mn,Fe)_3O_4$ (though not using the term jacobsite); this value approaches that of magnetite.

Occurrences of jacobsite are rare, and the Benallt occurrence is thus of particular interest. However, rock magnetism researchers have not examined either the Benallt or Nant ores, and there were, prior to the present survey, no reported values of magnetic susceptibility for these ores.

As part of the present study, susceptibility values have therefore been obtained for ore samples from the Benallt and Nant mines, providing three groups of data. Firstly, field measurements from ore exposed in situ at the two mines; secondly, field measurements on mined material which is abundant on dumps at Benallt and Nant, and at the site of the ore loading pier at Porth Alwm (Figure 2); and thirdly, laboratory measurements on samples cored from blocks of ore retrieved from the latter locality. Field measurements were made with a Scintrex SM-5 hand-held susceptibility meter, designed for use against any flat surface. Laboratory measurements were made with a Bison Instruments Model 3101 meter, designed for use with prepared core samples.

Exposed ore in situ can be seen at the Nant mine [2118 2673], and was reached by descending by rope into the glory-hole. Figure 5(a) shows the variation in magnetic susceptibility across the exposed face of ore in the northern wall of the glory-hole. Figure 5(b) shows the variation in magnetic susceptibility across the width of the

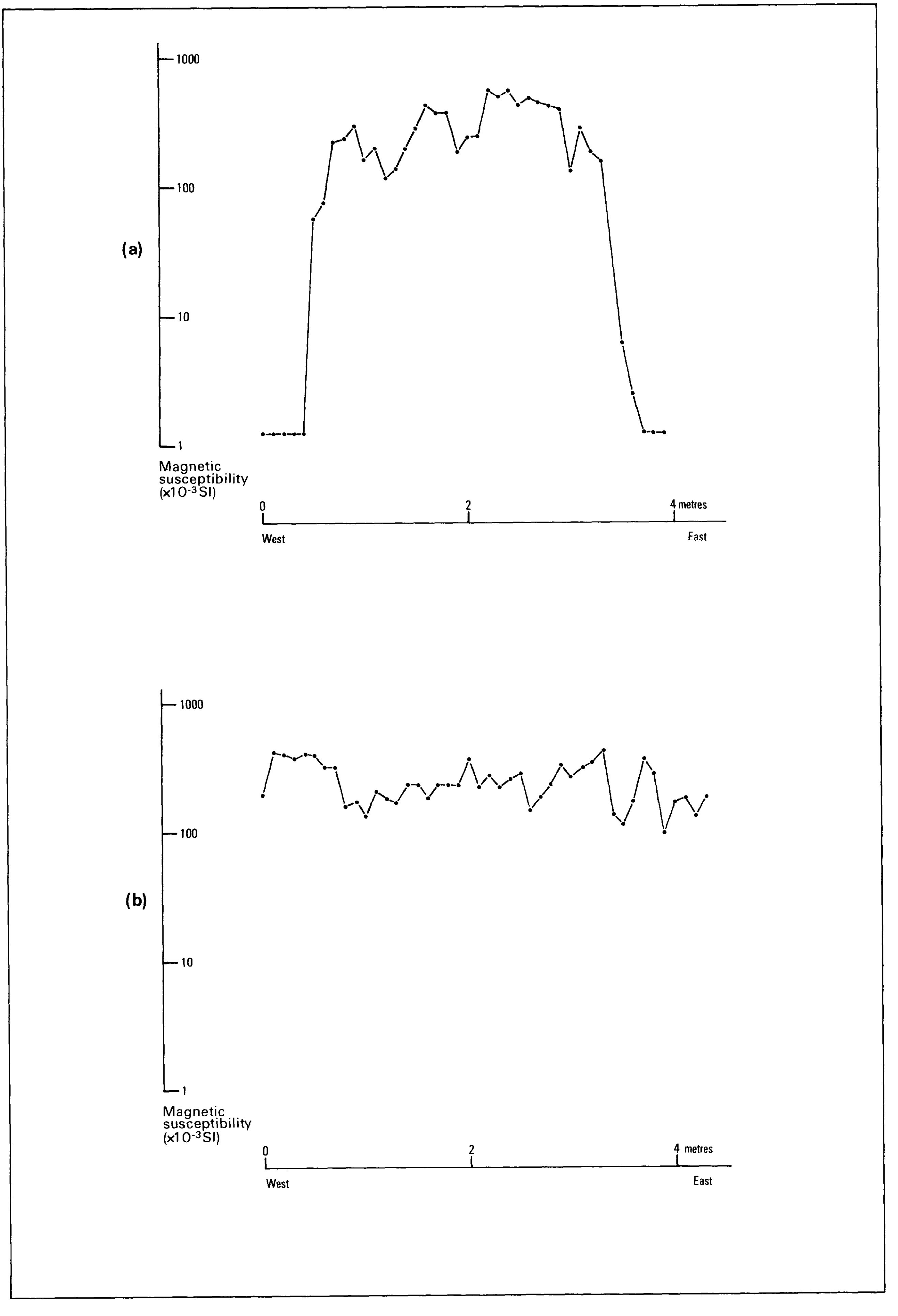

Figure 5 Magnetic susceptibility values, in situ ore, Nant mine

uppermost ore pillar (i.e. across the full width of the orebody). Observations are at approximately 0.1m intervals for both profiles. The profile in Figure 5(a) extends a little beyond the ore at each side, illustrating the very sharp cut-off of the magnetic material at the margins of the orebody. The average susceptibility value for the two sections is 0.27 (SI). (Note that for all of the magnetic susceptibility data presented here, logarithmic scales are used).

Other ore pillars are accessible by descending from the glory-hole into the stope beneath; susceptibility values comparable to the above are obtained for these. However, ore pillars accessible a short distance inside one of the mine entrances [2115 2668] (and identified as ore on the plan given by Groves (1952, Figure 41)) give values at least one order of magnitude lower than those observed across the glory-hole exposures. With much of the mine flooded or difficult to access, thorough investigation of these variations was not possible.

Susceptibility measurements were also made along the 'tramway' adit, at intervals of one metre from the entrance [2108 2662]. This adit penetrates sediments for a distance of 70m, and passes above the top of the orebody (Figure 11). No significant susceptibility values were recorded.

At Benallt, exposed ore is restricted to small patches within the opencut ([2218 2820] to [2218 2830]). Susceptibility values for these exposures range from 0.06 (SI) to 0.12 (SI) for material in situ, and from 0.12 (SI) to 0.44 (SI) for loose material on the floor of the workings.

To test the relationship between manganese grade and magnetisation, material from dumps at the two mines was sampled; Groves (1947; 1952, p.301) identified the Nant dumps (at the southern end of the tramway) as mine waste, and the large dump at Benallt [2221 2806] as low-grade ore (18% Mn). The results of this sampling are shown in Figure 6(b & c). The Benallt material has an average susceptibility of 0.036 (SI), while that at Nant gives an average value of 0.0085 (SI). It is notable that this more weakly magnetised manganiferous material is not always readily distinguishable from the ore itself.

A large quantity of ore is scattered at the shoreline, around the site of the old loading pier [2098 2632]. This pier was used during the first phase of mining at Benallt and Nant, with ore being conveyed to it by tramway (Down, 1980). It seems reasonable to suppose that this ore is a representative sample of the ore shipped from the two mines, and thus likely to be largely manganese-rich material. The ore is generally in large blocks (average dimension 0.2m) and is readily distinguished by its colour, ranging from blue/black through purple/brown to dark red. Susceptibility measurements were made on fifty blocks, with three measurements (on orthogonal faces) being taken for each block. The results are presented in Figure 6(c). Typical values for the more magnetic material (75% of the samples) are in the range 0.2 (SI) to 0.4 (SI).

Seven blocks of ore were retrieved from the above site, selected to cover a range of susceptibility values. Three cores (25mm diameter) were taken from each block, to provide samples for measurement of the remanent magnetisation carried by the ore. This was done for interest only, rather than to provide data to assist in the interpretation of the survey results, as the orientations of the samples were unknown. The opportunity was taken to measure the susceptibility of the cores, these possibly being less weathered than the outcropping ore described above. The distribution of values from the cores is of no consequence, since the blocks of ore were selected to provide a spread of values, rather than to reflect the distribution seen in Figure 6(c). However, it is notable that several of the cores gave values of susceptibility greater than any of those reported above.

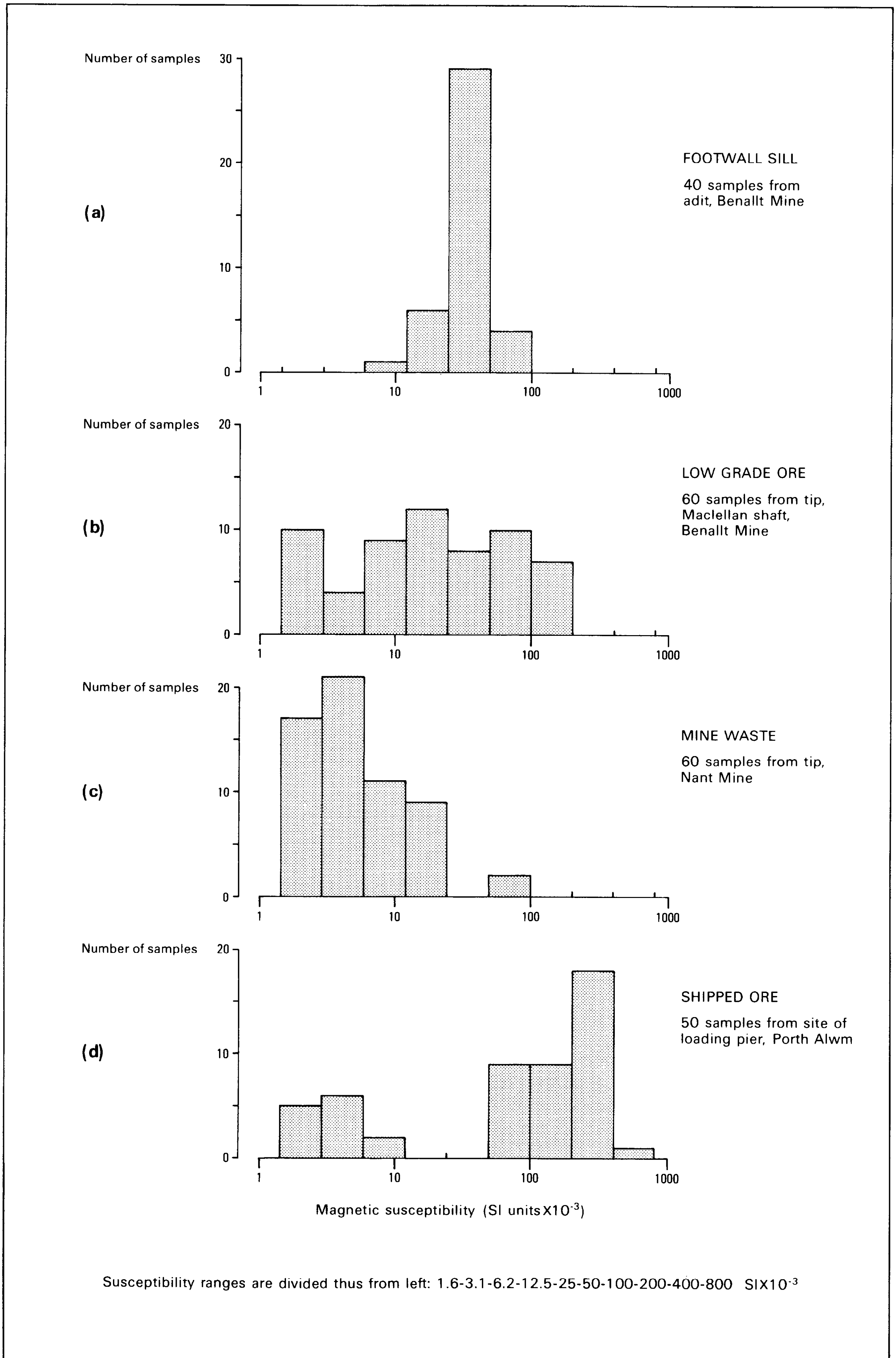

Figure 6 Magnetic susceptibility values, mined material

Thus the field susceptibility data indicate a typical value for the ore of around 0.3 (SI); the maximum value is 1.1 (SI) (from laboratory measurement for a core from one of the ore blocks). If we take the former value as representative, and assume a susceptibility of 1.5 (SI) for the jacobsite fraction, then the jacobsite must account for all of the reported typical iron content of the ore (7%, Groves (1952, p.308)). If instead we take as a suitable susceptibility value for the ore the average of all the values from Figure 6(c) (around 0.15 (SI)), then the required mean jacobsite content is halved; there is then room for a contribution to the iron content of the ore from other minerals.

For the samples of highest susceptibility, either a very high jacobsite content is needed or the jacobsite needs to be richer in iron, giving it a higher susceptibility. This need not affect the manganese grade of the ore significantly if, as the evidence of Mason (1943) suggests, the rise in susceptibility is disproportionate to the reduction in the Mn/Fe ratio. So, for example, the sample with a susceptibility of 1.1 (SI) could contain 73% jacobsite with ~45% Fe_3O_4 (susceptibility of ~1.5 (SI)), or only 30% jacobsite if its Fe_3O_4 content was ~65% (susceptibility of ~3.3 (SI)). The latter would give a lower total Fe content for the ore, all other things being equal.

So the susceptibility/grade relationship may indeed be valid, despite the inverse relationship being true for the causative mineral; it is the contribution to the total Mn content from other manganese minerals which is critical. The data presented above demonstrate the great increase in susceptibility when the Mn grade rises from around 20% to around 30%. Presumably, the chemical/metamorphic processes necessary to achieve this are the same processes which lead to the formation of jacobsite. This is a useful phenomenon when this grade difference represents the difference between economic and non-economic mineralisation, but less helpful if lower grades than those previously mined were to be the target of magnetic surveys.

Also as part of the present study, the magnetic properties of some samples of the manganese ore were examined by the Department of Physics at the University of Newcastle-upon-Tyne. The results are reported elsewhere (Cornwell and Evans, 1989), but indicate a saturation magnetisation close to that of magnetite. The Curie temperature is lower (250-300°C) than for most titanium-poor magnetites, although it is similar to that for pyrrhotite.

Density and porosity measurements were made for the core samples from the blocks of manganese ore described above; the results were not of particular relevance to the interpretation of the magnetic survey data, but have provided a useful addition to the Survey's database of rock physical properties. For the less strongly magnetic material (susceptibilities from 0.001 to 0.01 (SI)) densities are in the range 3.2-3.4 $Mg.m^{-3}$, whilst for the strongly magnetic material (susceptibilites from 0.1 to 1.0 (SI)) densities are around 3.6-3.7 $Mg.m^{-3}$. All of the samples are lithologically very compact, with porosities invariably less than 1%.

The Footwall Sill

The imbricated sediments at Benallt, within which the orebodies are found, are confined between the Lower Clip Lava (to the east) and a dolerite sill (to the west); these igneous rocks dip to the east at approximately 45°. The sill was named the Footwall Sill by Groves (1947), who showed from magnetometer profiles that it is magnetic. The Footwall Sill is not exposed in the vicinity of the mine, but there is a large tip of the dolerite in the uppermost part of the opencut, the result of an exploratory adit driven into the sill (described by Groves (1947)). Susceptibility measurements were made for 40 samples of material from this tip, and the results are shown in Figure 6(a). The average susceptibility is 0.034 (SI). By way of comparison, typical values (from drill core samples) for the well-known Whin Sill dolerite intrusion of northern England are generally within 10% of this figure (Bateson and others, 1984).

The Gallt y Mor Sill

The Gallt y Mor Sill (so named by Matley (1932)) is well exposed on the coast between Porth Ysgo and Porth Cadlan (Figure 2). (It will be shown later that this is most probably the same intrusion as the Footwall Sill). Its thickness here is estimated at 140m (Gibbons and McCarroll, in preparation). The top few metres of the sill are accessible on the west side of Porth Ysgo, and susceptibility sections were measured at two sites ([2055 2643] and [2074 2650]), at intervals of 0.1m, providing a total of 112 observations. The distribution of the susceptibility values is shown in Figure 7(a). Over 80% of the values fall within the range of values for the Footwall Sill (Figure 6(a)), though the average value for the Gallt y Mor Sill is somewhat less (0.019 (SI)).

Magnetite-rich sandstones

In the coastal section west of Porth Ysgo, the Gallt y Mor sill is overlain by sandstones. The susceptibility section described above was extended upwards to include these sandstones, which were found to be irregularly but strongly magnetised; the magnetite-rich bands are clearly visible. The distribution of the susceptibility values, from 104 observations, is shown in Figure 7(b). The difference in typical values between the lower part of the section and the upper part (with magnetite-rich bands) is clearly seen.

There are no sandstones mapped inland, and with the significant magnetic anomalies inland accounted for by the Footwall Sill, the north-eastward extent of these sandstones remains unknown. Magnetite-rich sandstones from elsewhere in North Wales have been described by Evans and Chacksfield (1987) who report susceptibility values for these of up to 0.6 (SI).

Other localities

Magnetic rocks are exposed at a number of localities additional to those noted above, and 'spot' measurements of susceptibility for these were made using the Scintrex SM-5 hand-held susceptibility meter. These rocks generally have susceptibility values in the range 0.01 (SI) - 0.03 (SI) and are located as follows :

(a) Over a width of a few metres on the west side of the sill exposed between Porth Alwm and Porth Ysgo (Figure 8).

(b) On both sides of the stream which runs from Ysgo to Porth Ysgo. On the basis of the mapping of Cattermole and Romano (1981) these exposures represent the upper part of the Gallt y Mor Sill and the lower part of the sill exposed between Porth Alwm and Porth Ysgo (Figure 8). The magnetic observations here are thus consistent with those noted at (a) above.

(c) On 'outcrops' piercing the drift in the valley between Penarfynydd and Ty'n Rhedyn. These appear to be the upper extremities of large boulders of the ultrabasic rocks of Mynydd Penarfynydd.

(d) At four locations on the western flank of Mynydd Rhiw ([2240 2882], [2242 2889], [2242 2898], [2255 2940]). These exposures thus most probably represent the northward extension of the Footwall Sill of Benallt.

Other exposures tested, where the rocks are clearly not magnetic, are as follows :

(a) The greater part of the sill exposed between Porth Alwm and Porth Ysgo.

(b) The two sills exposed further east along the coast ([2115 2625]) (Figure 8).

(c) The isolated outcrop between Bodlondeb and Ty'n Rhedyn ([2169 2697]), considered

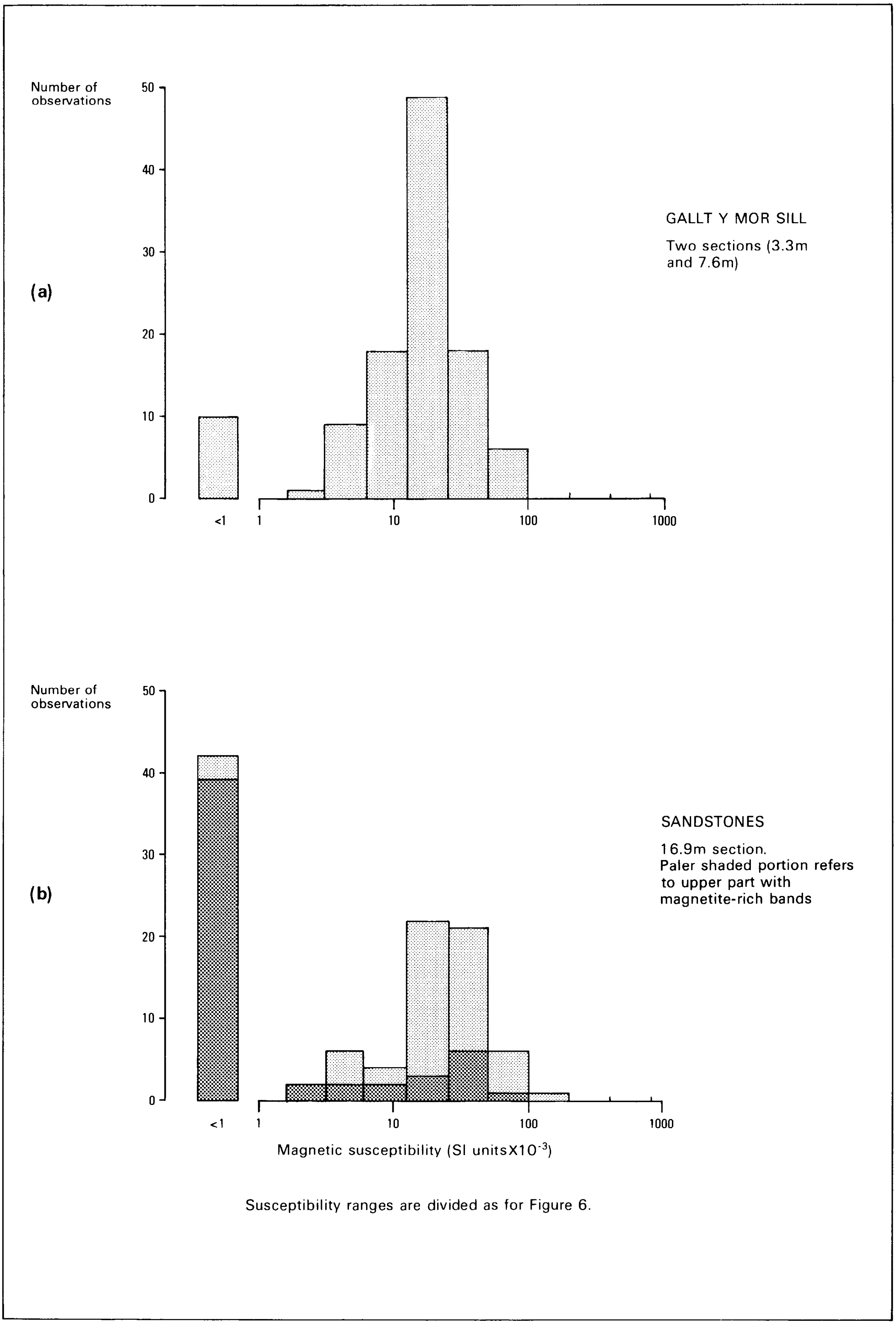

Figure 7 Magnetic susceptibility values, Porth Ysgo

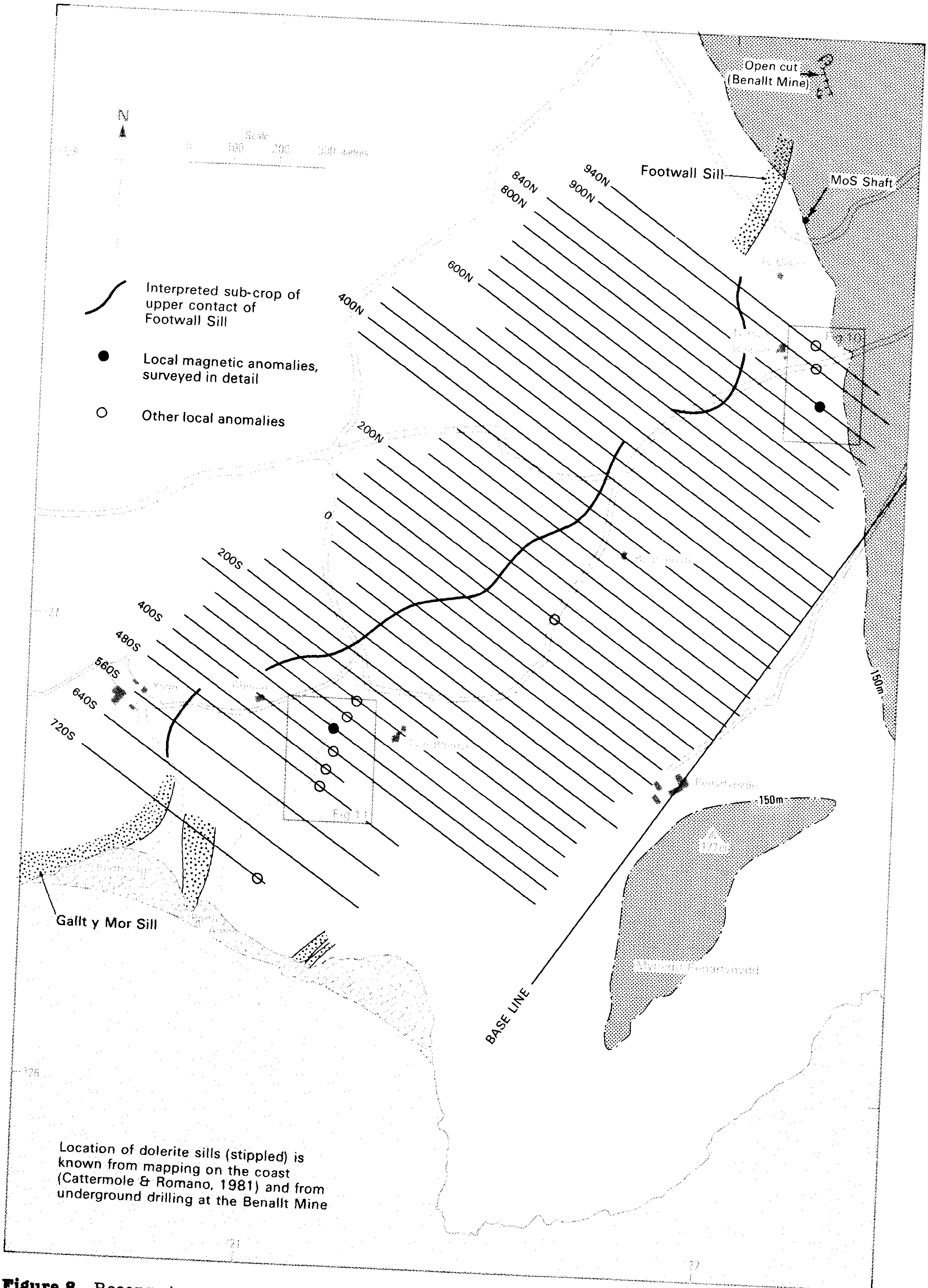

Figure 8 Reconnaissance magnetic survey—Penarfynydd area

by Matley (1932) to represent the southward extension of the Lower Clip Lava of Benallt.

(d) A substantial exposure of dolerite in an old quarry near Ty Engan (Figure 2). This has been mapped by Matley (1932) as the northward extension of the Footwall Sill at Benallt.

Reconnaissance magnetic surveys

Penarfynydd area

Thirty-four traverses were measured across the area between the Benallt and Nant mines (traverses 400S to 940N, Figure 8), surveyed from a base line approximately along the road to Penarfynydd Farm. The traverses were spaced 40m apart and were on average 900m in length. A further five traverses (440S to 720S) were measured to cover the area from the Nant mine to the coast, so that the rocks exposed in the coastal section might be better related to the magnetic anomalies observed inland. A traverse orientation of 130°/310° (magnetic) was used throughout. Observations were made with Geometrics G816 (1nT resolution) and G836 (10nT resolution) total-field proton magnetometers. The survey was carried out between 12th and 25th March 1984.

The magnetic data for the Penarfynydd area enable the sub-crop of the Footwall Sill to be positioned with some confidence; assuming the sill is not transgressive, the magnetic data thus determine the western limit of the area through which the manganese beds are believed to persist. As noted above, the sill is nowhere exposed southwards from Benallt towards Nant; the drift across this ground is known to be locally as thick as 25m (Groves, 1952, p.316). However, the magnetic anomaly associated with the sill is well illustrated in the Benallt area (Groves 1947), where the location of the sill is known from horizontal boreholes drilled from the 130-foot level of the re-opened Ministry of Supply workings. The sill was located as far south as a point [2203 2784] north-west of Ty Canol (Groves (1952), Figure 40), and the present survey has traced the sub-crop south-westwards from there (Figure 8).

The anomaly due to the sill is generally of the order of 600nT-800nT in amplitude, and 150m-200m in width. A typical profile, from part of traverse 760N, is shown in Figure 13. The anomaly is continuous for 1.4km south-westwards from Ty Canol, extending as far as Llanfaelrhys church. However, on two traverses (560N and 600N) it is less well defined. This may be due to impersistence of the intrusion, or to displacement of the sill by a fault; if the latter, then the displacement of the sill is to the west-south-west, as indicated by Matley (1932), Groves (1952, Figure 37) and Woodland (1956), but only by some 200m rather than the 600m indicated from this earlier mapping. The locality cannot be mapped in greater detail because of the presence here of several buildings and sources of extraneous magnetic anomalies.

The interpretation of the location of the sub-crop of the upper contact of the sill from the present survey data (Figure 8) is confirmed by drilling results reported by Groves (1952, pp.315-318). Six boreholes were put down in 1942 to explore the inferred prospective ground between Ty'n Rhedyn and Bodlondeb farms. The final borehole intersected the three principal components of the succession : the Lower Clip Lava, the mudstones (with a 4m section carrying 13% Mn), and the Footwall Sill. This borehole was drilled from a point approximately 30m west-north-west of the isolated outcrop at [2169 2697], inclined at 45° and directed north-west. The beds dip at 45° to the south-east, and the calculated position of the sub-crop of the upper contact of the sill (196m north-west of the borehole) matches the position interpreted from the magnetic data to within 10m. The intersected manganese bed here must sub-crop very close to the lane; a weak magnetic anomaly on traverse 80N (Figure 8) may be due to the mineralisation, but because of the effect of fences either side of the lane this cannot be demonstrated with certainty. An isolated anomaly for manganese in soil also occurs here (Figure 18).

South-west of Llanfaelrhys church (Figure 8) the interpretation of the magnetic data is less straightforward. Strong (600nT) positive anomalies are observed on traverses 480S and 560S, but these are of much shorter wavelength than the anomalies extending north-east to Benallt. Also, the southernmost traverse (720S) shows a rather irregular magnetic profile, with no single distinct feature. Nevertheless, the sharp anomalies on traverses 480S and 560S indicate a north-south trend for the source rocks, consistent both for location and trend with the mapped swing in strike of the Gallt y Mor sill, turning inland from its NE-SW trend on the coast, to a N-S trend south-west of Llanfaelrhys church (Figure 8) (Matley, 1932; Cattermole and Romano, 1981).

Thus although the magnetic data between the church and Porth Ysgo are less conclusive than might have been expected from the unambiguous data further to the north-east, it is difficult to interpret the data for the Penarfynydd area as a whole otherwise than indicating that the inland extension of the Gallt y Mor sill is also the south-westward extension of the Footwall Sill at Benallt. The magnetic susceptibility data described above support such an assumption, if the data for the upper (exposed) part of the Gallt y Mor sill are taken as representative of the whole thickness of this intrusion. Furthermore, Beckly (1988) has observed that the mudstone forming the northern half of the islet of Maen Gwenonwy, above the Gallt y Mor sill (Figure 2), is lithologically and faunally identical to the mudstone of the mining belt. This evidence also supports equating the Gallt y Mor and Footwall sills.

This view is in contrast to the mapping of Matley (1932), who equated the Footwall Sill instead with a sill seen *above* the mudstones on Maen Gwenonwy (via exposures on the west side of Nant y Gadwen and between Porth Alwm and Porth Ysgo), presumably on the basis that these represent the next sill below the ore bed at Nant. Groves (1952), and more recently Gibbons and McCarroll (in preparation) have concurred with this view. In the absence of significant exposure inland from Porth Ysgo towards Benallt, and in view also of the agreement between the geophysical interpretation and the drilling results of 1942 noted above, it seems reasonable to accept Figure 8 as correctly representing the sub-crop of the upper contact of the Footwall Sill, rather than the provisional revision of the mapping (Figure 3).

It is worth noting here a significant error made by Groves (1947) in the interpretation of his magnetic survey data. The traverse which he measured along the Aberdaron-Rhiw road located two anomalies west of Tyddyn Meirion, which he attributed to a pair of sills; the Footwall Sill causing the more easterly anomaly, with the anomaly to the west being considered to be due to the inland extension of the Gallt y Mor sill. The explanation for the error is evident from Figure 8; the road crosses the single anomaly due to the Footwall Sill in two places, because of the geometry of the sub-crop arising from the sill being displaced to the west-south-west.

Given the interpretation of the geophysical data proposed above, the sill forming the small promontory between Porth Alwm and Porth Ysgo needs to be fitted into the picture. Significantly, the map provided by Cattermole and Romano (1981) shows this sill and the Gallt y Mor sill both turning sharply inland at Porth Ysgo, and the possibility that these sills merge a little further north cannot be discounted - the Porth Alwm sill presumably being transgressive, in order to move down from its position above the 'manganese mudstones' at Maen Gwenonwy to a position below those beds at Nant.

This possibility is supported by magnetic data. As noted above, the sill exposed on the promontory between Porth Alwm and Porth Ysgo is moderately magnetised in part; also, a magnetic traverse across the islet of Maen Gwenonwy and its shingle bar (linking it to the mainland at low tide) showed irregular but significant magnetic anomalies up to about 200nT amplitude. Traverses to the north-east and south-west to confirm these anomalies were obviously not possible. Also, the magnetic susceptibility data show the presence of magnetic rocks on both sides of the stream which runs down from Ysgo to Porth Ysgo; these outcrops being respectively the extensions northwards of the coastal exposures of the Gallt y Mor sill and Porth Alwm sill, as illustrated by Cattermole and Romano (1981).

The magnetic survey data cannot help with the question posed by the mapping of where on the coast the dolerite exposed alongside the Nant tramway at [2110 2656] crops out; this dolerite is equated by Matley (1932) with the Lower Clip Lava, and by Groves (1952) with weathered igneous rock seen above the sediments hosting the ore at the eastern end of the southernmost adit at Nant. All of the available evidence is that the Lower Clip Lava is essentially non-magnetic, so the geophysical data cannot assist in resolving this question. The Lower Clip Lava could be very thin hereabouts (no thickness figures are reported), so its exposure may not be evident amongst the cliff debris.

The survey of the Penarfynydd area located four other significant anomalies or groups of anomalies (Figure 8). The most important are anomalies indicative of manganese ore near Tyddyn Meirion (traverses 840N, 900N and 940N) and near the Nant mine (traverse 360S), investigated by additional sets of detailed traverses, and described separately below. Anomalies were also observed on three traverses (400S, 440S and 480S) above the workings of the Nant mine, attributed to ore left in place to support the roof of the workings (as illustrated by Groves (1952, Figure 41)) and therefore not considered further. Finally, three very sharp anomalies were located on the trackbed of the old tramway, near the Nant mine (traverses 280S and 320S) and near the head of the incline to the old pier (traverse 720S). These have no obvious cause, and were dismissed after it was shown that these anomalies have no strike extent, and fall off rapidly over distances of only a few metres.

Mynydd Rhiw area

The northward extension of the sediments which host the ore at Benallt has historically been held to be barren ground, though with no firm evidence on which to base this assumption.

There is no visible, documented or mapped evidence of trial shafts or diggings on the ground to the north of the upper end of the Benallt opencut, and there is only one report of exploratory driving along strike, this being an adit driven during the wartime operations to test the source of a strong magnetic anomaly near the Clip y Gilfinhir (Groves, 1947) centred approximately at [2225 2835]. This adit extended only for 125m, and proved the anomaly to be due to the Footwall Sill being faulted eastwards across strike, and hence occurring where the ore bed might otherwise be expected. At about the same time, a borehole was put down from a point (approximately [2230 2860]) north-west of the Clip y Gilfinhir, which penetrated 75m of mudstones below the Lower Clip Lava (Groves, 1952, p.314); no ore was located.

Given the distance between the Benallt and Nant mines, and the known geology and mode of occurrence of the mineralisation, there is clearly no reason why ore might not also occur a comparable distance north of Benallt. Exposure is rather better across Mynydd Rhiw than in the Penarfynydd area, though it is the igneous rocks which are seen rather than the sediments.

Having covered the Penarfynydd area, some trial magnetic traverses were made across Mynydd Rhiw in June 1984. The results indicated that the Footwall Sill could be traced as far as the northern end of the high ground. Accordingly, a more detailed survey was carried out over the area, between 12th and 20th October 1984.

Thirty-seven traverses were measured across the area, with an orientation of 107°/287° (magnetic). These were spaced 60m apart over Mynydd Rhiw, and 120m apart over the northern flank of the hill (Figure 9). Geometrics magnetometers, as described for the Penarfynydd area, were again employed. The earlier reconnaissance (June 1984) had shown that the strong magnetic anomalies seen on the west flank of the hill could not readily be traced beyond Coch-y-Moel, and the detailed survey was therefore not extended beyond there towards Sarn, although the mapping by Matley (1932) indicates that the sequence of sediments and igneous rocks does persist in that direction.

The results of the detailed survey on Mynydd Rhiw reflect those for the Penarfynydd area; a single prominent positive anomaly persists for approximately 2.4 km north-north-west from the northern limit of the Benallt workings, where the Footwall Sill is clearly seen to be the cause of the anomaly. The sharp change in strike of the anomaly west of the Clip y Gilfinhir (Figure 9) marks the northern edge of the block of the Footwall Sill faulted across the ore beds, noted above.

The anomaly is almost continuous, reflecting the largely undisturbed nature of this ground as shown by Matley (1932), though in the less well exposed ground on the northern flank of the hill the magnetic data place the intrusion further to the east than suggested by the mapping. Between traverses 1460N and 1660N the anomaly is less clearly defined as a single feature, possibly due to impersistence of the intrusion, to transgression, or to minor faulting. The magnetic data indicate that on Mynydd Rhiw, and particularly on the northern flank of the hill, the sill is much thinner than it is in the Penarfynydd area. The interpreted position of the upper contact of the sill (Figure 9) is consistent with the locations of outcrops of magnetic rocks, noted in the details of rock physical properties above.

With little or no drift cover in parts of the Mynydd Rhiw area, the anomalies due to the sill are often much sharper than those observed in the Penarfynydd area. Assuming again that the sill is not transgressive, the anomaly defines the western limit of the area within which anomalies indicative of manganese mineralisation might be expected to occur. Of four such anomalies observed (Figure 9), two were particularly prominent, and were investigated in detail by additional sets of traverses, as described separately below.

Detailed magnetic surveys

Detailed magnetic surveys were carried out in four areas; Tyddyn Meirion, Nant y Gadwen, and at two sites on Mynydd Rhiw. Contoured magnetic data for three of these areas are shown in Figures 10, 11 and 12. Typical magnetic profiles across the principal anomalies are illustrated in Figure 13. For comparison, a profile showing the magnetic anomaly across the Footwall Sill near Tyddyn Meirion is also shown.

Tyddyn Meirion

The magnetic survey of the Penarfynydd area located small but significant anomalies on traverses 840N, 900N and 940N, of maximum amplitude 190nT. This result was of considerable interest; the anomalies were located on strike from those reported by Groves (1947), which were proved by mining to be due to manganese ore. Furthermore, this apparent extension of the ore bed indicated that the Rhiw Fault of Matley (1932) was, if present at all, located not along the Rhiw-Aberdaron road as he had indicated, but at least 100m further south.

The area of interest was therefore investigated in detail by a subsequent magnetic survey, carried out in June 1984. The traverse locations are shown in Figure 10.

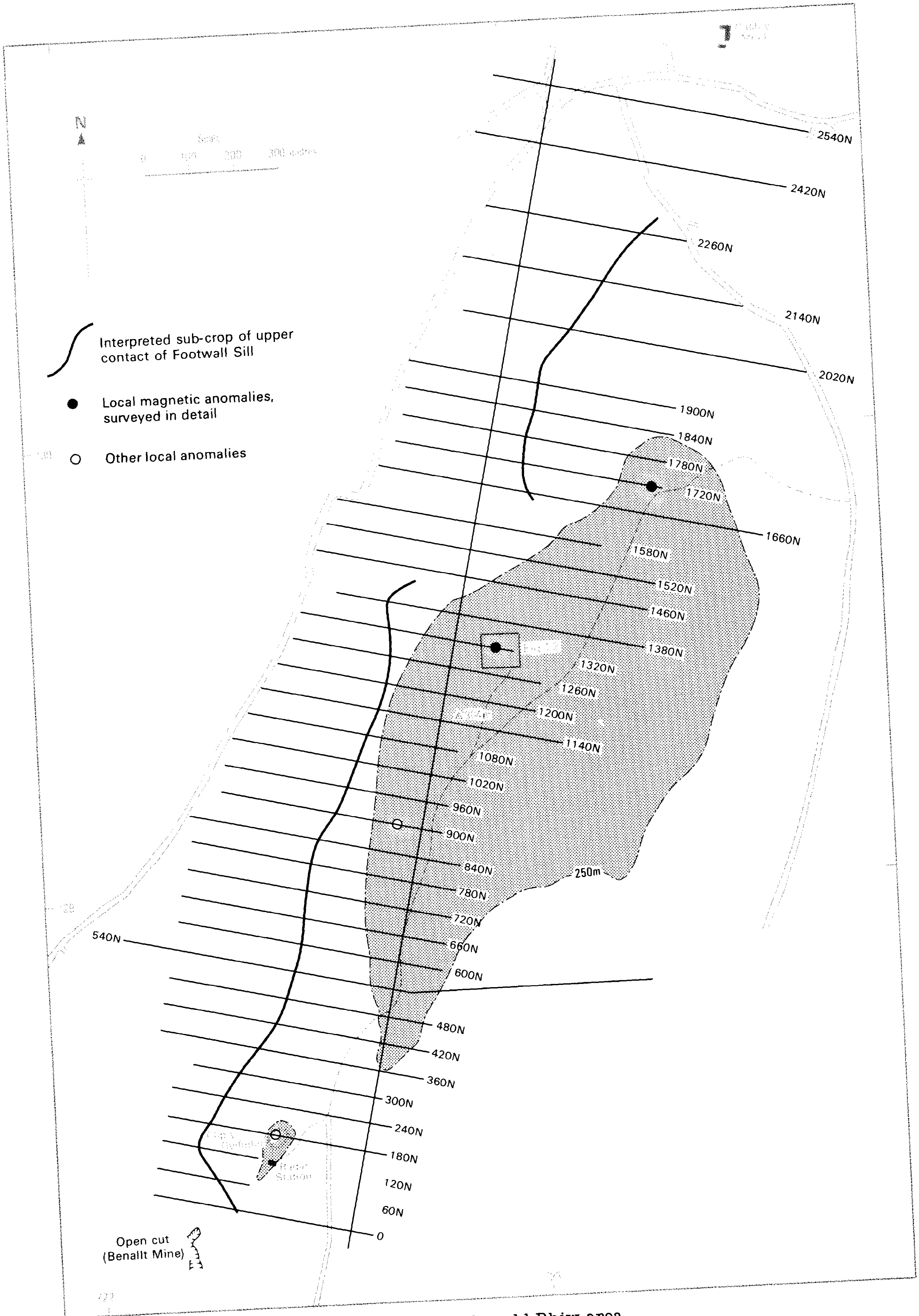

Figure 9 Reconnaissance magnetic survey—Mynydd Rhiw area

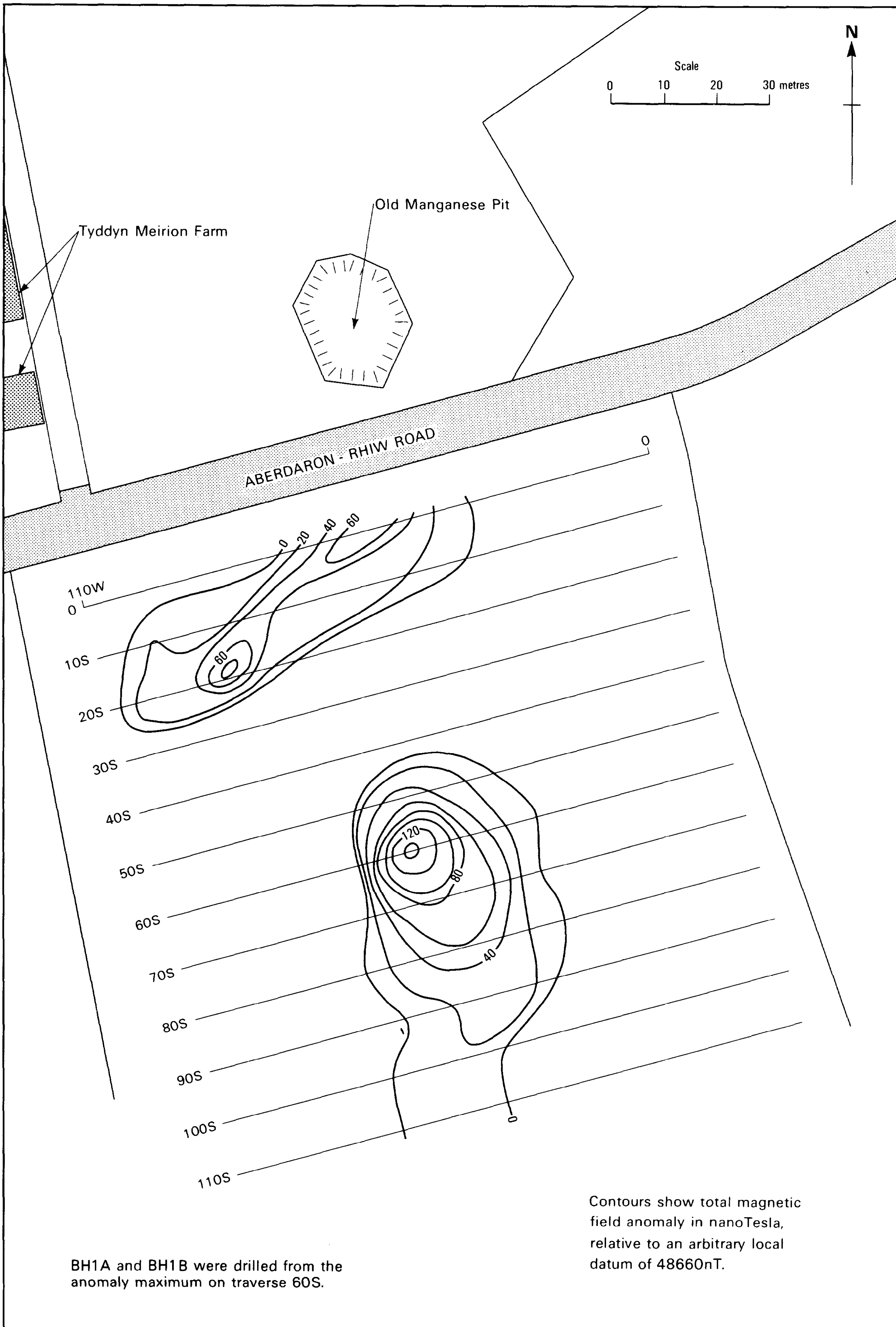

Figure 10 Detailed magnetic survey, Tyddyn Meirion

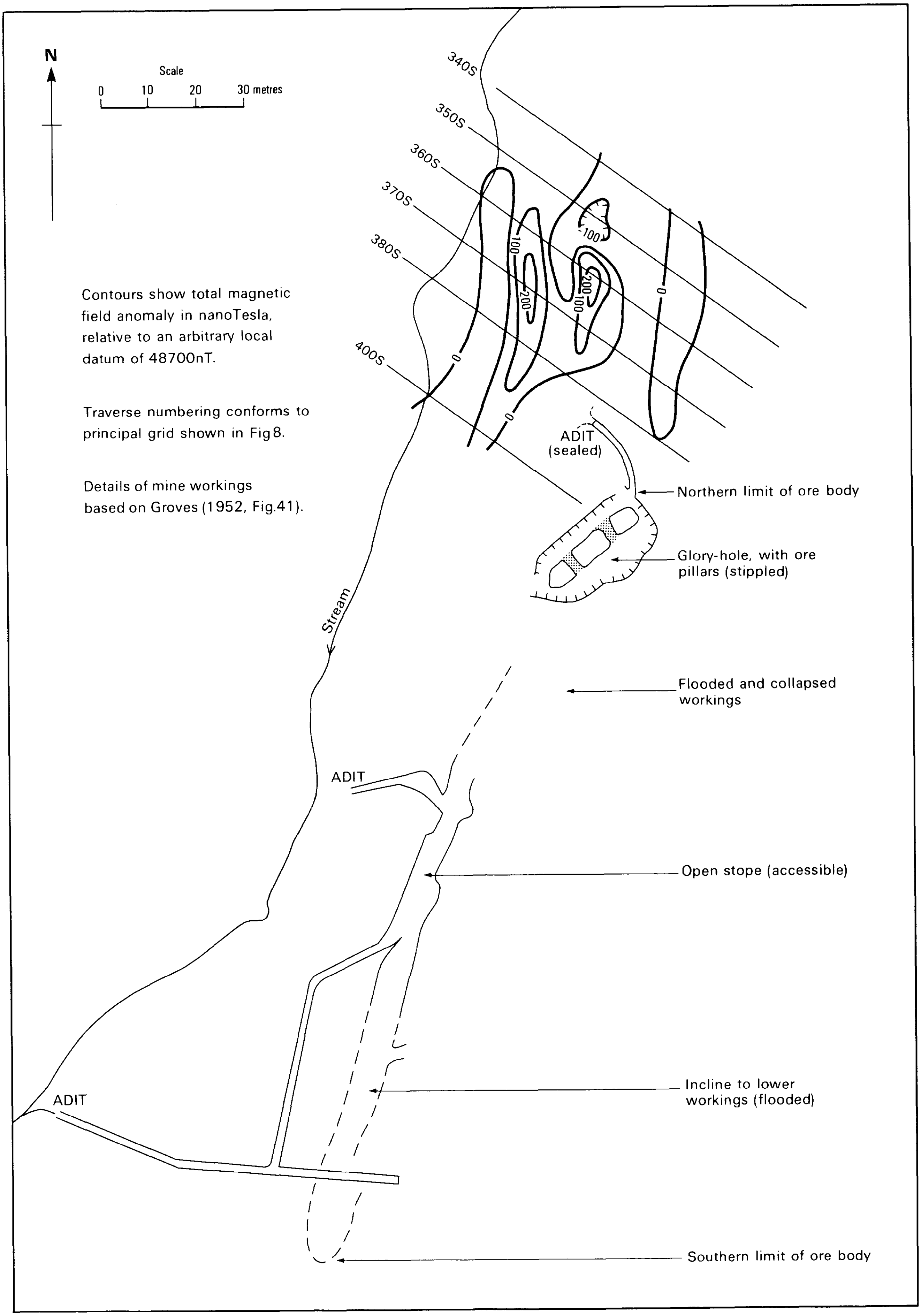

Figure 11 Detailed magnetic survey, Nant y Gadwen

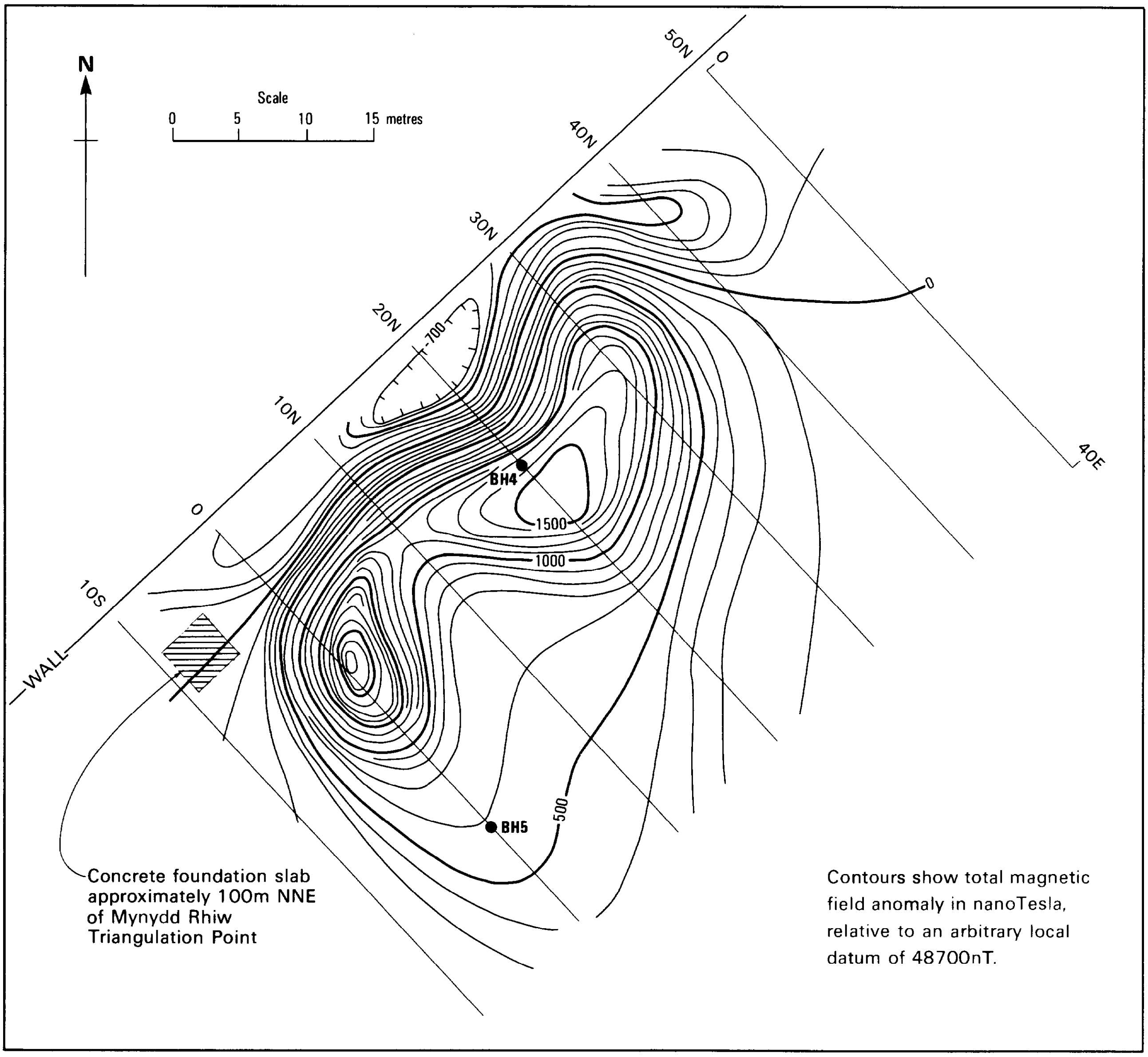

Figure 12 Detailed magnetic survey, Mynydd Rhiw

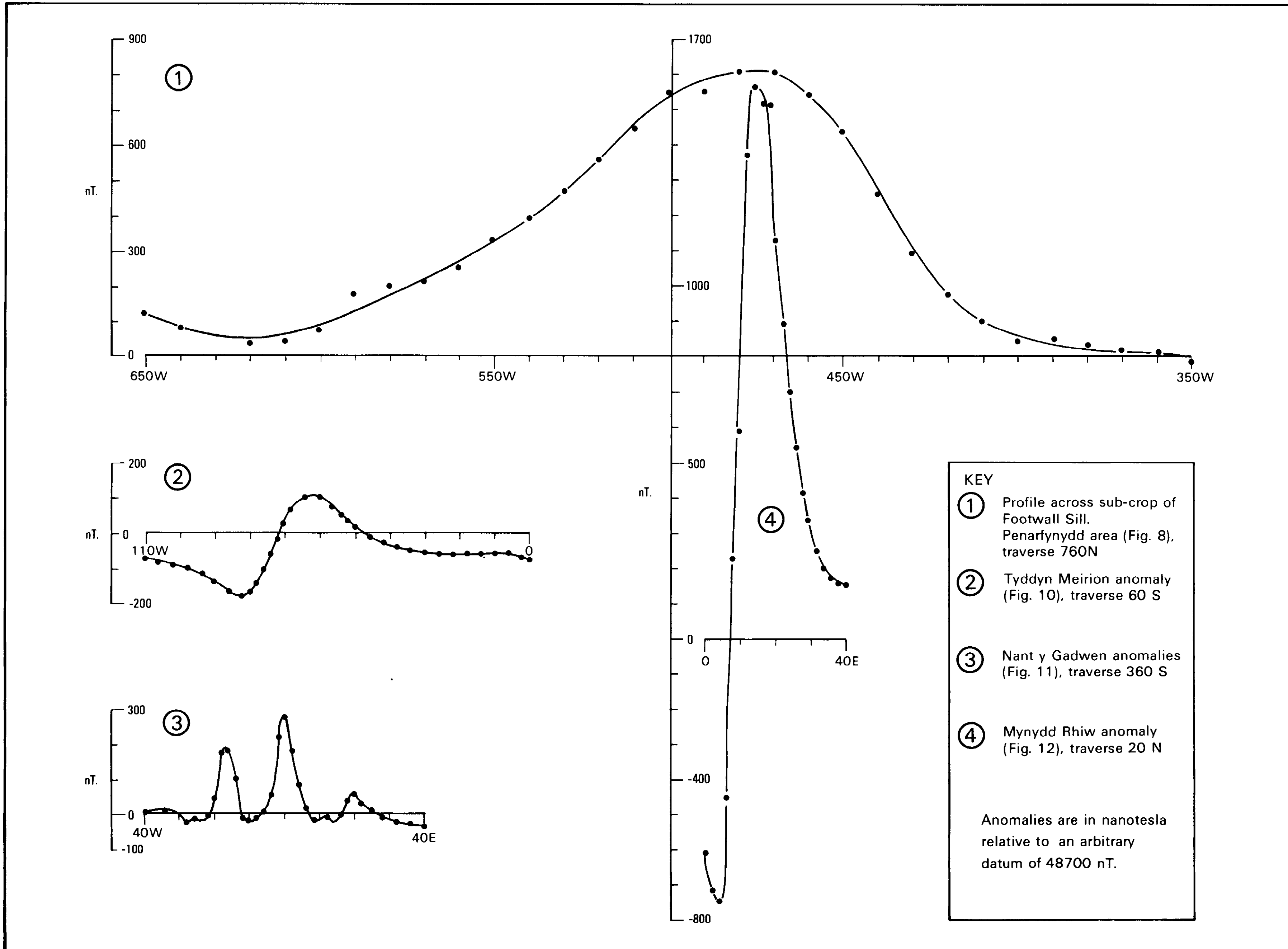

Figure 13 Examples of magnetic profiles across selected anomalies

Observations were made along these traverses (spaced 10m apart) at 2m intervals.

Figure 10 also shows the extent of the magnetic anomaly initially located on traverse 840N of the Penarfynydd area survey (Figure 8). In addition, a second anomaly was located close to the Rhiw-Aberdaron road.

This latter anomaly appears to extend away from the pit on the north side of the road, from which 50 tons of ore were raised during 1916 (Groves, 1947). Inspection shows that the excavations from this pit follow the trend of the magnetic anomaly, though for how far is not known. The anomaly thus clearly suggests the presence, near to surface, of manganese ore. Groves (1947) had identified this anomaly, though did not map it in detail, and suggested that the trend of the anomaly results from the ore being drawn out along the line of the postulated fault. However, the presence of the second anomaly to the south, centred at [2221 2753], suggests that the ore bed persists on strike rather than being displaced to the west-south-west as mapped (Matley, 1932). The extent and amplitude of this latter anomaly are such that it is comparable to the anomalies located by Groves (1947) in the fields east of the track from Tyddyn Meirion to Ty Canol, which were shown to be due to substantial bodies of economic manganese ore, lying within a few tens of metres of surface.

Consequently, this anomaly (the more southerly of the two shown in Figure 10) was investigated by drilling. On traverse 60S, which crosses the anomaly at its maximum, a negative anomaly accompanies the positive on its western side (Figure 13; not shown in Figure 10 to preserve clarity). This was interpreted as indicating that the sub-crop of the causative feature was located approximately beneath the steepest gradient, with the source of the anomaly having a moderate dip to the east (and thus consistent with the disposition of several of the Benallt orebodies). Accordingly, the initial borehole (BH1A) was sited on the anomaly maximum, and inclined to the west (azimuth 266°) at an inclination of 60°. A second borehole (BH1B) from this site was drilled vertically. The results of the drilling are described later in this report.

Gravity measurements were made at 5m intervals along traverse 60S, across the maximum of the magnetic anomaly; the density measurements noted above indicated that a manganese orebody should provide a small gravity anomaly. The regional gravity field in the Rhiw area shows a strong gradient, trending north-south, and possibly related to the source of the north-south magnetic anomaly noted above (Figure 4). Against this background, a gravity anomaly of approximately 0.05 mGal was observed, coincident with the maximum of the magnetic anomaly. This anomaly was considered to be of insufficient amplitude to justify further gravity measurements over the area of the magnetic anomaly.

Nant y Gadwen

The survey of the Penarfynydd area located strong magnetic anomalies (~200nT) of short wavelength in the steep-sided Nant y Gadwen valley, on traverse 360S immediately north of the Nant mine. The traverse grid was too coarse to resolve these anomalies adequately, and additional traverses were therefore measured to cover these anomalies in detail.

Six traverses were measured, parallel to the traverses of the 'primary' grid. These were 80m in length, with observations at 2m intervals. The sides of the Nant y Gadwen are steep, and this presented some difficulties in preserving plan (rather than slope) distances for this detailed work. The traverse locations are shown in Figure 11; there may be errors of a few metres in the position of the features shown, because of the topographic problems, and because the original plan by Groves (1952) on which it is based does not differentiate between magnetic and true north.

As is clearly seen in Figure 11, the detailed traverses define two elongate anomalies. These are located some 40m north-north-west of the north end of the Nant orebody. Figure 11 has been drawn to show the whole of the orebody worked at the Nant mine, so that the relative size of the magnetic anomalies can be seen. The anomalies are parallel, trending north-south, and over the strongest portions are approximately 20m and 30m in length respectively. A weaker positive anomaly lies parallel, some 20m to the east, and is approximately 30m in length. The two stronger anomalies have amplitudes of approximately 250nT and widths of approximately 10m (Figure 13). The easterly anomaly appears to develop into a strong (150nT) negative anomaly at its northern end.

The anomalies clearly suggest that thin, elongate pods of manganese ore may be present here, located only 10m or so beneath the valley floor. The position and trend of the anomalies (aligned on strike and *en echelon* with the Nant orebody) support this view. If this interpretation is correct, then the pattern of multiple orebodies seen at Benallt is thus represented (to a lesser degree) at Nant.

Drilling short vertical boreholes to test the anomalies was precluded by the lack of vehicle access to the deeply-incised Nant y Gadwen. It would have been possible, at best, to position a drilling rig in the field above the eastern side of the valley, to drill an inclined borehole to intersect the postulated ore (probably dipping steeply east, as does the Nant orebody). However, drilling at an angle shallower than 60° would not have been advisable, but had this angle been adopted it is quite possible that the borehole would have passed beneath the postulated orebodies (since there is no reason to suppose that the down-dip extent of the ore would necessarily be much greater than the strike extent). The anomalies have therefore not been tested by drilling.

Mynydd Rhiw

The locations of the two strongest anomalies of interest in the Mynydd Rhiw area are shown in Figure 9. Both are located only on single traverses (1320N and 1720N), so clearly have no significant strike extent.

Both anomalies were investigated in detail by additional closely-spaced traverses; seven traverses spaced 10m apart to cover the southern anomaly, and seven traverses spaced 5m apart to cover the northern anomaly, with observations at 2m intervals on all traverses.

The southern anomaly was shown to be elongate approximately along strike, though clearly over no more than 40m (Figure 12). It is of considerably greater amplitude (approximately 2000nT) than any of the anomalies located in the Penarfynydd area (Figure 13) and the steep magnetic gradient on its north-west side indicates a source within a few metres of surface.

The northern anomaly was found to be of even greater amplitude (~4000nT) but of limited areal extent, and with no evident strike alignment.

Both anomalies were considered to be suitable drilling targets. They were considered to be located close enough to the interpreted subcrop of the Footwall Sill to be possibly within the manganese mudstones, and thus possibly due to ore; there was no possibility of either being due to a concealed man-made source; drift was clearly very thin at both sites; and both sites were readily accessible to a drilling rig.

The results of the drilling are described later.

GEOCHEMICAL INVESTIGATIONS

Soil sampling

A total of 334 soil samples were collected from across-strike traverse lines from two areas, the first north of Benallt and the second between Nant and Benallt (Figure 14). Samples were collected at 25m intervals along NW-SE oriented lines, with a hand auger from a depth of 0.8-1.0m, after removal of near surface organic material. Drift cover on Mynydd Rhiw is relatively thin; in contrast, south of Benallt it is generally thick, though locally very variable. The results of drilling between the two mines (Groves, 1952, pp.315-318) have shown the cover at one locality to vary between 2m and 24m thick over a distance of less than 70m.

The soil samples were dried, sieved at minus 0.18mm (85mesh), mixed with binder and ground in a planetary ball-mill. The samples were submitted for X-ray fluorescence analysis for the elements Ti, V, Cr, Mn, Fe, Ni, Cu, Zn, Pb, Sr, Zr, Mo, U, Ba and As.

Analytical data for the soils are tabulated in Appendix 9 and summary statistics for the complete data set and for the two separate areas sampled are shown in Table 2. A correlation matrix for the total data set is shown in Table 3. Interpretation of the soil data was undertaken with the aid of single element cumulative frequency plots. Most elements show multi-modal distributions with the exception of Ba and U which show a normal distribution. Anomaly maps (Figures 15 - 19) were constructed by plotting the upper anomalous population taken from the cumulative frequency diagrams. In the case of Ti the upper two populations have been plotted.

Immobile elements which include Ti, V and Zr (Figures 15, 16 and 19) reflect bedrock chemistry in the north of the area and are useful in mapping the sub-crop of the basic rocks on Mynydd Rhiw. In the south, geochemical variation in soil is locally controlled by drift deposits and hydromorphic processes and no clear patterns related to the underlying bedrock can be discerned. For example, high Cr values in the south-east of the area (Figure 17) are most likely to be due to transported material from Mynydd Penarfynydd which is composed of hornblende picrite (Cattermole, 1969).

The distribution of Mn in soil (Figure 18) is affected by secondary redistribution processes and appears to be of little value. A small group of anomalies to the south of Benallt, coincident with a magnetic anomaly, were thought possibly to indicate a strike extension of the manganese mineralisation, but subsequent drilling (BH1A and BH1B) intersected ironstones (depleted in Mn) rather than manganese ore.

Rock sampling

Rock samples were collected for the two mine sites and available exposures throughout the area (Figure 14). Descriptions of the rocks collected are given in Appendix 1 and chemical analyses in Appendix 2.

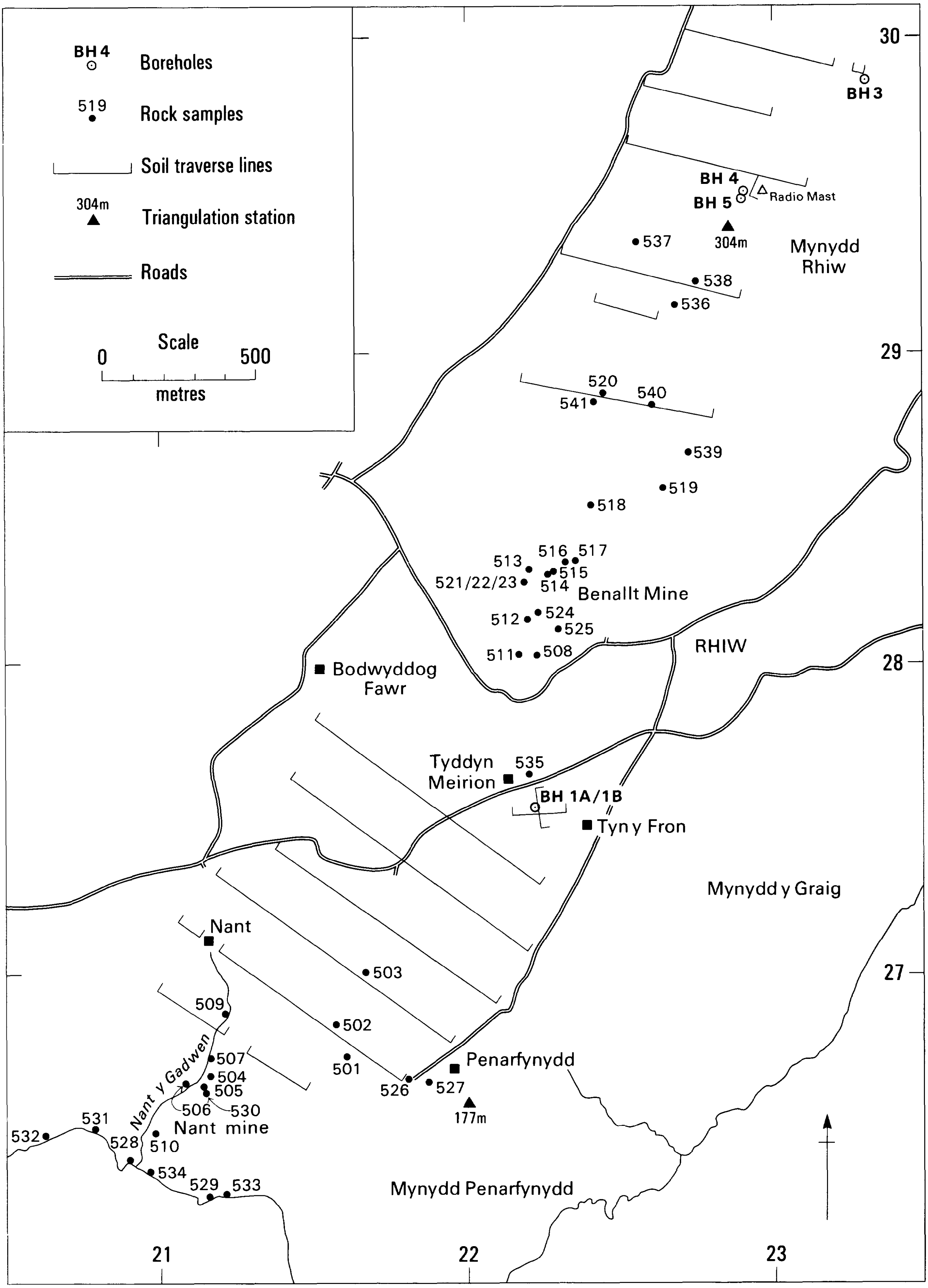

Figure 14 Location of soil traverse lines, boreholes and rock samples

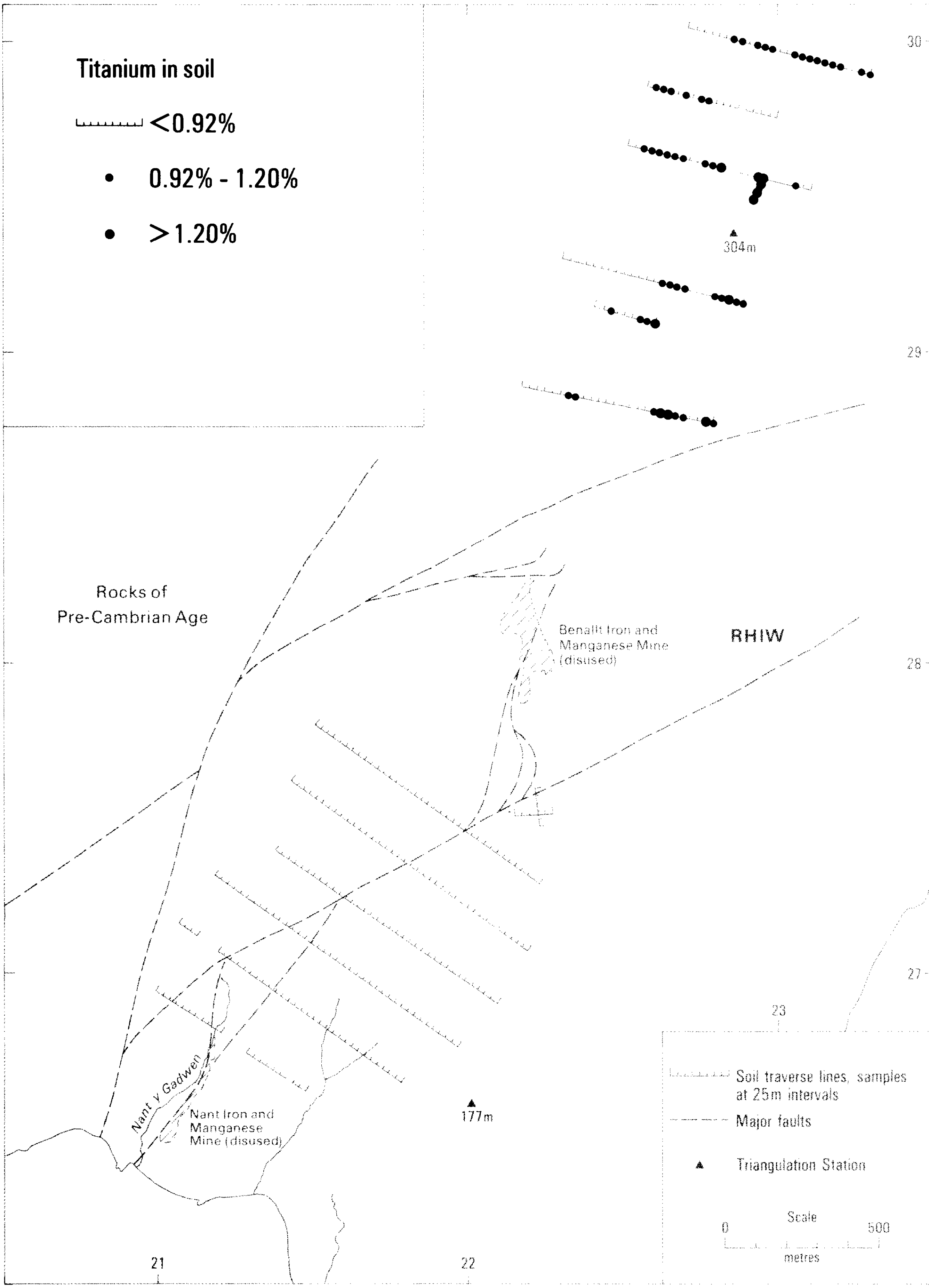

Figure 15 Distribution of Titanium in soil

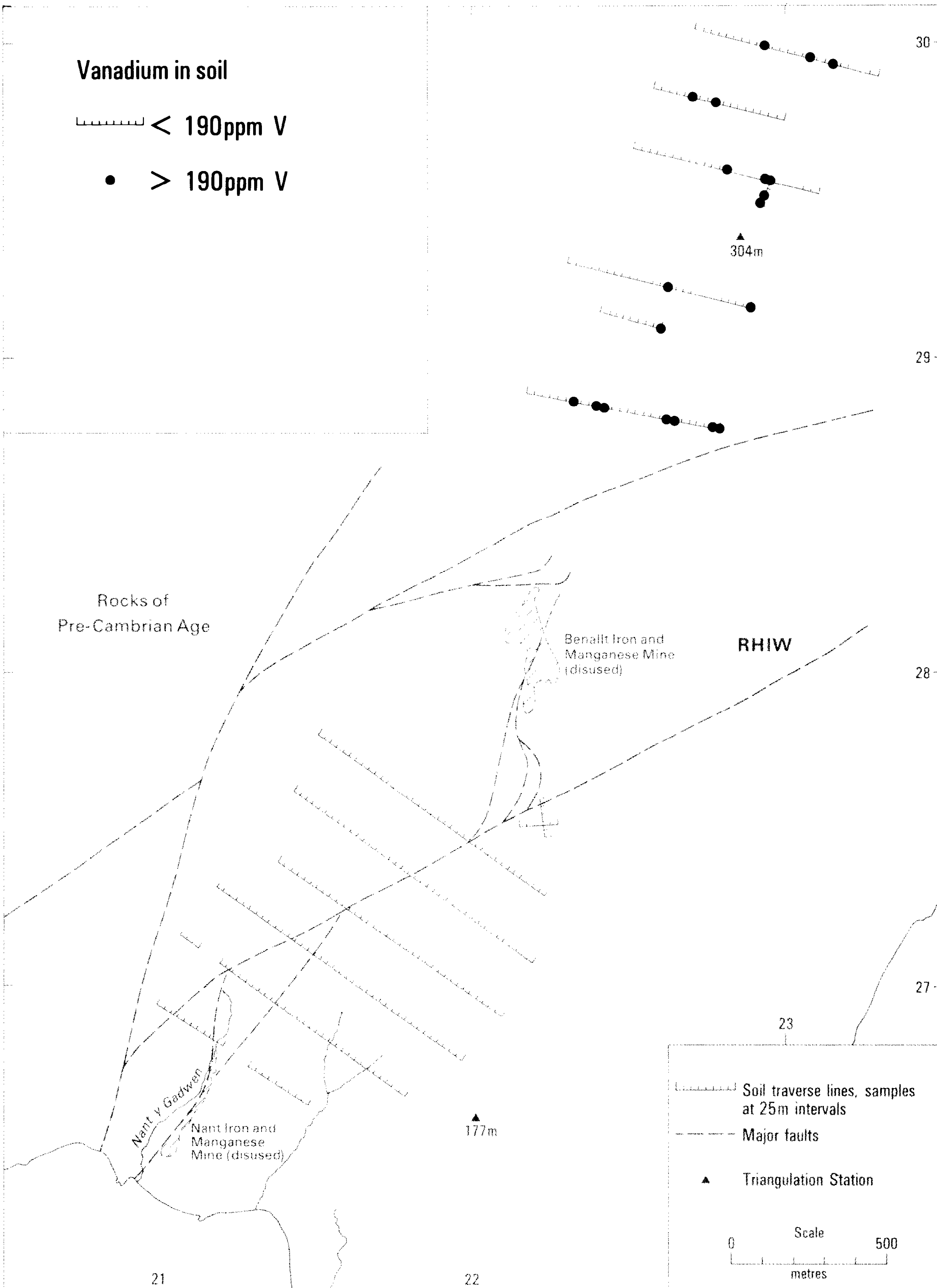

Figure 16 Distribution of Vanadium in soil

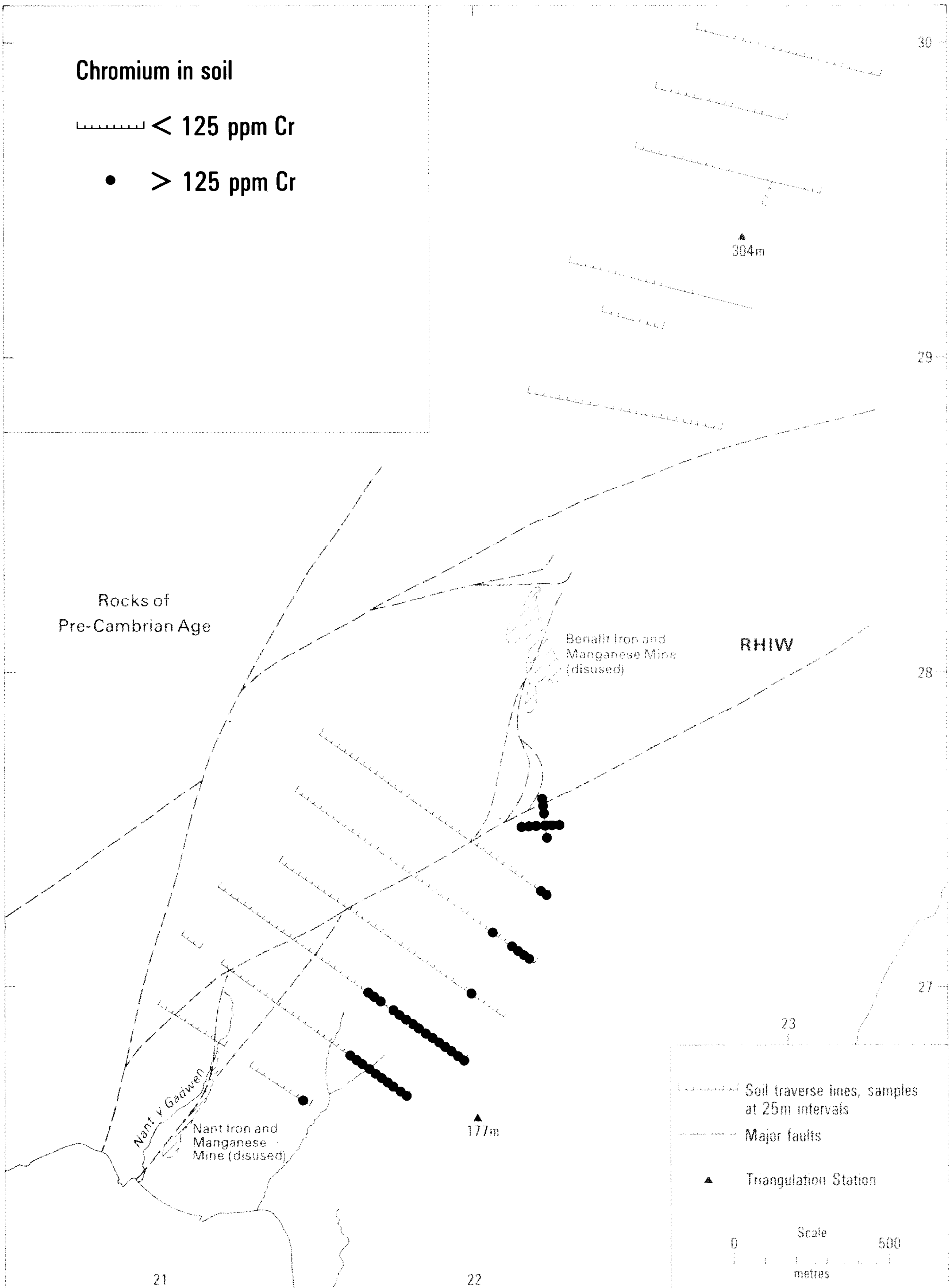

Figure 17 Distribution of Chromium in soil

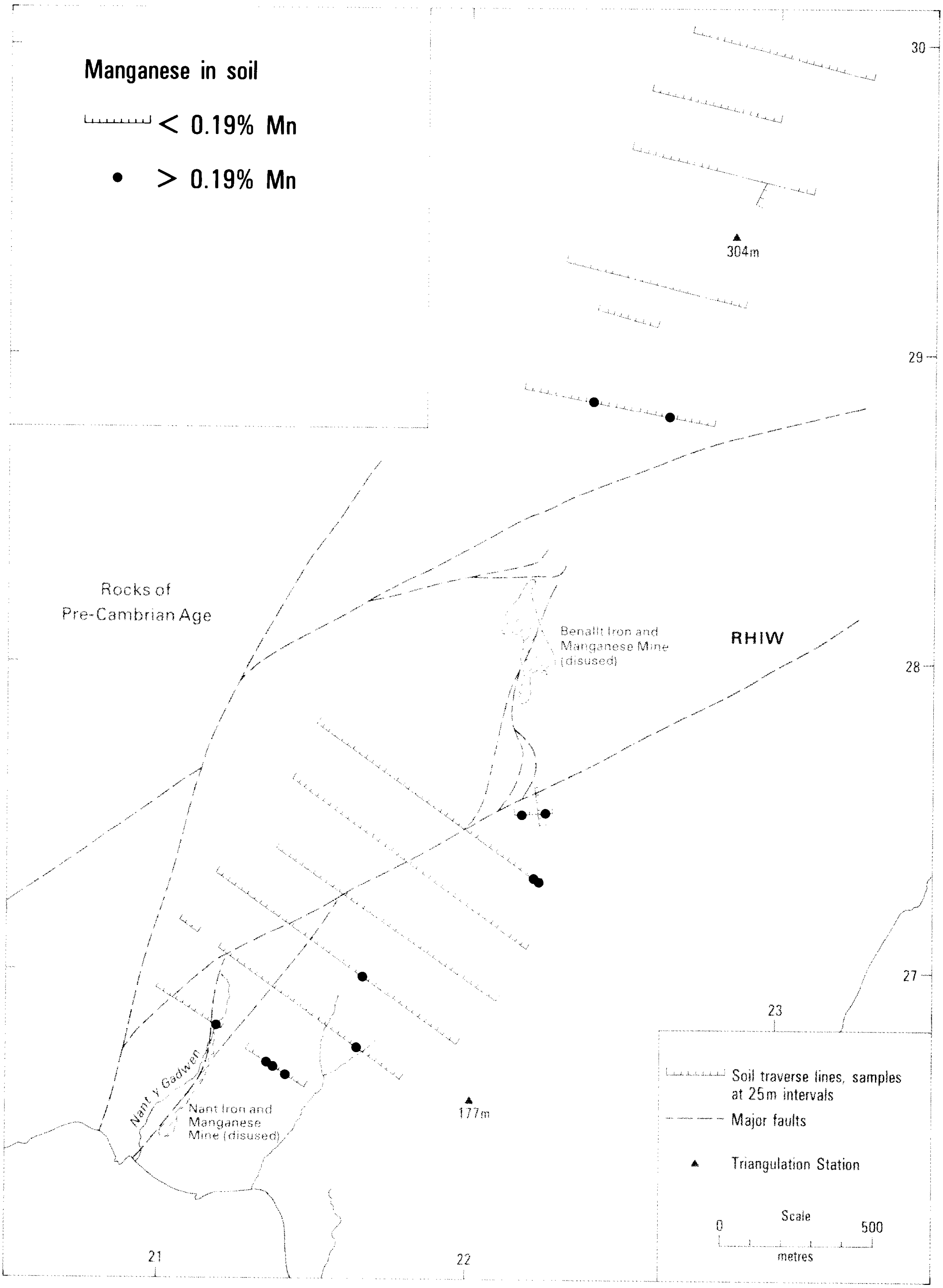

Figure 18 Distribution of Manganese in soil

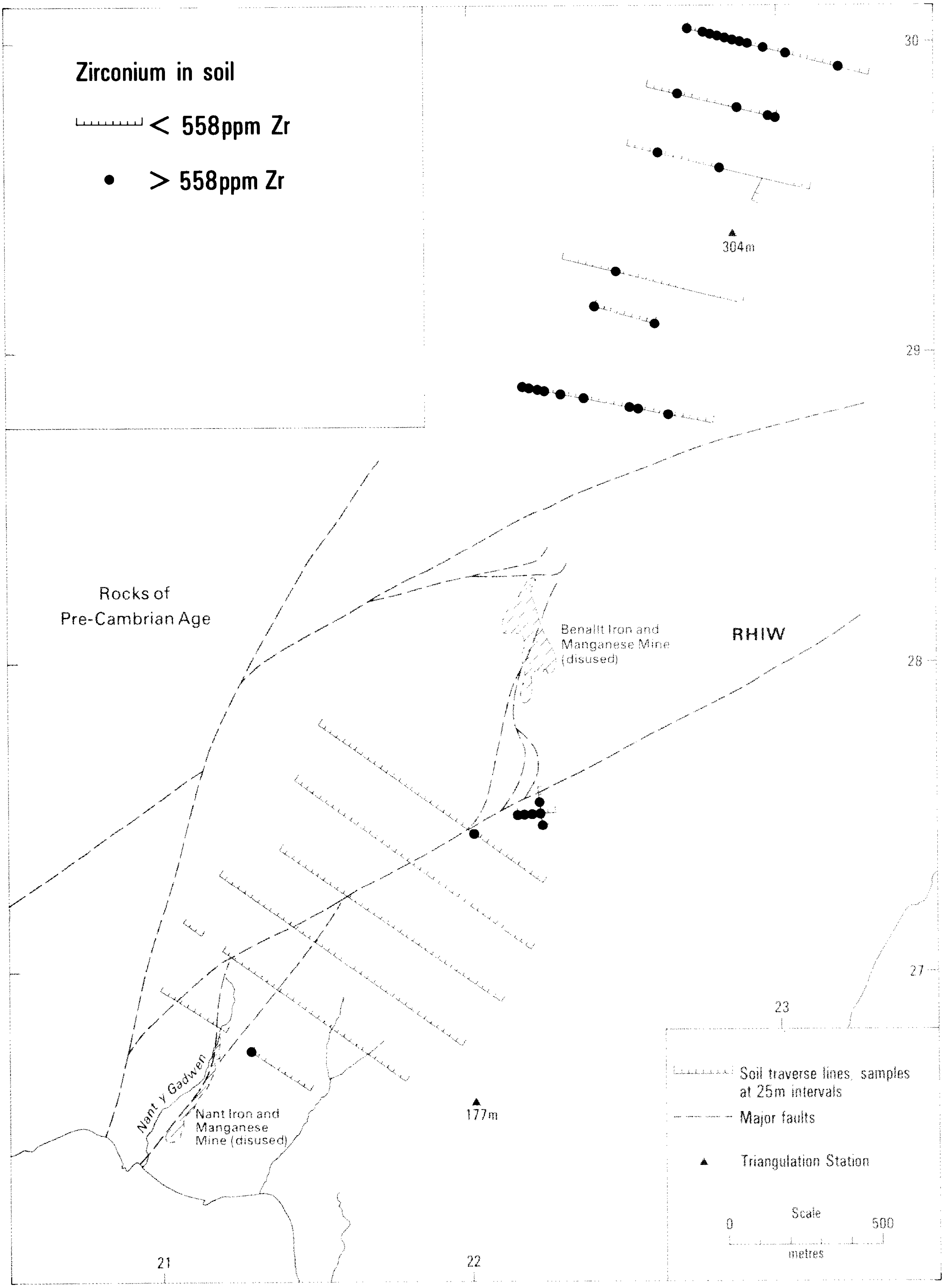

Figure 19 Distribution of Zirconium in soil

Elements	Minimun ppm	Maximum ppm	Geometric mean ppm	Standard Deviation (log)
Ti	5190	18140	7171	0.10
V	80	320	130	0.10
Cr	50	260	96	0.12
Mn	250	16590	915	0.22
Fe	9200	88100	38986	0.10
Ni	1	58	17	0.33
Cu	1	47	9	0.41
Zn	19	131	61	0.13
Pb	12	98	26	0.13
Sr	44	100	71	0.05
Zr	220	951	428	0.09
Mo	1	4	1	0.20
U	1	8	3	0.20
Ba	30	530	244	0.14

Total data set for Rhiw soils : n=334

Ti	5740	18140	9312	0.10
V	110	320	161	0.10
Cr	50	110	73	0.08
Mn	250	2760	802	0.20
Fe	9200	88100	41849	0.14
Ni	1	29	8	0.33
Cu	1	16	3	0.41
Zn	19	109	49	0.14
Pb	12	72	23	0.17
Sr	44	100	65	0.06
Zr	220	951	476	0.11
Mo	1	2	1	0.18
U	1	7	3	0.20
Ba	30	290	178	0.15

North data set for Rhiw soils : n=116

Ti	5190	7210	6241	0.02
V	80	150	116	0.04
Cr	80	260	111	0.10
Mn	250	16590	982	0.23
Fe	25700	54100	37546	0.06
Ni	10	58	25	0.10
Cu	3	47	15	0.17
Zn	37	131	68	0.08
Pb	17	98	28	0.09
Sr	61	93	74	0.03
Zr	240	695	404	0.07
Mo	1	4	1	0.21
U	1	8	4	0.19
Ba	170	530	289	0.05

South data set Rhiw soils : n=218

TABLE 2 Summary statistics for soil data

	>0.8	0.7-0.8	0.6-0.7	0.5-0.6	0.4-0.5	0.3-0.4
Ti	V	-Ni-Cu-Ba		-Cr-Fe	-Zn	-Sr
V	Ti	Fe	-Ni-Ba	-Cr-Cu		-Zn
Cr			Ni Cu	-Ti-V Zn Ba	Sr	
Mn				Zn		Cu
Fe		V				
Ni	Ba	-Ti Cu	-V Cr Zn Sr			
Cu		-Ti Ni Zn	Cr Ba	-V Sr		Mn
Zn		Cu	Ni	Cr Mn Ba	-Ti Sr	-V
Pb						
Sr			Ni	Cu Ba	Zn	Cr
Zr						
U						
Ba	Ni	-Ti	-V Cu	Cr Zn Sr		

TABLE 3 Correlation matrix for total soil data : n=334
(log transformed data)

DRILLING

Lithology and geochemistry

Five boreholes were drilled (Figures 3 and 14) to investigate the sources of magnetic anomalies, with one borehole (BH4) being extended to 97.7m for heat flow measurements. None of the holes intersected manganese ore although several occurrences of ironstone were noted. Detailed lithological logs of the boreholes are given in Appendices 3 - 7 and geochemical logs showing the levels of Ca, Ti, V, Cr, Mn, Fe, Co, Ni, Cu, Zn, Pb, Rb, Sr, Zr, Ba and As are shown in Figures 20-25. The analytical data for all elements determined from the borehole core are given in Appendix 8 and summary statistics are shown below (Table 4). Samples for chemical analysis were taken at marked changes in lithology or at 1m intervals where no change was apparent. In continuous sections of the same rock type only representative samples were taken from the core.

	Total data set			BH1A	BH1B	BH3	BH4	BH5
	Min n=63	Max n=63	Mean n=63	Mean n=12	Mean n=12	Mean n=6	Mean n=24	Mean n=9
Ca	1300	76600	22000	9300	1500	38200	20000	41800
Ti	1400	24200	13900	15400	1600	10500	13000	13600
V	30	550	325	381	430	275	250	344
Cr	10	190	71	62	62	112	75	58
Mn	200	3400	1600	1700	1900	1500	1300	1500
Fe	30200	494000	161000	190000	214000	83700	128000	193000
Co	6	52	29	29	33	27	28	28
Ni	9	72	27	21	29	25	29	27
Cu	2	99	27	25	30	31	27	28
Zn	48	580	138	113	115	118	162	150
Pb	1	233	16	7	7	5	27	18
Rb	1	181	27	14	10	3	55	7
Sr	8	467	176	164	137	273	188	145
Zr	18	375	182	158	180	177	201	170
Ba	40	990	252	210	256	100	368	92
As	1	55	80	27	22	3	19	21

TABLE 4 Summary statistics for drill-core data (ppm)

BH1A and BH1B (Appendices 3 and 4) were drilled from the same collar position, with BH1A inclined at 60° and BH1B vertical (Figures 20 and 21). A geological section constructed from geological data from these holes is shown in Figure 22. The rocks recovered consisted of highly weathered and altered dolerite, brecciated in several sections, altered ironstone and chert. The ironstone band dipping towards the east contains up to 70.62% Fe_2O_3 but shows lower levels of Mn when compared to the dolerite. The ironstone band also shows higher levels of Ca, Cr, Ni, Pb, Ba and As and lower levels of Ti, Co, Cu, Sr and Zr when compared with the dolerite. A black chert band below the ironstone (Figure 22) is enriched in Cu, Pb and As. High magnetic susceptibility values (maximum 0.46 (SI)) were recorded for the ironstone and the chert band.

BH3 (Appendix 5), located on a magnetic anomaly at the north end of the Mynydd Rhiw ridge, was drilled to 30.6m. Purple, fine-grained, hornfels passed into medium-grained dolerite which is exposed to the west of the drill site dipping to the

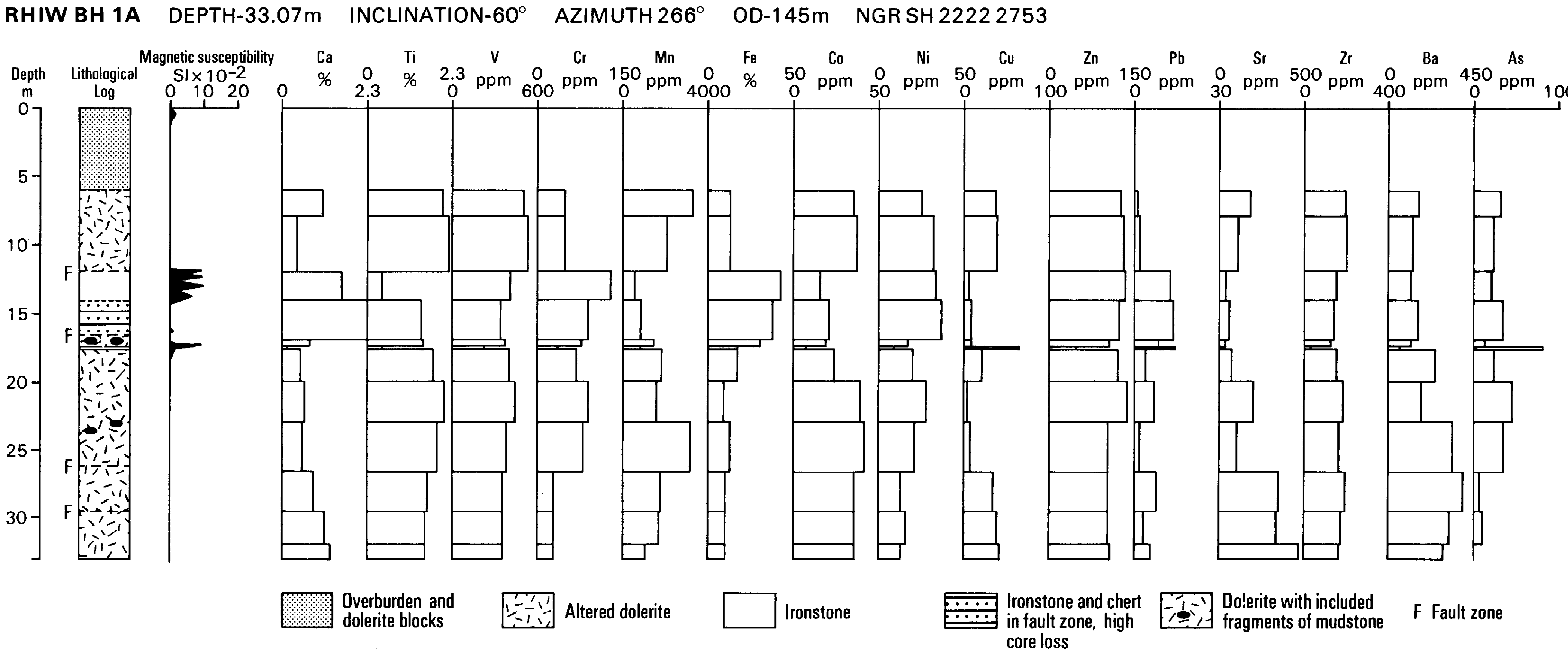

Figure 20 Graphical log of BH1A

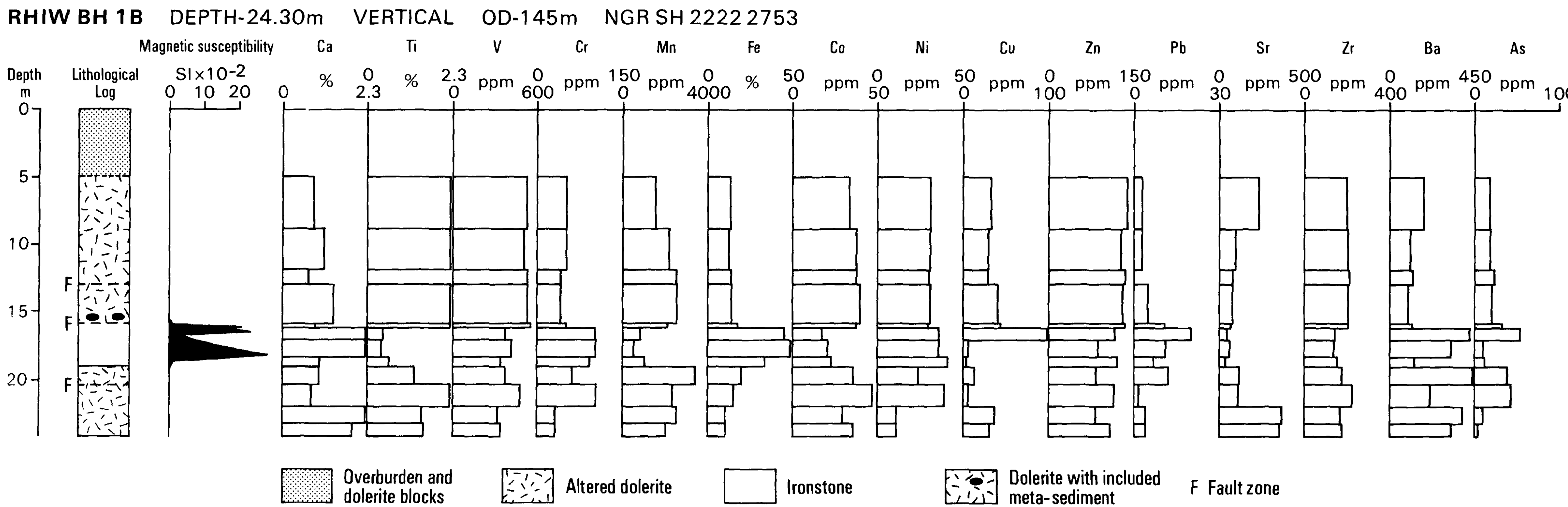

Figure 21 Graphical log of BH1B

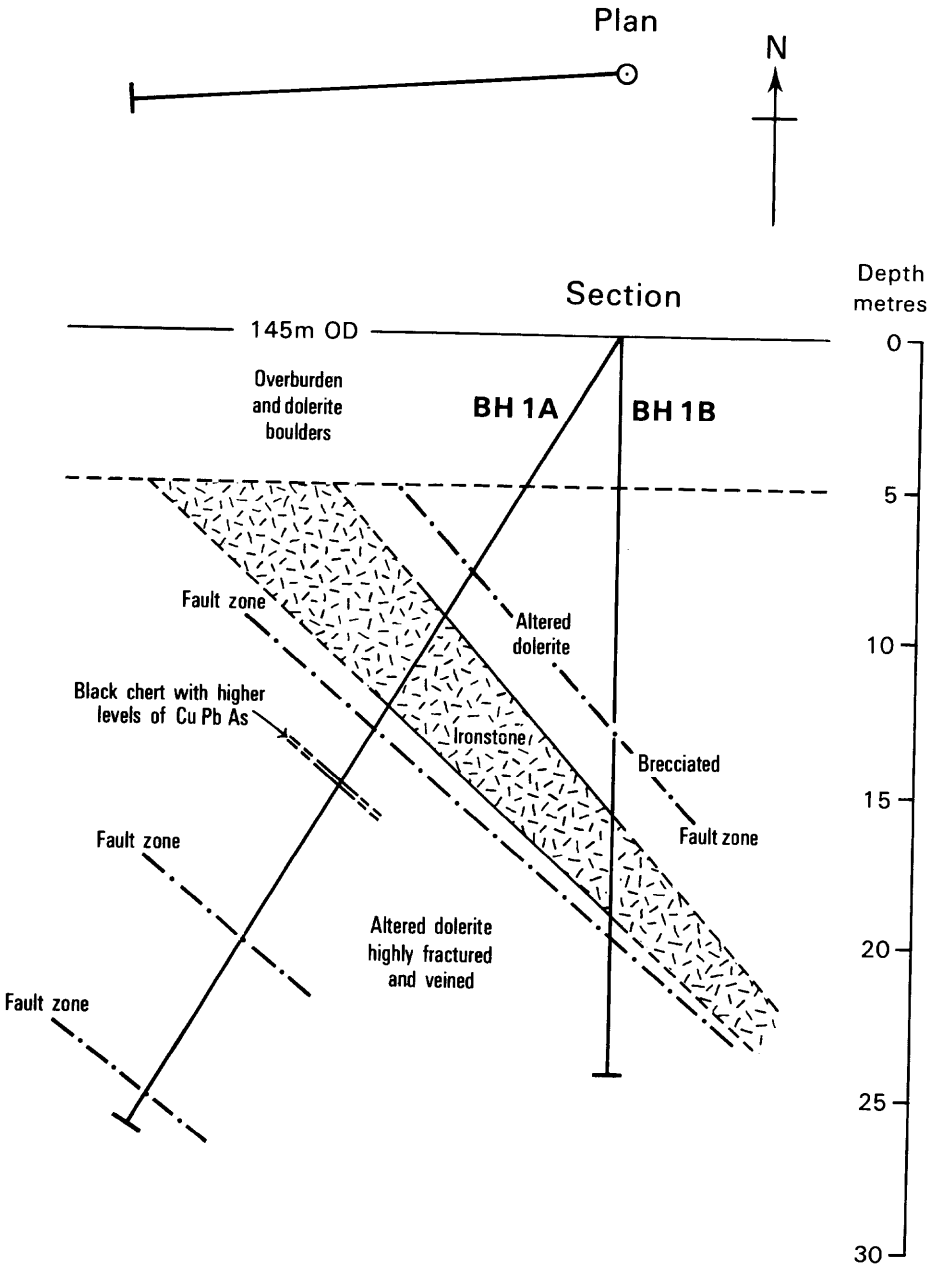

Figure 22 Plan and section of BH1A and BH1B

east. There is little significant chemical change down-hole (Figure 23) except in a fault zone at the sediment/dolerite contact, where higher levels of Ti, V, Ni, Mn, Fe and Co are apparent. The flinty hornfels is known to have been used for Neolithic stone implements from excavations of an axe factory near the drill site (Houlder, 1961). Magnetic susceptibility values for the core were low (less than 0.01 (SI)) and no explanation can be given for the magnetic anomaly either from the lithology or the chemistry of the drill core.

BH4 (Appendix 6), located north-west of the radio mast on Mynydd Rhiw, was sited on a coincident magnetic and geochemical anomaly. The borehole was extended on behalf of the BGS Geothermal Programme to reach a depth suitable for the long-term observation of bottom-hole temperature. An ironstone band occurs near surface some 5m thick, highly broken and weathered, and with a high magnetic susceptibility (maximun 0.18 (SI)). This ironstone contains up to 70% Fe_2O_3 (Figure 24) and also shows higher levels of Ca, V, Cr and Pb when compared with the underlying mudstones. The weathered mudstones pass into 43m of basalt dipping at 15° to the east (41m true thickness). Below the basalt a mudstone/siltstone sequence was encountered containing another thin basalt flow (Figure 24).

BH5 (Appendix 7) was positioned up-slope of BH4 to gain a better intersection of the ironstone and was terminated at 17.6m once through the ground of interest (Figure 25). The hole commenced in altered vesicular basalt and then passed into a fault zone giving poor recovery of a vesicular cherty rock which becomes more iron-rich with depth (up to 47.32% Fe_2O_3). Higher levels of Zn and Pb occur within the fault zone and lower levels of Ca, Ti, V, Mn, Co, Cu, Sr Zr, Ba and As compared with the overlying basalts. The geological mapping (Figure 3) indicates that the ironstone encountered in BH4 and BH5 is stratigraphically above the manganese lithologies seen at the Nant and Benallt mines .

Geophysical borehole logging

A full suite of geophysical logs were run in the deepest of the five boreholes drilled (BH4), for the purposes of the British Geological Survey's Geothermal Programme, for whom this borehole had been deepened. The log data are not directly relevant to the exploration for manganese reported here, and are therefore not illustrated in this report. Penn (1987) has briefly described some of the log data in the context of Welsh stratigraphy. The data are available for inspection by arrangement with the Head, Regional Geophysics Research Group, British Geological Survey, Keyworth, and are also available in digital format. These log data have provided useful physical property information for a section of Lower Palaeozoic rocks for which log data from elsewhere in the UK are scarce or non-existent. The borehole logging was carried out by BPB Instruments Ltd. The logs run were : caliper; resistivity (focussed electric); SP; Single Point Resistance; natural gamma; density; dual-spaced neutron; and multi-channel sonic (Evans, 1986).

The remaning boreholes drilled to test the various magnetic anomalies described above were too shallow to justify full-suite logging. Water levels in these holes were too low for basic electrical logging to be worthwhile.

Element-specific methods in borehole logging are rare, but the use of neutron logging specifically for manganese has been reported by Fel'dman (1963); its scientific basis is the relatively large capture cross-section of manganese, which (in comparison with other rock-forming elements) makes it a neutron absorber. The unexpected results of the drilling (no intersection of manganese ore) precluded an opportunity to test this technique.

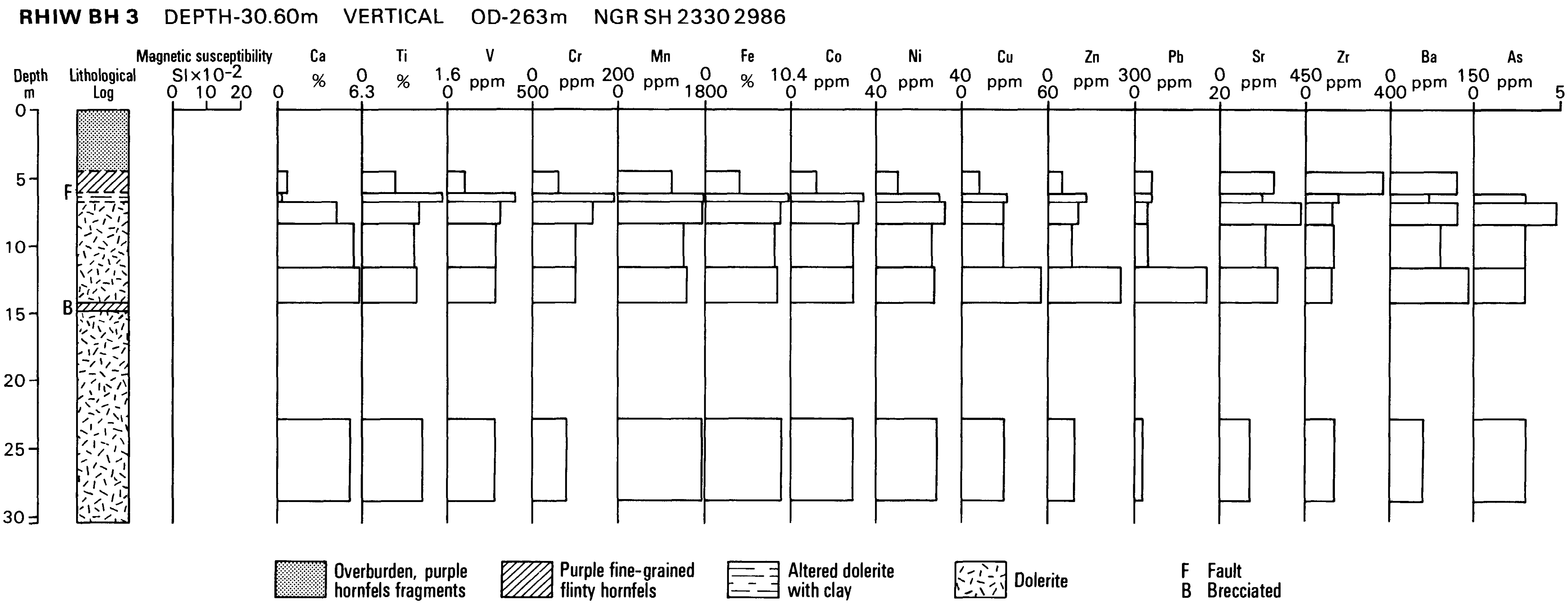

Figure 23 Graphical log of BH3

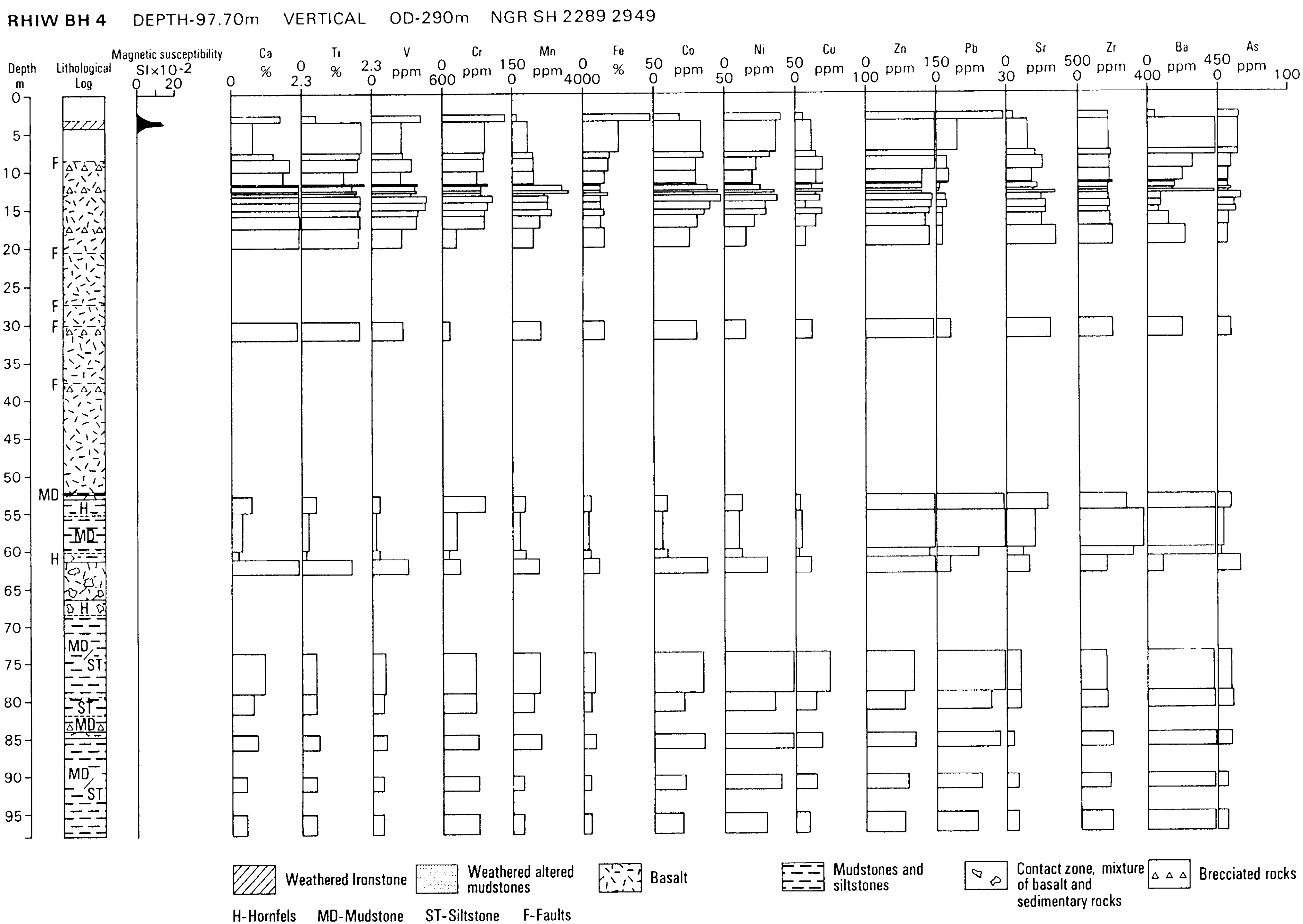

Figure 24 Graphical log of BH4

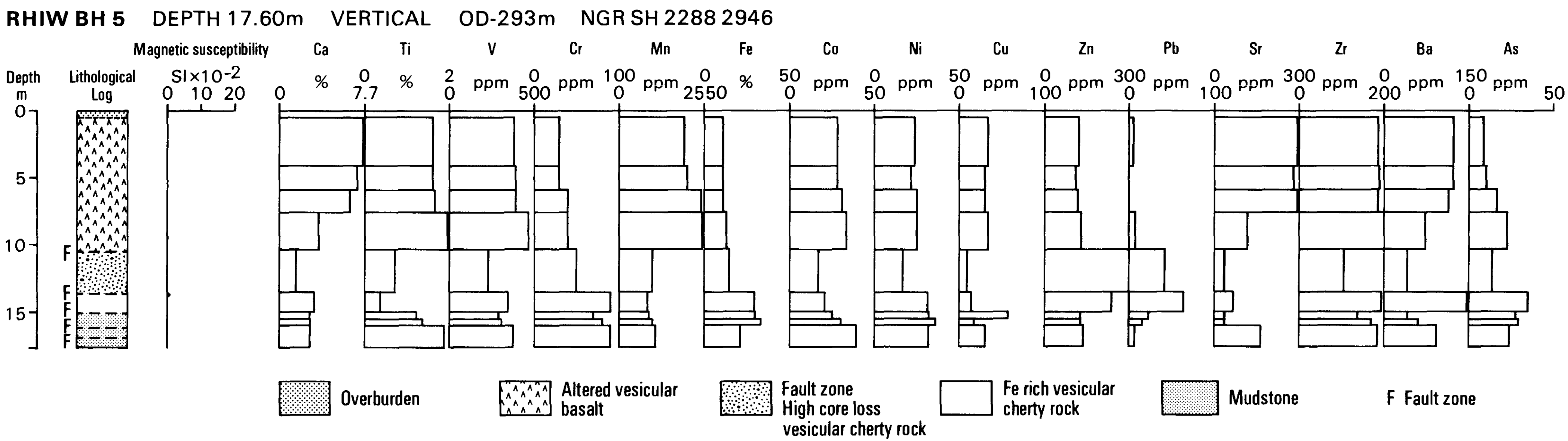

Figure 25 Graphical log of BH5

Discussion

The results of the drilling have shown the magnetic anomalies at two of the three drill sites to be caused by stratabound ironstones, occurring in both cases near surface (maximum depth 16m, BH1B). The ironstone lithologies intersected in the boreholes are approximately 4m thick both at Tyddyn Meirion and on Mynydd Rhiw. If these ironstone bands form distinct beds within the succession then the limited extent of the magnetic anomalies may be due to a variable magnetite content related to intensity of alteration. Another possibility is that the ironstones occur as lenses of limited lateral extent. Recent mapping (Figure 3) indicates that the ironstone intersected in BH4 and BH5 is stratigraphically above the manganese-bearing lithologies but that the ironstone intersected in BH1A and BH1B may be the lateral equivalent of the manganese mineralisation of Benallt, with iron replacing the manganese. The magnetic anomaly tested by BH3 on Mynydd Rhiw remains unexplained, whilst those in Nant y Gadwen are still considered likely to be due to manganese ore, because of their very close proximity to the Nant orebody.

The occurrence of the Ordovician ironstones in North Wales can be correlated with eustatic falls in the sea level; the ironstones appear at the transition from a regressive to a transgressive phase (Trythall and others, 1987). There is no obvious correlation between ironstone deposition and volcanic activity and it is more probable they were introduced by lateritic weathering of a low-lying land mass.

CONCLUSIONS

1. Magnetic anomalies indicative of ore between the Benallt and Nant mines have been located only in the immediate vicinity of the old workings. One of two anomalies close to Benallt was tested by drilling and shown to be due to ironstone. Anomalies *en echelon* with the Nant orebody could not easily be tested by drilling, but are thought most likely to be due to small manganese orebodies.

2. There is no evidence of any other substantial manganese orebody near to surface between the Benallt and Nant mines. This conclusion is made on the basis of the magnetic survey data (which show no significant anomalies in this part of the survey area), coupled with the magnetic susceptibility data for the manganese-bearing rocks, which show that ore-grade material is generally strongly magnetic, with lower-grade material very much less so. The sub-economic mineralisation proved by drilling in 1942 clearly does not develop laterally to ore grade.

3. North of Benallt there is again no evidence of any substantial manganese orebody, though some strong short-wavelength magnetic anomalies are present. Drilling the two most prominent of these has shown one to be due to ironstone, the other remaining unexplained.

4. There is little possibility of there being prospective ground outwith the area covered by the magnetic survey, since the Footwall Sill which bounds the ore-bearing sediments to the west has now, from the magnetic survey data, been clearly mapped between its coastal and inland exposures.

5. Strongly magnetic stratabound ironstones with a maximum dimension of only a few tens of metres have thus been proved at two localities, though it is clear from the magnetic data that over the 4km strike length of ground surveyed such ironstone bodies are certainly not common. The example south of Benallt appears to be a lateral equivalent of the Benallt ore. The ironstone on Mynydd Rhiw appears to be stratigraphically above the ore-bearing mudstones.

The ironstones contain up to ~70% Fe_2O_3, but low levels of manganese compared to adjacent rocks. They are altered and fractured and are as strongly magnetic as the manganese ores of Benallt and Nant.

6. Data from the soil sampling programme were of limited use, particularly in the southern area, near to the coast, due to the variable thickness of drift deposits and more recent blown sand. Only five elements showed readily interpreted patterns but these are not directly related to mineralisation. In areas of relatively thin drift cover the sub-crop of the basic igneous rocks on Mynydd Rhiw is detected by enhanced levels of Ti and V. At Tyddyn Meirion (BH1A and BH1B) high levels of Cr, Mn and Zr in soil are coincident with a strong magnetic anomaly, although the ironstone intersected is depleted in Mn.

7. The possibility remains that the manganese ore at the Benallt and Nant mines persists with depth. However, because of the relatively small dimensions of the typical orebodies, coupled with the steep dip of the host sediments, detailed magnetic surveys over the old workings would be unlikely to prove either the presence or absence of any down-dip extensions. Short-wavelength anomalies due to remanent ore would present difficulties for data interpretation in these areas.

ACKNOWLEDGEMENTS

The British Geological Survey is indebted to land owners within the area for allowing access for geochemical sampling, geophysical surveying, and drilling operations. Particular thanks for assistance go to Mr H Jones of Penarfynydd Farm, Mr W G Williams of Craig Ewig, Mrs M Evans of Nant, and Major J R Harden of Nanhoron Hall. The assistance of Mr G Roberts of the National Trust and Mr R B White of the Gwynedd Archaeological Trust is also acknowledged. The authors would like to thank Mr J D Burnell, Consultant Land Agent, for arranging access for drilling and dealing with planning applications.

The magnetic survey was carried out by Steven Barrie, Chris Marsden, Ray Macklin and Jackie Vigurs. The magnetic survey data were converted to digital format by Work Experience students from two Nottingham schools. The analysis of the geochemical samples was undertaken by members of the BGS Mineral Resources and Applied Geochemistry Research Group in London, and the data processing and generation of computer maps undertaken by D G Cameron. The illustrations were prepared in the Drawing Office at BGS Keyworth under the supervision of R J Parnaby.

For helpful discussions, thanks are also due to J D Cornwell and D C Cooper of BGS, and Tim Young and Wes Gibbons of the University of Wales, College of Cardiff.

REFERENCES

Allen, P.M. 1982. Lower Palaeozoic volcanism in Wales, the Welsh Borderland, Avon, and Somerset. 65-91 *in* Igneous Rocks of the British Isles. Sutherland, D.S. (editor). (Chichester : John Wiley and Sons.)

Bateson, J.H., Evans, A.D. and Johnson, C.C. 1984. Investigation of magnetic anomalies and potentially mineralized structures in Whin Sill, Northumberland, England. Transactions of the Institution of Mining and Metallurgy (Section B : Applied Earth Science), Vol.93, B71-B77.

Beckinsale, R.D., Evans, J.A., Thorpe, R.S., Gibbons, W. and Harmon, R.S. 1984. Rb-Sr whole-rock isochron ages, $d^{18}O$ values and geochemical data for the Sarn Igneous Complex and the Parwyd gneisses of the Mona complex of Llŷn, N Wales. Journal of the Geological Society of London, Vol.141, 701-709.

Beckly, A.J. 1985. The Arenig Series in North Wales. Unpublished PhD thesis, Imperial College, University of London.

Beckly, A.J. 1987. Basin development in North Wales during the Arenig. 19-30 *in* Sedimentation and tectonics of the Welsh basin. Fitches, W.R and Woodcock, N.H. (editors). (Geological Journal, Vol.22, Spring Thematic Issue). (Chichester : John Wiley and Sons.)

Beckly, A.J. 1988. The stratigraphy of the Arenig Series in the Aberdaron to Sarn area, western Llŷn, North Wales. Geological Journal, Vol.23, 321-337.

Bennett, M.A. 1987. Genesis and diagenesis of the Cambrian manganese deposits, Harlech, North Wales. 7-18 *in* Sedimentation and tectonics of the Welsh Basin. Fitches, W.R. and Woodcock, N.H. (editors). (Geological Journal, Vol.22, Spring Thematic Issue). (Chichester : John Wiley and Sons.)

Bhimasankaram, V.L.S. and Rao, B.S.R. 1958. Manganese ore of south India and its magnetic properties. Geophysical Prospecting, Vol.6, 11-24.

Campbell Smith, W., Bannister, M.A. and Hey, M.H. 1946. Pennantite, a new manganese-rich chlorite from Benallt mine, Rhiw, Carnarvonshire. Mineralogical Magazine, Vol.27, 217-220.

Cattermole, P.J. 1969. A preliminary geochemical study of the Mynydd Penarfynydd intrusion, Rhiw Igneous Complex, south-west Lleyn. 435-446 *in* Precambrian and Lower Palaeozoic rocks of Wales. Wood, A. (editor). (Cardiff : University of Wales Press.)

Cattermole, P.J. 1976. The crystallisation and differentiation of a layered intrusion of hydrated alkali olivine-basalt parentage at Rhiw, North Wales. Geological Journal, Vol.11, 45-70.

Cattermole, P.J. and Romano, M. 1981. Lleyn Peninsula. Geologists' Association Guide, No.39. (London : The Geologists' Association.)

Cornwell, J.D. 1979. Geophysical investigations of some mineral deposits in North Wales. Applied Geophysics Unit Report, Institute of Geological Sciences, No.146.

Cornwell, J.D. and Evans, A.D. 1989. Magnetic properties of manganese ores from the Rhiw area, western Llŷn, North Wales. Project Note, Regional Geophysics Research Group, British Geological Survey, No.89/7.

Crimes, T.P. 1970. A facies analysis of the Arenig of western Lleyn, North Wales. Proceedings of the Geologists' Association, Vol.81, 221-239.

De Villiers, J.E. 1945. Some minerals occurring in South African manganese deposits. Transactions of the Geological Society of South Africa, Vol.48, 17-25.

Deb, S. 1939. Données nouvelles sur les propriétés physiques des constituants minéralogiques de la vredenburgite des Indes. Comptes Rendus de l'Académie des Sciences, Vol.209, 518-520.

Deb, S. 1943. Optical, X-ray and magnetic studies of the mineralogical constituents of vredenburgite from different occurrences in India. Quarterly Journal of the Geological, Mining and Metallurgical Society of India, Vol.15, 137-141.

Dewey, H. and Dines, H.G. 1923. Tungsten and manganese ores. Memoir of the Geological Survey - Special reports on the mineral resources of Great Britain, Vol.1 (3rd edition).

Down, C.G. 1980. The manganese mines of North Wales. British Mining (Monograph of the Northern Mine Research Society), No.14.

Essene, E.J. and Peacor, D.R. 1983. Crystal chemistry and petrology of coexisting galaxite and jacobsite and other spinel solutions and solvi. American Mineralogist, Vol.68, 449-455.

Evans, A.D. 1986. Geophysical logging of the Rhiw (Mynydd Rhiw No.4) borehole, Lleyn Peninsula, North Wales. Project Note, Regional Geophysics Research Group, British Geological Survey, No.86/3.

Evans, R.B. and Chacksfield, B.C. 1987. Magnetic anomalies in Snowdonia, North Wales, and their relationship to magnetite-rich sediments. Report of the Regional Geophysics Research Group, British Geological Survey, No.87/20.

Fel'dman, I.I. 1963. The discovery of manganese beds by neutron methods of examining boreholes. 44-46 *in* Industrial and exploratory geophysical prospecting. Zhigach, K.F. (editor). (New York : Consultants Bureau.) [Authorised translation from the Russian.]

Fermor, L.L. 1908. Three new manganese-bearing minerals - vredenburgite, sitaparite and juddite. Records of the Geological Survey of India, Vol.37, 137-141.

Fermor, L.L. 1909. Manganese ore deposits of India. Memoir of the Geological Survey of India, Vol.37.

Fortey, R.A. and Owens, R.M. 1978. Early Ordovician (Arenig) stratigraphy and faunas of the Carmarthen district, south-west Wales. Bulletin of the British Museum (Natural History), Geology, Vol.30, 225-294.

Fortey, R.A. and Owens, R.M. 1987. The Arenig Series in South Wales - stratigraphy and palaeontology. Bulletin of the British Museum (Natural History), Geology, Vol.41, 69-307.

Frenzel, G. 1980. The manganese ore minerals. 25-157 *in* Geology and geochemistry of manganese. Varentsov, I.M. and Grasselly, G. (editors). Proceedings of the 2nd International Symposium on the Geology and Geochemistry of Manganese, Sydney, 1976. (Stuttgart : E.S.V.)

Gibbons, W. 1980. The geology of the Mona Complex of the Lleyn Peninsula and Bardsey Island, North Wales. Unpublished Ph.D. thesis, Portsmouth Polytechnic.

Gibbons, W. 1983. The Monian 'Penmynydd Zone of Metamorphism' in Llŷn, North Wales. Geological Journal, Vol.18, 21-41.

Gibbons, W. and McCarroll, D. *In preparation.* Bardsey Island. Memoir of the British Geological Survey, Sheet 133 (England and Wales).

Groves, A.W. 1938. Manganese (2nd edition). (Reports of the mineral industry of the British Empire and foreign countries). (London : The Imperial Institute.)

Groves, A.W. 1947. Results of magnetometric survey at Benallt manganese mine, Rhiw, Caernarvonshire. Bulletin of the Institution of Mining and Metallurgy, No.484, 1-24; No.486, 37-47; No.490, 29-32.

Groves, A.W. 1952. Wartime investigations into the haematite and manganese ore resources of Great Britain and Northern Ireland. Ministry of Supply, Permanent Records of Research and Development, Monograph No.20-703.

Halse, E. 1892. Notes on the occurrence of manganese ore near the Arenigs, Merionethshire. Transactions of the Federated Institution of Mining Engineers, Vol.3, 940-952.

Harker, A. 1888. The eruptive rocks in the neighbourhood of Sarn, Caernarvonshire. Quarterly Journal of the Geological Society of London, Vol.44, 442-462.

Hawkins, T.R.W. 1983. Structure of the Ordovician succession around Aberdaron, south-west Llŷn, North Wales. Geological Journal, Vol.18, 169-181.

Houlder, C.H. 1961. The excavation of a Neolithic stone implement factory on Mynydd Rhiw in Caernarvonshire. The Prehistoric Society, No.5, 108-143.

Le Bas, M.J. 1982. The Caledonian granites and diorites of England and Wales. 191-201 *in* Igneous Rocks of the British Isles. Sutherland, D.S. (editor). (Chichester : John Wiley and Sons.)

Machamer, J.F. 1987. A working classification of manganese deposits. Mining Magazine, Vol.157, 348-351.

Mason, B. 1943. Mineralogical aspects of the system FeO-Fe_2O_3-MnO-Mn_2O_3. Geologiska Foreningens i Stockholm Fornhandlingar, Vol.65, 97-180.

Matley, C.A. 1932. The geology of the country around Mynydd Rhiw and Sarn, south-western Lleyn, Carnarvonshire. Quarterly Journal of the Geological Society of London, Vol.88, 238-273.

Nancarrow, P.H.A. 1987. Manganese minerals from Mynydd Rhiw, North Wales. Mineralogy and Petrology Report, British Geological Survey, No.87/6.

Penn, I.E. 1987. Geophysical logs in the stratigraphy of Wales and adjacent offshore and onshore areas. Proceedings of the Geologists' Association, Vol.98, 275-314.

Povarennykh, A.S. 1964. On the magnetic properties of minerals. 451-463 *in* Aspects of theoretical mineralogy in the USSR. Battey, M.H. and Tomkeieff, S.I. (editors). (Oxford : Pergamon.)

Ramsay, A.C. 1866. The Geology of North Wales. Memoir of the Geological Survey of Great Britain.

Ramsay, A.C. 1881. The Geology of North Wales. Memoir of the Geological Survey of Great Britain (2nd edition).

Roy, S. 1981. Manganese deposits. (London : Academic Press.)

Sedgwick, A. 1843. Outline of geological structure of North Wales. Proceedings of the Geological Society of London, Vol.4, 212-268.

Sedgwick, A. 1852. On the classification and nomenclature of the Lower Palaeozoic rocks of England and Wales. Quarterly Journal of the Geological Society of London, Vol.8, 136-168.

Shackleton, R.M. 1956. Notes on the structure and relations of the Pre-Cambrian and Ordovician rocks of south-western Lleyn (Caernarvonshire). Liverpool and Manchester Geological Journal, Vol.1, 400-409.

Sharpe, D. 1846. Contributions to the geology of North Wales. Quarterly Journal of the Geological Society of London, Vol.2, 283-316.

Shaw, H. 1936. Applied geophysics : A brief summary of the development of apparatus and methods employed in the investigation of subterranean structural conditions and the location of mineral deposits (3rd edition). (London : HMSO, for the Science Museum.)

Trythall, C.E., Molyneux, S.G. and Taylor, W.E.G. 1987. Age and controls of ironstone deposition (Ordovician), North Wales. 31-43 *in* Sedimentation and tectonics of the Welsh Basin. Fitches, W.R. and Woodcock, N.H. (editors). (Geological Journal, Vol.22, Spring Thematic Issue). (Chichester : John Wiley and Sons.)

Woodland, A.W. 1939. The petrography and petrology of the manganese ore of the Rhiw district (Carnarvonshire). Proceedings of the Geologists' Association, Vol.50, 205-222.

Woodland, A.W. 1956. The manganese deposits of Great Britain. 197-218 *in* Symposium sobre yacimientos de manganeso, Vol.5. Reyna, J.G. (editor). 20th Session of the International Geological Congress, Mexico, 1956.

APPENDIX 1

ROCK SAMPLES RHIW

Sample No	NGR	Rock Description	
RPR 501	SH 2159 2670	Dolerite	A
RPR 502	SH 2157 2683	Mudstone	A
RPR 503	SH 2167 2699	Basalt and Chert	A
RPR 504	SH 2116 2664	Mudstone	A
RPR 505	SH 2112 2660	Basic tuff and mudstone	A
RPR 506	SH 2106 2660	Manganese Ore	
RPR 507	SH 2114 2669	Mudstone; manganese rich	A
RPR 508	SH 2223 2802	Manganese Ore	
RPR 509	SH 2121 2682	Mudstone; manganese rich	A
RPR 510	SH 2098 2647	Tuff; manganese rich with pyrite	
RPR 511	SH 2216 2802	Mudstone with siliceous bands	A
RPR 512	SH 2219 2813	Mudstone; cherty with pyrite	A
RPR 513	SH 2219 2829	Mudstone and tuff abundant pyrite	A
RPR 514	SH 2227 2828	Basalt with fine disseminated pyrite	A
RPR 515	SH 2228 2829	Basalt; chert with fine dissem. pyrite	A
RPR 516	SH 2230 2831	Dolerite?	A
RPR 517	SH 2234 2833	Dolerite?	
RPR 518	SH 2238 2849	Basalt and chert	
RPR 519	SH 2262 2855	Dolerite? with disseminated fine pyrite	A
RPR 520	SH 2242 2884	Dolerite; coarse	
RPR 521	SH 2217 2826	Mudstone	A
RPR 522	SH 2217 2827	Mudstone/tuff manganese rich	
RPR 523	SH 2219 2825	Mudstone; cherty	
RPR 524	SH 2222 2814	Mudstone; cherty	
RPR 525	SH 2228 2809	Dolerite? abundant fine pyrite	
RPR 526	SH 2184 2664	Dolertite; coarse	A
RPR 527	SH 2189 2664	Mudstone/shale	A
RPR 528	SH 2088 2636	Dolerite; abundant fine pyrite	
RPR 529	SH 2114 2625	Dolerite some disseminated pyrite	
RPR 530	SH 2114 2662	Dolerite? some disseminated pyrite	
RPR 531	SH 2077 2649	Sandstone	A
RPR 532	SH 2062 2646	Dolerite	
RPR 533	SH 2119 2626	Mudstone (hornfelsed)	A
RPR 534	SH 2094 2634	Manganese Ore (highly magnetic)	A
RPR 535	SH 2219 2763	Mudstone; cherty	A
RPR 536	SH 2266 2912	Basalt (pillow structures) and chert	
RPR 537	SH 2255 2936	Dolerite; coarse	
RPR 538	SH 2272 2919	Dolerite? some disseminated pyrite	
RPR 539	SH 2275 2867	Basalt; vesicular	
RPR 540	SH 2260 2883	Basalt	
RPR 541	SH 2243 2682	Dolerite; coarse	

A - Samples analysed

Appendix 2 : Rhiw Rock Data

Sample	Ca (ppm)	Ti (ppm)	V (ppm)	Cr (ppm)	Mn (ppm)	Fe (ppm)	Co (ppm)	Ni (ppm)	Cu (ppm)	Zn (ppm)	Pb (ppm)	Rb (ppm)	Sr (ppm)	Zr (ppm)	Mo (ppm)
RPR501	41600	1460	60	2180	1560	90900	101	952	40	64	2	3	110	15	3
RPR502	900	7590	120	110	310	53100	15	34	23	106	31	193	79	241	5
RPR503	40800	17860	400	80	1810	119100	36	34	27	128	0	23	268	174	2
RPR504	900	6780	110	100	5720	62400	46	54	27	119	20	179	41	208	1
RPR505	3400	6830	190	70	1310	86800	16	25	5	72	5	52	51	145	3
RPR507	2300	5950	130	80	22030	90900	69	62	39	146	28	151	66	166	3
RPR509	1800	4650	110	50	16000	116100	54	93	34	115	37	95	171	125	18
RPR511	1100	5380	140	60	14410	81300	76	116	63	106	8	142	57	161	19
RPR512	6600	3580	150	30	16630	187700	40	136	22	91	81	45	205	145	7
RPR513	3200	4890	190	60	14070	193600	138	331	12	180	23	35	29	203	9
RPR514	48900	17180	330	10	1970	110000	26	12	13	106	1	6	198	250	1
RPR515	44800	15840	320	20	1630	114500	25	13	10	103	36	20	204	235	0
RPR516	60100	16360	240	10	2090	116000	22	10	9	121	1	7	305	178	2
RPR519	74500	16400	370	30	2140	105700	27	21	28	105	4	1	144	178	0
RPR521	700	6730	110	90	840	51400	2	20	20	43	36	184	48	194	2
RPR526	36300	2630	110	2860	1710	102300	100	903	72	84	2	2	70	23	1
RPR527	800	7630	120	100	270	28400	2	7	15	24	16	170	126	264	3
RPR531	6100	5420	110	60	860	93600	19	21	9	57	4	63	117	209	2
RPR533	4100	7880	120	100	1490	44800	17	43	2	23	4	130	103	262	4
RPR534	80500	2450	100	0	21160	166800	83	422	55	229	99	33	1459	113	6
RPR535	600	6470	110	80	4970	54400	50	41	27	153	29	170	33	200	2

All Analysis by X-Ray Fluorescence

Appendix 2 : Rhiw Rock Data

Sample	U (ppm)	Ba (ppm)	As (ppm)
RPR501	0	30	1
RPR502	4	600	12
RPR503	1	510	5
RPR504	4	1240	34
RPR505	2	500	28
RPR507	3	1870	39
RPR509	2	700	62
RPR511	3	4970	22
RPR512	2	14000	21
RPR513	3	610	13
RPR514	0	320	3
RPR515	1	610	4
RPR516	1	180	1
RPR519	0	30	4
RPR521	2	2230	22
RPR526	0	20	1
RPR527	4	660	1
RPR531	1	850	1
RPR533	2	950	4
RPR534	2	43000	130
RPR535	3	3170	46

All Analysis by X-Ray Fluorescence

APPENDIX 3

RHIW BH1A TYDDYN MEIRION

NGR SH 2222 2753 DEPTH - 33.07m
Inclination - 60° Azimuth - 266° OD - 145m
Date of sinking - 3 October 1985 Rig - EDECO STRATADRILL

Sample Nos	Lithology	Thickness m	Depth m
	Overburden. Quartz pebbles; dolerite blocks; dolerite fragments.	6.00	6.00
	Dolerite/basalt? highly broken; vesicular; weathered.	1.30	7.30
RPD 801	Dolerite; vesicular; light grey; weathered areas dark brown; hornblende calcite and abundant pyrite.	0.60	7.90
	Dolerite; altered fine-grained with high Fe content.	0.73	8.63
	Highly broken altered; secondary Fe and Mn on fractures.	2.07	10.70
	Highly altered, less broken, Mn on fractures.	0.30	11.00
RPD 802	Black ironstone some Mn, high specific gravity, some chert; high magnetic susceptability.	0.90	11.90
	Highly altered and broken ironstone with small pebbles of chert.	2.00	13.90
RPD 803	Less broken ironstone with some manganese, fractured.	0.10	14.00
	Contact of brown/orange cherty rock with fine-grained altered grey/black dolerite.	0.20	14.20
	High core loss; fault zone?	2.56	16.76
RPD 804	Dolerite; altered, highly disturbed with included small blocks of mudstone.	0.14	16.90
RPD 805	Highly broken; distinct Fe staining; (magnetic susceptibility highly variable).	0.50	17.40
RPD 806	Dolerite; altered; black chert high Fe/Mn content; high magnetic susceptability.	0.10	17.50
RPD 807	Dolerite; altered; shattered; abundant secondary Fe/Mn (very poor recovery).	2.40	19.90
RPD 808	As above but more Fe rich; very poor recovery.	3.00	22.90
	Highly altered; abundant secondary Fe/Mn.	0.30	23.20
	Dolerite with included shale fragements; secondary Fe/Mn on fracture planes.	0.55	23.75
	Fault zone; shattered dolerite		

RPD 809	Fe stained.	2.75	26.50
RPD 810	Dolerite; dark grey medium-grained and some fine-grained dolerite; less altered than previous core.	3.00	29.50
RPD 811	Dolerite; medium-grained with fractures parallel to core with abundant Mn/Fe on fracture planes; possible fault zone at 29.50m.	2.40	31.90
RPD 812	Dolerite; medium-grained less altered; Mn on joints.	1.17	33.07

APPENDIX 4

RHIW BH1B TYDDYN MEIRION

NGR SH 2222 2753 DEPTH - 24.30m
Inclination - vertical OD - 145m
Date of sinking - 16 September 1985 Rig - EDECO STRATADRILL

Sample Nos	Lithology	Thickness m	Depth m
	Overburden.	4.60	4.60
	Boulder - quartz rich dolerite.	0.37	4.97
RPD 813	Dolerite; altered; broken brown/orange; vesicular in part; secondary Fe/Mn.	3.93	8.90
	Dolerite; less altered fine-grained with some brecciated sections.	2.13	11.03
RPD 814	Dolerite; soft orange/brown altered; Fe/Mn on fractures.	0.87	11.90
RPD 815	Highly broken; possible fault zone.	1.10	13.00
	Dolerite; altered.	0.70	13.70
RPD 816	Dolerite; brecciated at 14.2m with included meta-sediment.	2.20	15.90
RPD 817	Contact with black/brown ironstone in possible fault zone; high magnetic susceptibility.	0.90	16.19
RPD 818	Solid black Fe/Mn ore; pyrite abundant in some sections; highly magnetic.	0.91	17.10
RPD 819	Black ironstone with some Mn; possible pisolithic structure?	1.30	18.40
RPD 820	Black non-magnetic rock; Fe staining becoming more grey in colour at contact with dolerite.	0.60	19.00
	Dolerite; brown/black altered.	0.30	19.30
RPD 821	Possible fault zone; highly shattered; brecciated; clay matrix.	1.10	20.40
	Dolerite? highly disturbed; clay rich; possible fault zone.	0.20	20.60
RPD 822	Less Fe rich dolerite.	1.46	22.06
RPD 823	Dolerite? Fe rich; abundant fine veining throughout.	1.28	23.34
	Dolerite? highly broken with secondary Fe/Mn.	0.71	24.05
RPD 824	Dolerite? less broken with quartz.	0.25	24.30

APPENDIX 5

RHIW BH3 MYNYDD RHIW

NGR SH 2330 2986 — Depth - 30.60m
Inclination - vertical — OD - 263m
Date of sinking - 23 September 1985 — Rig - EDECO STRATADRILL

Sample Nos	Lithology	Thickness m	Depth m
	Overburden. Fragments of vesicular dolerite and blocks of flinty purple hornfels within boulder clay.	4.60	4.60
	Boulder clay in fractures in bedrock surface.	0.10	4.70
	Purple fine-grained flinty hornfels; vertical fractures with sericite, chlorite and calcite on fracture planes.	1.00	5.70
RPD 825	Broken flinty rock near contact with dolerite; quartz veins.	0.50	6.20
	Soft altered clay rich doleritic material in fault zone at contact.	0.17	6.37
RPD 826	Dolerite; buff coloured; altered; vesicular; infilled with soft clay; hornblende crystals of varying size; secondary Fe/Mn on fracture planes.	0.47	6.84
	Dolerite; vesicular less altered; infilled with soft white mineral.	0.57	7.41
RPD 827	Dolerite; less vesicular; medium-grained; high quartz; hornblende crystals of varying size and abundant blebs of pyrite; some vesicles infilled with secondary Fe/Mn and chlorite.	1.09	8.50
RPD 828	Dolerite; rapid change to more porphyritic texture; non-vesicular; more hornblende.	5.79	14.29
	Contact with brecciated fine-grained purple hornfels; interbedded with dolerite.	0.41	14.70
	Dolerite; medium-grained; quartz rich.	2.30	17.00
	Dolerite; medium-grained.	1.95	18.95
RPD 829	Dolerite; fine-grained.	0.10	19.05
	Dolerite; medium-grained.	0.18	19.23
	Dolerite; fine-grained.	0.02	19.25
	Dolerite; medium-grained.	0.18	19.43
	Dolerite; fine-grained.	0.09	19.52
	Dolerite; medium-grained.	1.82	21.34
	Dolerite; fine-grained; vesicular with soft white sericite on fractures.	0.44	21.78
RPD 830	Dolerite; medium-grained some blebs of pyrite throughout; vesicular close to fractures; Mn/Fe on fracture planes.	7.02	28.80
	Dolerite; medium-grained.	1.80	30.60

APPENDIX 6

RHIW BH4 MYNYDD RHIW

NGR SH 2289 2949 — Depth - 97.70m
Inclination - vertical — OD - 290m
Date of sinking - 8 October 1985 — Rig EDECO STATADRILL

Sample Nos	Lithology	Thickness m	Depth m
	Overburden; dolerite debris.	3.00	3.00
RPD 831	Ironstone with some manganese; broken rusty brown sediment with possible ooliths; very high magnetic susceptability.	1.00	4.00
RPD 832	As above but highly broken.	4.00	8.00
RPD 833	Fine-grained mudstone light grey; Fe/Mn on fracture planes; brecciated and possible fault at 8.30m; thin quartz veins.	0.80	8.80
RPD 834	Basalt? light grey; fractures vertical.	1.60	10.40
RPD 835	Basalt; brecciated; vesicular in part with Fe/Mn in cavities.	1.70	12.10
RPD 836	Basalt; fine-grained with blebs of small white mineral - albite?	0.20	12.30
RPD 837	Basalt; fine-grained.	0.70	13.00
RPD 838	Basalt; highly vesicular and altered.	0.36	13.36
RPD 839	Breccia; fine grain matrix of basalt with fine quartz veins.	0.44	13.80
	Basalt; fine-grained highly altered.	0.20	14.00
RPD 840	Basalt; less altered; fractured.	0.50	14.50
RPD 841	Basalt; fine-grained vesicular; fractures vertical.	1.00	15.50
RPD 842	Basalt; highly broken fine-grained.	0.80	16.30
	Contact of 2 basalt flows; brecciated with country rock included at 16.76m; large fractures infilled with clay, Fe or quartz.	1.40	17.70
RPD 843	Basalt; highly broken; vesicular.	0.10	17.80
RPD 844	Basalt; dark grey fine-grained with small quartz veins; basalt more altered near fractures; large cavities with albite crystals; highly brecciated at 20.30m; cavity with clay and quartz at 20.50m.	2.70	20.50
	Basalt; fine-grained; brecciation associated with veining at 20.80m; good recovery.	1.60	22.10
	Basalt; altered broken; less broken from 22.70m with thin veins; brecciation within veins 22.90m - 23.40m; more broken from 24.40m.	2.70	24.80
	Basalt; dark grey with white albite? crystals; fractures infilled with quartz at 25.60m; basalt more altered adjacent to veining.	2.50	27.30

	Possible fault zone.	0.10	27.40
	Basalt; fine-grained; good recovery.	1.30	28.70
	Fault zone; clay, Fe and Mn.	0.70	29.40
	Basalt; fine-grained; veined.	0.30	29.70
	Brecciated; fractured	0.15	29.85
RPD 845	Basalt; grey fine-grained; good recovery; veined in some sections; distinct white albite? crystals.	2.55	32.40
	Basalt; dark grey; alternating fine-grained basalt with basalt containing albite phenocrysts; thin veins of soft white mineral common.	3.05	35.45
	Vein; quartz/sericite/feldspar?	0.10	35.55
	Basalt; fine-grained; possible fault at 37.40m; some veins brecciated. Contact of 2 basalt flows at 38.90m.	5.05	40.60
	Basalt; large crystals of albite.	0.40	41.00
	Basalt; altered and vuggy.	0.35	41.35
	Basalt; fine-grained; altered; some medium-grained basalt/dolerite with albite crystals; contact of 2 flows at 42.30m.	2.15	43.50
	Basalt; vesicular.	0.10	43.60
	Basalt; dark grey with thin veins of soft white/pink mineral.	4.00	47.60
	Basalt; broken; fractures vertical.	0.66	48.26
	Basalt; dark grey; veins.	2.34	50.60
	Basalt; vesicular altered.	0.15	50.75
	Basalt; drab grey altered.	0.91	51.66
	Basalt; ligh grey; fine-grained; abundant discontinuous thin veins.	0.34	52.00
	Thin band of mudstone.	0.06	52.06
	Basalt; fine-grained; altered; veined.	0.94	53.00
	Contact; hornfelsed mudstone; purple fine-grained.	0.37	53.37
	Banded highly disturbed meta-sediment; dark bands of mudstone and light bands of siltstone.	0.09	53.46
	Tuff?	0.08	53.54
	Mudstone; dark grey fine-grained; veined.	0.26	53.80
RPD 846	Mudstone; broken fractured; flinty/cherty in part; veins with secondary Fe vertical to core; some intercalated siltstones.	1.35	55.15
RPD 847	Change from banded mudstone to dark grey hard mudstone; fractured; secondary Fe/Mn on fractures; some banded sediments apparent at 57m; less disturbed from 57m; banding apparent; at 58.60m; veining more common; very hard cherty throughout.	5.05	60.20
	Contact; cherty hard sediment with included fragments of basalt.	0.15	60.35
	Transition to light grey cherty hard hornfels.	0.07	60.42

RPD 848	Hornfels; broken with thin quartz veins.	0.98	61.40
	Contact; basalt grey/green fine-grained abundant thin veins.	0.20	61.60
	Basalt; vesicular brecciated; veined quartz with included fragments of country rock.	0.76	62.36
	Basalt; brecciated; veined; cherty.	0.20	62.56
RPD 849	Fine-grained; light grey basalt forming matrix for breccia of mudstone fragments; cavities at 63.20m; highly broken; fractures vertical.	1.04	63.60
	Basalt; included country rock.	1.20	64.80
	Basalt; large cavities.	0.30	65.10
	Basalt; highly brecciated.	0.25	65.35
	Basalt; abundant white albite crystals.	0.55	65.90
	Transitional contact with country rock; disturbed; cherty; highly brecciated in part.	1.10	67.00
	Brecciated; basalt/mudstone.	2.50	69.50
	Mudstone dominant; fine-grained; some light grey siltstone.	4.10	73.60
	Breccia; included volcanic material with pyrite.	0.17	73.77
RPD 850	Mudstone dominant some siltstone with volcanic material; hornfelsed and cherty.	5.43	79.20
RPD 851	Siltstone; some fine-grained cherty sections; some mudstone.	2.40	81.60
	Mudstone; highly broken.	0.30	81.90
	Mudstone/siltstone.	0.70	82.60
	Mudstone; brecciated with quartz veins.	1.00	83.60
	Contact; grey/green vesicular basalt.	1.00	84.60
RPD 852	Contact; disturbed mudstone/siltstone sequence hornfelsed. some fine pyrite.	2.00	86.60
RPD 853	Mudstone/siltstone.	5.40	92.00
RPD 854	Mudstone/siltstone.	5.70	97.70

APPENDIX 7

RHIW BH5 MYNYDD RHIW

NGR SH 2288 2946 | Depth - 17.60m
Inclination - vertical | OD - 293m
Date of sinking - 5 November 1985 | Rig - EDECO STRATADRILL

Sample No	Lithology	Thickness m	Depth m
	Overburden.	0.50	0.50
RPD 861	Basalt; dark grey weathered; large white crystals (albite?) visible.	3.60	4.10
RPD 862	Basalt; fine-grained less weathered; good recovery.	1.90	6.00
RPD 863	Basalt; vesicular; broken; Fe stained from 7.60m.	1.60	7.60
RPD 864	Basalt; highly broken and Fe stained; secondary Fe/Mn on fractures; high core loss.	2.80	10.40
RPD 865	HIGH CORE LOSS; small fragments only recoverd; Fe rich cherty vesicular rock from possible fault zone.	3.20	13.60
RPD 866	Vesicular cherty rock; broken; some pieces have high specific gravity; Fe rich some Mn; conglomeritic in part.	0.90	14.50
RPD 867	Altered meta mustone dark grey; highly broken.	0.50	15.00
	Mudstone; disturbed brecciated country rock.	0.50	15.50
RPD 868	Fine-grained meta-mudstone dominant.	0.50	16.00
RPD 869	Fault at 16.00m; fine-grained meta-siltstone with black blebs (manganese?); fractures vertical filled with quartz; fault at 16.60m (highly broken); large cavity at 17.50m; secondary Fe/Mn on fractures.	1.60	17.60

Appendix 8: BH1A Rhiw Borehole Data

Sample	Top Depth	Bottom Depth	Ca (ppm)	Ti (ppm)	V (ppm)	Cr (ppm)	Mn (ppm)	Fe (ppm)	Co (ppm)	Ni (ppm)	Cu (ppm)	Zn (ppm)	Pb (ppm)	Rb (ppm)	Sr (ppm)	Zr (ppm)	Mo (ppm)	Th (ppm)	U (ppm)
RPD801	6.00	7.90	11100	20620	500	50	3330	134600	35	25	37	130	1	1	186	198	2	0	0
RPD802	7.90	11.90	3800	22610	530	50	2140	139000	37	32	38	134	2	0	115	202	2	1	0
RPD803	11.90	14.00	16000	4010	410	130	610	425700	16	33	5	136	13	9	45	156	3	13	5
RPD804	14.00	16.90	22600	14550	340	90	860	381900	21	36	8	126	14	5	58	148	0	4	1
RPD805	16.90	17.40	7600	15100	370	80	1540	309000	19	16	8	108	9	8	32	128	0	3	1
RPD806	17.40	17.50	1300	1980	150	20	840	172200	12	9	63	49	14	6	8	18	0	2	1
RPD807	17.50	19.90	4900	18000	400	70	1870	176900	24	19	21	122	4	20	70	155	2	1	2
RPD808	19.90	22.90	6100	20900	440	90	1600	97200	39	27	2	139	7	10	204	187	1	1	1
RPD809	22.90	26.50	5200	19140	380	80	3170	130700	41	20	6	104	2	32	102	166	1	2	0
RPD810	26.50	29.50	8300	16290	350	30	1800	104500	35	12	34	104	8	23	349	194	3	4	0
RPD811	29.50	31.90	11400	15630	350	30	1690	106900	35	15	38	102	3	32	333	175	2	3	2
RPD812	31.90	33.07	12900	15560	350	30	1040	104200	35	13	41	108	6	22	467	169	2	4	0

All Analysis by X-Ray Fluorescence

Appendix 8: BH1A Rhiw Borehole Data

Sample	Top Depth	Bottom Depth	Sb (ppm)	Ba (ppm)	As (ppm)
RPD801	6.00	7.90	1	160	33
RPD802	7.90	11.90	1	130	23
RPD803	11.90	14.00	0	120	21
RPD804	14.00	16.90	2	160	34
RPD805	16.90	17.40	3	120	12
RPD806	17.40	17.50	2	60	80
RPD807	17.50	19.90	1	250	23
RPD808	19.90	22.90	1	170	44
RPD809	22.90	26.50	0	340	34
RPD810	26.50	29.50	0	400	6
RPD811	29.50	31.90	1	320	9
RPD812	31.90	33.07	0	290	1

All Analysis by X-Ray Fluorescence

Appendix 8: BH1B Rhiw Borehole Data

Sample	Top Depth	Bottom Depth	Ca (ppm)	Ti (ppm)	V (ppm)	Cr (ppm)	Mn (ppm)	Fe (ppm)	Co (ppm)	Ni (ppm)	Cu (ppm)	Zn (ppm)	Pb (ppm)	Rb (ppm)	Sr (ppm)	Zr (ppm)	Mo (ppm)	Th (ppm)	U (ppm)
RPD813	4.97	8.90	8600	22500	520	50	1520	134200	34	31	32	138	3	1	233	197	2	0	1
RPD814	8.90	11.90	11400	22120	500	50	2180	127600	38	31	29	127	3	1	98	201	1	0	1
RPD815	11.90	13.00	7200	22860	520	40	2490	136300	38	30	28	134	0	4	79	205	0	2	0
RPD816	13.00	15.90	13800	22110	520	40	2550	139800	40	31	40	130	5	3	79	200	2	2	1
RPD817	15.90	16.19	8900	23130	550	50	2130	181400	38	29	42	134	11	4	70	203	0	2	0
RPD818	16.19	17.10	22200	3700	360	100	820	454900	18	36	99	116	20	3	44	137	2	12	3
RPD819	17.10	18.40	28400	3530	400	100	520	494000	21	36	4	86	11	4	61	132	4	10	4
RPD820	18.40	19.00	10000	5460	330	90	1010	338500	23	41	2	121	7	3	36	146	1	9	3
RPD821	19.00	20.40	9900	12250	360	60	3360	199600	36	24	12	83	12	45	116	172	1	7	3
RPD822	20.40	22.06	7700	24220	460	100	2300	153400	47	39	4	115	2	13	109	218	3	2	1
RPD823	22.06	23.34	33900	14190	310	30	2490	102700	30	11	36	83	4	31	364	167	3	3	0
RPD824	23.34	24.30	18700	14800	330	30	1970	104700	36	11	30	109	4	15	351	172	2	2	2

All Analysis by X-Ray Fluorescence

Appendix 8: BH1B Rhiw Borehole Data

Sample	Top Depth	Bottom Depth	Sb (ppm)	Ba (ppm)	As (ppm)
RPD813	4.97	8.90	1	180	17
RPD814	8.90	11.90	0	110	17
RPD815	11.90	13.00	0	120	22
RPD816	13.00	15.90	0	100	18
RPD817	15.90	16.19	0	120	31
RPD818	16.19	17.10	1	420	55
RPD819	17.10	18.40	2	320	8
RPD820	18.40	19.00	1	130	10
RPD821	19.00	20.40	0	660	36
RPD822	20.40	22.06	2	210	43
RPD823	22.06	23.34	1	380	8
RPD824	23.34	24.30	2	320	2

All Analysis by X-Ray Fluorescence

Appendix 8: BH3 Rhiw Borehole Data

Sample	Top Depth	Bottom Depth	Ca (ppm)	Ti (ppm)	V (ppm)	Cr (ppm)	Mn (ppm)	Fe (ppm)	Co (ppm)	Ni (ppm)	Cu (ppm)	Zn (ppm)	Pb (ppm)	Rb (ppm)	Sr (ppm)	Zr (ppm)	Mo (ppm)	Th (ppm)	U (ppm)
RPD825	4.60	6.20	7700	6230	100	60	1100	41700	12	10	12	48	4	4	288	370	2	9	0
RPD826	6.20	6.84	3700	15270	400	190	1780	104200	34	29	31	133	4	1	223	159	3	2	2
RPD827	6.84	8.50	43900	10610	310	140	1740	91600	32	32	29	105	3	3	428	132	2	1	1
RPD828	8.50	11.70	57400	9730	280	100	1360	85700	29	26	29	82	3	3	236	134	2	1	1
RPD829	11.70	14.29	62300	10250	280	100	1410	86300	29	27	55	251	17	4	300	127	1	2	0
RPD830	22.80	28.80	54300	11480	280	80	1790	93000	29	28	30	92	2	1	161	141	1	2	1

All Analysis by X-Ray Fluorescence

Appendix 8: BH3 Rhiw Borehole Data

Sample	Top Depth	Bottom Depth	Sb (ppm)	Ba (ppm)	As (ppm)
RPD825	4.60	6.20	1	120	0
RPD826	6.20	6.84	1	70	3
RPD827	6.84	8.50	0	120	6
RPD828	8.50	11.70	1	90	3
RPD829	11.70	14.29	1	140	3
RPD830	22.80	28.80	4	60	3

All Analysis by X-Ray Fluorescence

Appendix 8: BH4 Rhiw Borehole Data

Sample	Top Depth	Bottom Depth	Ca (ppm)	Ti (ppm)	V (ppm)	Cr (ppm)	Mn (ppm)	Fe (ppm)	Co (ppm)	Ni (ppm)	Cu (ppm)	Zn (ppm)	Pb (ppm)	Rb (ppm)	Sr (ppm)	Zr (ppm)	Mo (ppm)	Th (ppm)	U (ppm)
RPD831	3.00	4.00	16600	5100	400	130	190	485600	17	40	13	168	42	5	36	181	5	13	2
RPD832	4.00	8.00	6800	19860	250	90	930	236200	33	36	26	151	9	92	141	170	2	2	2
RPD833	8.00	8.80	13800	19140	260	90	1130	179300	34	31	33	160	0	95	206	185	2	1	1
RPD834	8.80	10.40	19300	18620	330	90	1150	167200	29	23	37	145	4	16	264	179	1	2	0
RPD835	10.40	12.10	16800	13830	240	70	1170	144600	29	19	29	121	5	9	173	174	1	1	0
RPD836	12.10	12.30	28800	20810	380	100	1010	101900	24	20	38	99	4	1	192	204	3	2	1
RPD837	12.30	13.00	44300	16950	370	80	2680	123800	37	26	26	120	1	4	218	165	1	0	1
RPD838	13.00	13.36	36000	18000	380	80	3050	119000	45	33	41	125	1	3	181	170	2	2	1
RPD839	13.36	13.80	29900	17510	320	80	1800	164400	27	23	28	116	0	32	324	177	2	1	0
RPD840	13.80	14.50	32800	19080	450	110	1950	120600	52	37	35	139	4	2	229	188	0	0	0
RPD841	14.50	15.50	33500	19230	440	100	1920	122600	39	27	16	137	5	3	266	196	2	1	1
RPD842	15.50	16.30	29500	18000	390	90	2160	139700	35	28	37	133	3	1	264	173	1	0	2
RPD843	16.30	17.80	30300	19250	370	90	1530	125600	30	21	30	126	3	5	248	189	2	1	0
RPD844	17.80	20.50	36900	18370	250	30	1250	138700	24	14	17	134	3	15	324	199	0	1	1
RPD845	29.85	32.40	39200	19150	260	20	1540	150300	30	14	24	145	6	15	303	207	0	1	1
RPD846	53.00	55.15	6200	4950	70	90	560	40700	9	13	7	503	189	56	266	281	1	9	2
RPD847	55.15	60.20	3500	2690	30	30	400	30200	6	10	9	580	233	41	188	375	2	13	2
RPD848	60.20	61.40	1800	1430	50	10	660	46000	9	13	5	137	18	41	110	321	3	8	0
RPD849	61.40	63.60	28700	15300	300	40	1430	114200	37	30	23	203	6	8	170	173	2	2	1
RPD850	73.77	79.20	10400	5090	100	70	1510	80400	33	58	47	100	33	175	92	167	3	9	2
RPD851	79.20	81.60	6900	5170	90	70	1180	57600	21	33	27	79	22	174	94	171	1	9	3
RPD852	84.60	86.60	8500	5870	110	80	1540	79600	35	72	38	103	27	160	60	206	2	12	2
RPD853	90.00	92.00	5600	5620	90	80	620	53000	21	39	29	89	19	181	80	188	2	12	1
RPD854	95.00	97.70	5600	5520	90	80	570	47400	19	30	22	81	17	180	81	199	2	12	3

All Analysis by X-Ray Fluorescence

Appendix 8: BH4 Rhiw Borehole Data

Sample	Top Depth	Bottom Depth	Sb (ppm)	Ba (ppm)	As (ppm)
RPD831	3.00	4.00	0	50	28
RPD832	4.00	8.00	1	990	28
RPD833	8.00	8.80	1	990	28
RPD834	8.80	10.40	0	290	16
RPD835	10.40	12.10	1	210	13
RPD836	12.10	12.30	0	60	11
RPD837	12.30	13.00	1	170	14
RPD838	13.00	13.36	0	150	16
RPD839	13.36	13.80	1	660	13
RPD840	13.80	14.50	1	90	33
RPD841	14.50	15.50	1	90	20
RPD842	15.50	16.30	0	70	23
RPD843	16.30	17.80	0	120	14
RPD844	17.80	20.50	0	250	13
RPD845	29.85	32.40	0	210	20
RPD846	53.00	55.15	1	670	20
RPD847	55.15	60.20	1	500	9
RPD848	60.20	61.40	0	500	6
RPD849	61.40	63.60	0	100	33
RPD850	73.77	79.20	1	650	18
RPD851	79.20	81.60	1	620	22
RPD852	84.60	86.60	1	440	19
RPD853	90.00	92.00	2	480	17
RPD854	95.00	97.70	0	480	15

All Analysis by X-Ray Fluorescence

Appendix 8: BH5 Rhiw Borehole Data

Sample	Top Depth	Bottom Depth	Ca (ppm)	Ti (ppm)	V (ppm)	Cr (ppm)	Mn (ppm)	Fe (ppm)	Co (ppm)	Ni (ppm)	Cu (ppm)	Zn (ppm)	Pb (ppm)	Rb (ppm)	Sr (ppm)	Zr (ppm)	Mo (ppm)	Th (ppm)	U (ppm)
RPD861	0.50	4.10	76600	15870	370	30	1940	110500	28	24	33	115	5	3	294	184	3	0	1
RPD862	4.10	6.00	70700	15960	380	30	2050	111900	28	22	30	106	1	4	274	186	0	1	1
RPD863	6.00	7.60	62800	16280	380	40	2470	109700	31	25	30	110	0	5	301	182	2	1	0
RPD864	7.60	10.40	35300	19470	460	40	2510	128600	34	25	33	124	8	3	113	197	2	1	0
RPD865	10.40	13.60	15200	6980	220	50	1030	147300	17	17	9	294	42	4	32	105	2	4	0
RPD866	13.60	15.00	31800	3490	340	90	850	291400	21	32	14	229	64	21	65	193	1	11	2
RPD867	15.00	15.50	27500	12080	280	70	870	292600	26	32	57	121	23	6	35	133	2	3	2
RPD868	15.50	16.00	28200	13400	300	80	1010	331000	31	36	17	122	17	9	34	166	0	3	0
RPD869	16.00	17.60	28300	18840	370	90	1100	214600	40	32	30	131	7	6	159	183	0	1	1

All Analysis by X-Ray Fluorescence

Appendix 8: BH5 Rhiw Borehole Data

Sample	Top Depth	Bottom Depth	Sb (ppm)	Ba (ppm)	As (ppm)
RPD861	0.50	4.10	2	120	9
RPD862	4.10	6.00	1	120	10
RPD863	6.00	7.60	2	110	17
RPD864	7.60	10.40	1	70	23
RPD865	10.40	13.60	1	40	14
RPD866	13.60	15.00	0	180	36
RPD867	15.00	15.50	1	40	28
RPD868	15.50	16.00	1	60	29
RPD869	16.00	17.60	1	90	24

All Analysis by X-Ray Fluorescence

Appendix 9 : Rhiw Soil Data

Sample	Easting	Northing	Ti (ppm)	V (ppm)	Cr (ppm)	Mn (ppm)	Fe (ppm)	Ni (ppm)	Cu (ppm)	Zn (ppm)	Pb (ppm)	Sr (ppm)	Zr (ppm)	Mo (ppm)	U (ppm)	Ba (ppm)
RPS4401	221965	326762	6150	110	150	1130	35500	33	27	90	43	75	418	0	5	310
RPS4402	221944	326777	6320	110	180	1150	33800	31	24	90	34	79	436	1	4	320
RPS4403	221924	326791	6370	110	190	990	33900	33	25	88	40	79	437	1	3	320
RPS4404	221903	326806	6280	110	160	1130	35200	32	21	77	30	77	433	1	3	320
RPS4405	221883	326821	6330	110	190	1450	32000	30	24	90	31	74	436	0	1	330
RPS4406	221862	326835	6350	110	170	1250	34700	29	21	82	35	74	447	3	4	330
RPS4407	221842	326850	6150	110	180	1160	34300	29	24	82	30	75	420	1	4	310
RPS4408	221821	326864	6270	110	210	1580	32600	31	22	88	34	76	433	1	4	300
RPS4409	221801	326879	6200	110	230	1730	34500	32	28	93	47	75	406	2	3	290
RPS4410	221780	326894	6130	110	160	1380	32600	27	18	78	27	73	413	1	4	290
RPS4411	221759	326908	6140	100	130	1240	30700	25	16	77	29	73	428	1	4	280
RPS4412	221739	326923	5920	130	140	1000	42500	33	20	79	24	75	336	0	7	300
RPS4413	221718	326938	6100	120	120	1340	36800	28	22	95	29	73	361	1	5	290
RPS4414	221698	326952	6190	120	130	1390	38000	27	18	81	24	73	385	1	5	290
RPS4415	221677	326967	6230	120	150	1680	38100	26	21	83	29	71	384	2	2	290
RPS4416	221657	326981	6480	110	130	1970	37900	27	26	93	31	77	436	0	5	240
RPS4417	221636	326996	6160	110	100	1100	35300	25	12	69	22	73	402	2	4	290
RPS4418	221615	327011	6170	130	110	560	41700	30	17	68	26	81	344	0	6	330
RPS4419	221595	327025	6260	120	100	700	37900	25	15	64	29	78	347	1	5	290
RPS4420	221574	327040	6340	110	100	620	33000	20	12	60	33	75	355	1	5	270
RPS4421	221554	327055	6330	120	100	610	34600	21	10	55	28	72	368	1	4	270
RPS4422	221533	327069	5980	100	90	900	29900	22	10	58	23	73	415	0	2	260
RPS4423	221513	327084	6530	120	90	440	32600	17	6	52	28	75	361	0	3	260
RPS4424	221492	327098	6070	130	100	520	43200	29	14	68	36	76	307	1	3	290
RPS4425	221472	327113	6370	130	100	410	40200	20	9	49	33	74	353	0	4	280
RPS4426	221451	327128	6080	120	100	600	38800	23	16	65	31	69	344	1	4	280
RPS4427	221430	327142	6340	120	100	460	36700	21	12	54	34	74	375	1	2	280
RPS4428	221410	327157	6300	120	100	560	36200	24	14	63	54	77	348	1	4	300
RPS4429	221389	327172	6150	130	100	420	42900	30	12	60	23	78	300	0	4	310
RPS4430	221369	327186	6430	120	90	350	33400	21	14	61	27	75	367	2	4	280
RPS4431	221348	327201	6430	120	90	650	35700	22	12	55	32	74	374	1	4	300
RPS4432	221328	327215	6100	120	100	900	39000	27	13	63	20	76	352	1	3	310
RPS4433	221307	327230	6210	110	90	1040	35000	24	14	72	36	71	363	1	6	270
RPS4434	221286	327245	6100	130	100	1000	32000	22	13	75	39	74	378	0	5	290
RPS4435	221266	327259	6240	130	100	1330	38400	22	10	62	30	75	375	0	5	310
RPS4436	221245	327274	6170	130	100	600	39900	23	11	65	35	74	410	0	7	260
RPS4437	221225	327289	5850	120	90	1780	36700	23	10	76	37	84	361	1	5	330
RPS4438	221204	327303	5920	110	100	870	39700	27	16	52	25	79	436	1	6	300
RPS4439	221184	327318	6250	110	90	680	30800	19	7	54	27	73	411	1	4	280
RPS4440	221785	326648	6750	110	210	560	37500	30	16	54	28	91	397	1	5	420
RPS4441	221765	326663	6770	110	190	1290	30000	30	19	99	35	89	378	1	3	370
RPS4442	221744	326677	6640	110	200	990	32300	31	24	77	33	81	387	1	5	350
RPS4443	221724	326692	6150	120	150	1270	39800	34	26	80	29	79	352	2	5	320
RPS4444	221703	326706	6400	120	180	1630	37700	32	22	82	23	77	379	1	4	340
RPS4445	221683	326721	6310	110	180	1520	36700	31	20	82	28	81	410	3	4	310
RPS4446	221662	326735	6350	110	170	1690	35700	31	17	87	29	76	325	0	2	330
RPS4447	221642	326750	6570	120	160	1900	41000	32	16	79	29	75	338	0	3	290
RPS4448	221622	326765	6500	130	200	1660	42800	40	16	83	31	72	316	0	2	300

All Analysis by X-Ray Fluorescence

Appendix 9 : Rhiw Soil Data

Sample	Easting	Northing	Ti (ppm)	V (ppm)	Cr (ppm)	Mn (ppm)	Fe (ppm)	Ni (ppm)	Cu (ppm)	Zn (ppm)	Pb (ppm)	Sr (ppm)	Zr (ppm)	Mo (ppm)	U (ppm)	Ba (ppm)
RPS4449	221601	326779	7030	140	260	1480	50200	58	19	87	34	76	325	0	0	330
RPS4450	221581	326794	6590	130	230	1200	41800	45	18	81	25	75	338	3	0	330
RPS4451	221560	326808	6190	140	120	880	46300	32	18	72	29	72	316	2	0	310
RPS4452	221540	326823	6620	120	120	590	36500	27	14	79	32	77	368	1	2	330
RPS4453	221519	326837	6340	120	100	1740	41000	27	19	92	36	73	375	2	4	300
RPS4454	221499	326852	6310	120	100	1450	38900	27	19	88	37	72	374	0	4	290
RPS4455	221478	326866	6270	100	90	1690	31900	22	11	80	26	75	402	0	4	270
RPS4456	221458	326881	6190	110	100	1780	34900	24	16	87	32	70	419	0	6	290
RPS4457	221438	326896	6310	100	90	1750	28500	15	14	81	32	70	410	1	2	280
RPS4458	221417	326910	6050	100	100	1150	32700	23	21	89	29	72	411	1	3	290
RPS4459	221397	326925	6190	110	100	1600	36500	25	20	77	34	72	458	0	4	280
RPS4460	221376	326939	6230	110	100	1670	34600	22	29	76	27	71	447	0	5	290
RPS4461	221356	326954	6450	110	90	1390	31600	21	19	79	31	70	405	0	4	270
RPS4462	221335	326968	6240	110	100	1690	36300	24	17	82	21	72	398	1	2	290
RPS4463	221315	326983	6340	120	100	1490	36700	24	20	84	27	68	402	1	4	260
RPS4464	221295	326998	6120	120	100	1370	39200	28	24	87	30	77	382	0	5	300
RPS4465	221274	327012	6410	110	110	2160	35900	21	19	88	35	69	411	1	7	280
RPS4466	221254	327027	6270	130	110	750	45000	32	22	70	25	78	333	2	4	320
RPS4467	221233	327041	6360	110	100	1020	33900	22	16	71	31	73	414	0	3	290
RPS4468	221213	327056	6430	120	100	1100	40900	28	19	75	31	79	380	0	6	310
RPS4469	221192	327070	6310	110	100	1360	37400	26	18	76	34	80	420	2	3	270
RPS4470	221130	327122	6220	110	100	970	34400	24	13	65	31	75	417	0	6	270
RPS4471	221108	327136	6060	110	100	670	40400	26	15	53	25	79	382	2	4	300
RPS4472	221087	327151	5870	100	100	640	33900	25	9	54	20	70	488	1	2	250
RPS4473	221065	327165	5700	100	90	490	36100	23	14	56	31	68	376	1	5	250
RPS4474	222090	326905	6190	120	120	1050	35600	26	13	68	25	73	407	0	4	290
RPS4475	222070	326919	6080	110	120	1010	36900	29	17	67	26	73	420	1	5	290
RPS4476	222049	326933	6150	110	120	1190	35100	26	13	73	27	70	395	0	5	270
RPS4477	222029	326947	6220	110	120	1370	36700	25	15	75	28	72	399	0	2	280
RPS4478	222009	326962	6330	120	120	1190	38800	29	20	85	27	75	355	2	6	280
RPS4479	221988	326976	5900	130	140	1300	39500	34	19	82	31	74	457	0	3	280
RPS4480	221968	326990	6030	130	120	1040	45900	38	22	80	27	77	343	1	4	310
RPS4481	221948	327004	6040	130	120	1010	43200	34	22	85	35	72	367	1	1	290
RPS4482	221928	327018	6100	120	110	930	43700	31	20	72	30	77	364	0	5	300
RPS4483	221907	327032	5930	110	110	1000	34200	23	15	73	27	72	419	1	3	260
RPS4484	221887	327046	6080	140	110	870	45800	29	17	66	29	76	359	1	6	300
RPS4485	221867	327060	5930	130	110	490	35400	23	10	53	21	64	278	0	3	170
RPS4486	221846	327075	6180	140	110	560	47900	30	17	62	25	79	326	1	3	310
RPS4487	221826	327089	6190	130	110	530	47100	28	18	66	27	74	340	1	4	300
RPS4488	221806	327103	6080	120	110	450	43600	31	16	67	22	77	368	1	5	310
RPS4489	221785	327117	6160	130	100	720	47200	30	16	64	27	82	353	0	2	330
RPS4490	221765	327131	6410	120	100	460	31400	18	7	58	31	73	401	1	5	260
RPS4491	221745	327145	6090	100	100	470	37800	35	13	66	23	71	455	0	4	280
RPS4492	221724	327159	6230	120	100	350	45100	27	9	59	20	75	380	0	3	300
RPS4493	221704	327173	5950	100	100	460	38600	24	8	56	25	68	495	2	2	240
RPS4494	221684	327188	6260	100	90	470	28500	22	10	52	19	71	419	0	5	260
RPS4495	221663	327202	6000	100	100	600	31100	21	7	54	27	72	414	1	3	260
RPS4496	221643	327216	6200	110	90	1130	31900	22	6	53	24	71	404	1	4	280

All Analysis by X-Ray Fluorescence

Appendix 9 : Rhiw Soil Data

Sample	Easting	Northing	Ti (ppm)	V (ppm)	Cr (ppm)	Mn (ppm)	Fe (ppm)	Ni (ppm)	Cu (ppm)	Zn (ppm)	Pb (ppm)	Sr (ppm)	Zr (ppm)	Mo (ppm)	U (ppm)	Ba (ppm)
RPS4497	221623	327230	6050	110	100	700	38400	31	15	69	29	81	376	1	5	310
RPS4498	221603	327244	6220	120	100	590	38500	24	9	60	27	75	393	0	4	290
RPS4499	221582	327258	6160	130	100	680	40600	27	15	63	30	79	368	0	3	300
RPS4500	221562	327272	6310	120	100	910	40600	29	13	73	29	79	384	1	4	320
RPS4501	221542	327286	6100	120	100	1120	35000	25	17	75	29	72	406	1	4	280
RPS4502	221521	327301	6290	110	90	720	31100	19	9	55	30	72	486	1	4	270
RPS4503	221501	327315	6100	120	100	1390	39600	26	8	60	27	78	449	1	6	310
RPS4504	221481	327329	6340	130	100	1330	35200	27	11	71	31	83	358	1	4	330
RPS4505	221460	327343	6520	120	100	950	37700	25	13	61	24	78	380	4	6	320
RPS4506	221440	327357	6120	130	110	970	47800	40	21	66	31	86	331	0	3	340
RPS4507	221420	327371	6180	120	100	910	39200	26	12	63	29	77	368	0	6	300
RPS4508	221399	327385	6110	110	90	1040	30600	23	9	74	27	76	462	0	6	260
RPS4509	221379	327399	6200	110	90	1160	35100	25	15	64	32	78	440	1	2	300
RPS4510	222195	327070	6090	100	120	930	37100	29	19	66	27	78	451	1	4	270
RPS4511	222175	327085	6140	120	130	1020	43800	34	23	70	31	80	393	0	7	310
RPS4512	222155	327099	6190	110	160	1500	35600	30	29	75	30	74	478	0	4	250
RPS4513	222134	327114	6120	120	170	1800	34700	28	47	86	28	71	425	1	3	240
RPS4514	222114	327129	6210	130	160	1820	39000	29	32	85	29	69	445	0	4	260
RPS4515	222094	327143	5980	110	120	1050	38000	30	24	73	27	68	428	2	6	270
RPS4516	222074	327158	6180	120	120	960	40000	30	22	70	30	75	398	0	4	300
RPS4517	222054	327172	6230	110	130	650	34300	27	16	67	31	72	463	1	4	250
RPS4518	222034	327187	6130	120	120	900	37500	30	16	67	25	75	404	1	4	280
RPS4519	222013	327202	6260	110	110	1200	42400	32	19	62	23	82	519	1	5	290
RPS4520	221993	327216	6120	120	110	830	42200	36	20	66	27	85	400	1	5	320
RPS4521	221973	327231	6100	110	100	660	37000	25	11	53	23	76	461	1	3	280
RPS4522	221953	327246	5950	110	100	1260	40700	27	19	56	28	80	399	1	3	300
RPS4523	221933	327260	6280	100	100	900	28700	20	9	57	24	74	452	2	4	260
RPS4524	221912	327275	6260	110	100	1170	38900	26	11	81	22	80	412	0	6	290
RPS4525	221892	327289	6190	120	110	1240	46200	32	20	54	24	82	449	1	5	280
RPS4526	221872	327304	6170	120	100	980	43400	32	15	65	30	77	370	3	3	330
RPS4527	221852	327319	5980	110	100	960	43300	30	15	57	24	75	445	1	2	280
RPS4528	221832	327333	6220	110	100	880	35800	26	15	65	32	76	456	1	2	270
RPS4529	221811	327348	6220	110	100	550	37600	25	9	55	17	72	483	1	3	280
RPS4530	221791	327363	6130	130	100	1080	47700	34	18	64	25	84	356	1	4	330
RPS4531	221771	327377	6090	140	110	740	50600	34	23	76	27	83	304	1	5	340
RPS4532	221751	327392	6330	120	100	450	42200	27	9	59	23	80	359	0	5	300
RPS4533	221731	327406	6070	130	100	1210	48400	40	20	71	23	93	328	1	3	340
RPS4534	221711	327421	6390	120	90	440	37000	25	8	62	25	92	317	0	4	320
RPS4535	221690	327436	6610	150	110	250	40900	29	9	62	27	86	240	0	5	330
RPS4536	221670	327450	6490	140	110	280	37400	28	14	61	33	87	311	0	3	310
RPS4537	221650	327465	6160	140	110	790	49500	34	20	68	24	82	332	0	3	330
RPS4538	221630	327480	6270	120	90	830	39700	22	14	54	34	74	423	4	5	280
RPS4539	221610	327494	6190	120	100	510	41400	29	10	61	24	76	404	1	4	300
RPS4540	221589	327509	6530	120	100	660	30300	18	8	50	24	74	430	2	4	270
RPS4541	221569	327523	6360	130	110	1030	54100	32	17	58	25	83	346	1	3	300
RPS4542	221549	327538	6090	120	100	960	38100	21	9	61	35	69	421	1	3	260
RPS4543	221529	327553	6210	110	100	1230	38400	28	11	66	31	78	475	2	4	290
RPS4544	221509	327567	6280	130	100	440	43900	25	12	57	24	77	388	2	2	290

All Analysis by X-Ray Fluorescence

Appendix 9 : Rhiw Soil Data

Sample	Easting	Northing	Ti (ppm)	V (ppm)	Cr (ppm)	Mn (ppm)	Fe (ppm)	Ni (ppm)	Cu (ppm)	Zn (ppm)	Pb (ppm)	Sr (ppm)	Zr (ppm)	Mo (ppm)	U (ppm)	Ba (ppm)
RPS4545	221488	327582	6070	120	110	480	46300	29	21	56	28	74	378	2	3	300
RPS4546	221468	327597	5790	100	90	620	32400	22	6	49	24	71	460	1	3	270
RPS4547	221448	327611	6100	120	100	1530	37900	26	13	55	29	77	442	1	4	300
RPS4548	221428	327626	5910	100	90	510	36700	20	6	47	26	68	445	0	1	240
RPS4549	222230	327290	6270	100	160	2180	34900	23	32	87	31	69	504	2	5	230
RPS4550	222210	327304	6470	110	140	2080	36000	22	31	76	30	69	513	2	5	220
RPS4551	222190	327319	6220	100	120	1670	36300	24	28	78	25	68	487	0	1	240
RPS4552	222169	327333	6050	90	100	1080	34700	22	25	73	37	75	502	1	4	260
RPS4553	222149	327348	6610	120	120	1450	37200	26	27	93	38	75	439	1	2	260
RPS4554	222129	327362	6260	110	100	1260	39500	28	23	72	30	75	435	1	5	290
RPS4555	222109	327377	5900	100	100	1180	38300	29	23	70	27	72	471	1	2	280
RPS4556	222089	327391	6000	100	100	1190	33800	25	17	77	34	70	448	1	5	260
RPS4557	222069	327406	6090	110	100	1190	37900	26	19	70	26	72	434	1	4	270
RPS4558	222048	327420	6110	100	100	1160	34800	22	14	63	22	71	480	1	4	240
RPS4559	222028	327434	6450	110	100	1100	32800	19	17	63	23	70	455	1	3	260
RPS4560	222008	327449	5910	90	100	780	31600	25	11	56	22	75	603	1	5	250
RPS4561	221988	327463	6310	100	100	810	31500	19	14	66	28	72	465	0	8	260
RPS4562	221968	327478	6270	100	100	520	27500	18	9	61	32	73	485	1	5	260
RPS4563	221947	327492	6190	100	90	1050	34300	20	11	68	34	72	482	1	6	280
RPS4564	221927	327507	6520	110	100	1730	35300	19	10	84	34	69	540	2	3	270
RPS4565	221907	327521	6340	100	90	760	32200	17	14	69	35	71	525	1	5	240
RPS4566	221887	327535	5970	130	100	1440	52000	41	20	76	30	82	319	1	2	370
RPS4567	221867	327550	6190	130	100	810	45500	26	12	58	26	77	332	0	4	330
RPS4568	221846	327564	6050	120	100	1190	41900	26	12	54	24	77	443	0	5	290
RPS4569	221826	327579	6370	120	90	920	33000	19	11	77	28	75	414	1	5	260
RPS4570	221806	327593	6130	120	100	1120	41900	26	13	53	26	82	372	1	5	320
RPS4571	221786	327608	6010	130	100	1130	39600	29	12	58	24	82	368	1	5	320
RPS4572	221766	327622	6180	120	90	1080	34400	22	8	69	37	73	391	1	5	290
RPS4573	221746	327637	6650	120	90	580	32700	24	6	63	27	80	378	1	5	290
RPS4574	221725	327651	6580	130	100	680	47400	22	8	60	22	80	386	1	2	310
RPS4575	221705	327665	7010	120	90	540	25700	10	3	37	26	69	416	1	5	240
RPS4576	221685	327680	6080	110	100	510	37100	23	12	52	23	71	418	1	4	270
RPS4577	221665	327694	6730	120	90	720	31600	18	10	72	31	74	434	1	5	280
RPS4578	221645	327709	6610	130	100	1260	43000	18	10	71	31	66	532	2	4	230
RPS4579	221624	327723	7010	120	90	300	25900	10	8	49	36	67	524	0	4	220
RPS4580	221604	327738	6840	130	90	690	32900	18	8	80	42	78	367	2	6	270
RPS4581	221584	327752	5520	90	80	780	35100	22	13	55	21	66	464	1	4	250
RPS4582	221564	327766	5980	120	100	1080	43600	31	41	131	98	74	398	2	4	350
RPS4583	221544	327781	6650	120	90	450	27700	16	7	51	31	69	401	2	4	260
RPS4584	221523	327795	6340	120	90	370	35700	22	10	46	23	73	390	0	3	270
RPS4585	221503	327810	6090	120	100	350	47100	29	17	56	22	74	375	0	2	300
RPS4586	222789	328775	11200	220	70	1240	62200	18	12	72	14	88	398	0	4	190
RPS4587	222764	328780	14120	320	50	1880	76300	11	12	78	26	90	340	1	1	170
RPS4588	222740	328785	7500	160	70	1150	38800	19	8	54	16	72	511	1	4	210
RPS4589	222715	328789	7160	140	70	1060	41600	18	10	62	12	76	487	0	4	210
RPS4590	222690	328794	9710	180	50	1700	54600	17	9	70	18	73	356	1	2	200
RPS4591	222666	328799	11170	180	50	870	50900	10	5	59	17	73	436	0	2	160
RPS4592	222641	328804	13600	260	60	2760	63800	7	6	55	36	76	568	1	3	130

All Analysis by X-Ray Fluorescence

Appendix 9 : Rhiw Soil Data

Sample	Easting	Northing	Ti (ppm)	V (ppm)	Cr (ppm)	Mn (ppm)	Fe (ppm)	Ni (ppm)	Cu (ppm)	Zn (ppm)	Pb (ppm)	Sr (ppm)	Zr (ppm)	Mo (ppm)	U (ppm)	Ba (ppm)
RPS4593	222616	328808	12830	230	60	1550	63600	9	3	60	15	80	473	0	3	160
RPS4594	222592	328813	9380	180	70	1470	51000	10	5	64	26	63	460	0	3	220
RPS4595	222567	328818	8490	170	80	1130	52300	17	6	75	23	61	514	2	2	210
RPS4596	222542	328823	8210	150	80	1180	42900	18	9	67	19	68	604	1	4	230
RPS4597	222517	328827	8480	160	80	970	44300	20	3	68	23	69	580	0	3	230
RPS4598	222493	328832	7010	140	70	860	37600	17	6	60	19	65	494	2	4	230
RPS4599	222468	328837	8190	160	60	970	42400	11	3	43	17	66	384	0	4	200
RPS4600	222443	328842	5740	110	80	440	35900	17	7	51	20	64	546	0	3	240
RPS4601	222419	328846	10780	210	50	1570	58100	7	9	57	22	83	441	2	3	170
RPS4602	222394	328851	10120	210	50	2060	71800	7	5	56	19	89	392	0	3	190
RPS4603	222369	328856	7440	130	80	1130	41100	18	7	61	13	68	606	0	5	220
RPS4604	222345	328861	10090	180	60	920	57900	8	3	43	15	63	440	0	2	170
RPS4605	222320	328865	11630	230	50	1210	65200	6	3	47	22	74	462	2	3	140
RPS4606	222295	328870	8470	180	70	1050	52100	15	6	57	12	76	627	0	3	200
RPS4607	222271	328875	7380	150	80	1000	45400	19	6	72	22	68	539	0	3	230
RPS4608	222246	328880	6710	120	80	1000	36400	15	5	52	16	70	630	0	2	220
RPS4609	222221	328884	7140	130	80	950	38600	17	5	55	20	70	581	0	4	220
RPS4610	222197	328889	7160	140	80	800	38100	16	8	56	17	71	657	1	4	220
RPS4611	222172	328894	7180	140	80	830	37800	16	5	55	13	72	707	1	7	220
RPS5501	223100	329515	6660	120	90	550	43300	15	5	52	13	63	420	0	3	220
RPS5502	223075	329523	8110	170	80	690	56000	10	4	54	15	71	386	0	4	170
RPS5503	223050	329530	10710	120	90	470	27400	11	1	47	20	67	516	2	2	180
RPS5508	222931	329559	15810	320	70	880	88100	6	1	72	22	46	237	0	2	80
RPS5514	222810	329590	14280	220	80	1300	62300	6	4	64	34	64	663	1	4	50
RPS5515	222785	329596	10510	160	70	800	53800	7	5	56	69	63	545	1	3	210
RPS5516	222760	329602	10920	170	60	890	45600	3	5	47	38	65	326	0	2	210
RPS5517	222735	329607	7180	110	70	940	41600	12	16	62	28	44	323	0	4	260
RPS5518	222711	329613	7640	130	80	960	46000	19	10	78	66	59	420	2	4	290
RPS5519	222686	329619	9200	160	80	840	50100	12	7	58	33	54	468	1	4	220
RPS5520	222661	329625	10100	160	70	900	46400	5	3	43	29	57	364	1	1	190
RPS5521	222636	329631	10820	180	70	890	53000	6	1	50	24	62	468	0	4	200
RPS5522	222611	329637	10920	170	80	1150	56100	10	4	57	16	69	614	1	3	210
RPS5523	222586	329642	9920	170	90	1270	52600	13	5	57	22	70	498	1	5	220
RPS5524	222561	329648	9890	170	80	1290	54900	15	10	57	20	78	517	2	3	240
RPS5525	222536	329654	8560	150	80	990	40900	14	8	55	21	69	509	1	5	230
RPS5526	222512	329660	8100	140	80	1250	42900	17	9	66	20	70	451	0	4	250
RPS5527	222300	329300	7070	110	80	1760	27100	9	8	74	18	65	494	1	4	240
RPS5528	222324	329294	6960	110	80	1290	28400	11	4	49	16	66	518	1	4	260
RPS5529	222348	329288	7200	120	90	1160	26900	9	7	56	25	68	530	2	1	240
RPS5530	222372	329282	7120	120	80	920	31800	11	7	50	16	67	521	2	6	250
RPS5531	222396	329276	7540	120	80	980	36700	13	8	54	17	75	511	1	4	280
RPS5533	222444	329264	8170	150	90	1170	42700	14	10	65	27	70	499	0	4	240
RPS5534	222468	329258	8240	130	80	990	46900	21	12	64	17	71	609	1	2	290
RPS5535	222492	329252	7270	120	80	830	45500	17	7	65	19	60	426	0	3	270
RPS5536	222516	329246	8360	140	70	800	40300	5	3	44	24	57	353	1	3	220
RPS5537	222540	329240	9450	150	70	650	43400	5	4	44	47	55	333	1	3	170
RPS5538	222564	329234	8250	130	60	440	30700	2	5	36	59	46	286	2	4	130
RPS5539	222588	329228	11950	200	60	1060	56300	3	3	49	28	57	333	1	4	150

All Analysis by X Ray Fluorescence

Appendix 9 : Rhiw Soil Data

Sample	Easting	Northing	Ti (ppm)	V (ppm)	Cr (ppm)	Mn (ppm)	Fe (ppm)	Ni (ppm)	Cu (ppm)	Zn (ppm)	Pb (ppm)	Sr (ppm)	Zr (ppm)	Mo (ppm)	U (ppm)	Ba (ppm)
RPS5540	222612	329222	11060	190	70	920	57200	7	6	58	24	55	371	0	3	190
RPS5541	222636	329216	10590	170	60	1060	46000	2	7	51	37	57	353	0	4	180
RPS5542	222660	329210	10470	170	80	1560	52700	4	9	60	35	53	503	0	3	180
RPS5547	222785	329180	9540	180	80	1030	56100	15	8	66	22	72	421	1	4	210
RPS5548	222809	329173	9170	170	80	470	44600	15	6	55	12	59	423	1	2	190
RPS5549	222833	329167	13810	280	60	780	42600	3	3	54	25	49	220	1	2	30
RPS5552	223288	329881	9490	160	60	530	23300	1	0	30	38	63	296	0	2	80
RPS5553	223260	329891	10000	170	60	460	20300	3	5	26	49	58	346	0	3	70
RPS5556	223190	329909	8890	150	100	630	40800	7	4	45	39	62	827	0	2	140
RPS5557	223166	329915	9920	180	60	530	41000	4	1	37	51	60	381	0	2	160
RPS5558	223142	329921	10990	200	70	880	43000	3	5	44	72	74	376	0	3	120
RPS5559	223117	329927	10620	190	80	630	51800	6	3	53	37	60	465	0	3	140
RPS5560	223093	329933	10160	190	90	600	53000	8	4	60	25	63	411	1	3	160
RPS5561	223069	329939	11460	210	80	1240	47900	10	5	109	34	84	373	1	6	170
RPS5562	223045	329945	9980	160	80	1670	30900	5	2	43	39	100	422	3	3	130
RPS5563	223020	329951	8380	130	80	1160	26700	7	3	55	24	82	648	1	3	150
RPS5564	222996	329957	8570	150	80	590	36200	8	2	42	31	62	534	0	6	190
RPS5565	222972	329963	10810	180	80	650	44600	6	2	39	33	68	536	0	4	140
RPS5566	222948	329969	11660	190	80	640	46200	4	3	33	32	67	615	0	1	130
RPS5567	222923	329975	11670	200	90	1290	51200	5	2	44	16	72	553	1	3	170
RPS5568	222899	329981	9000	150	70	720	37400	5	3	41	43	57	583	0	4	140
RPS5569	222875	329987	10220	180	80	740	51900	8	3	44	15	63	662	2	1	190
RPS5570	222851	329993	9790	170	70	490	44000	5	0	30	16	57	634	1	1	160
RPS5571	222826	329999	8240	140	90	1060	40600	16	6	63	20	66	631	0	5	210
RPS5572	222802	330005	8190	140	90	930	38500	18	7	69	20	73	604	1	4	240
RPS5573	222778	330011	7360	120	90	730	40900	21	8	68	20	67	569	1	3	250
RPS5574	222754	330017	7890	140	90	890	37400	15	6	58	24	66	626	2	4	230
RPS5575	222729	330023	7770	130	90	940	39600	29	12	82	19	73	504	0	4	270
RPS5576	222705	330029	7560	130	90	780	42700	22	10	63	24	69	585	0	5	270
RPS5577	222406	329145	7730	110	80	620	31100	12	5	44	15	78	776	0	5	230
RPS5578	222431	329138	8520	130	60	410	34600	4	1	31	21	59	400	1	1	190
RPS5579	222457	329131	8450	130	70	600	34700	4	3	29	16	62	414	0	4	220
RPS5580	222482	329124	8280	140	60	350	33500	2	0	24	21	53	392	1	4	180
RPS5581	222507	329118	10080	180	70	660	48000	3	2	23	14	62	416	0	1	190
RPS5582	222532	329111	8290	140	70	470	37800	3	5	28	21	52	404	1	6	180
RPS5583	222558	329104	8590	140	60	640	42000	3	1	25	18	54	415	0	2	200
RPS5584	222583	329097	9400	150	60	550	36800	2	3	30	20	54	400	0	5	180
RPS5585	222608	329090	11510	180	60	1160	53600	4	2	46	29	67	487	0	6	140
RPS5587	222655	329089	14650	210	50	1030	62700	3	5	41	43	64	694	1	2	100
RPS5588	222274	327521	6830	130	170	1530	38600	25	24	79	28	66	544	1	3	250
RPS5589	222249	327519	6710	120	160	2240	37500	18	21	61	23	74	529	0	3	250
RPS5590	222224	327517	6550	110	140	1700	36400	21	15	71	28	65	652	0	3	260
RPS5591	222199	327514	6690	110	130	1700	36000	16	14	57	28	66	601	1	4	260
RPS5592	222174	327512	6880	120	130	2040	38100	14	14	58	24	66	651	0	2	250
RPS5593	222149	327510	6660	110	130	1890	35600	14	19	72	31	63	565	0	5	230
RPS5594	222236	327473	6600	110	140	1560	35300	19	15	71	32	66	695	1	3	240
RPS5595	222232	327498	6270	100	130	1240	32900	20	15	67	30	67	595	1	4	250
RPS5596	222228	327523	6780	120	150	1890	37200	17	17	71	26	66	601	1	4	240

All Analysis by X-Ray Fluorescence

Appendix 9 : Rhiw Soil Data

Sample	Easting	Northing	Ti (ppm)	V (ppm)	Cr (ppm)	Mn (ppm)	Fe (ppm)	Ni (ppm)	Cu (ppm)	Zn (ppm)	Pb (ppm)	Sr (ppm)	Zr (ppm)	Mo (ppm)	U (ppm)	Ba (ppm)
RPS5597	222223	327548	6780	130	140	1780	38400	21	15	63	27	68	614	1	1	240
RPS5598	222219	327573	6670	130	160	1280	37300	23	14	57	29	70	558	0	2	230
RPS5599	222215	327598	7210	130	170	1690	38900	21	15	58	22	71	547	0	4	260
RPS5600	220990	326940	6110	130	100	420	48800	27	17	58	24	79	338	1	3	350
RPS5601	221012	326927	6160	130	100	1140	40900	29	20	71	28	75	344	1	3	340
RPS5602	221034	326913	6140	140	100	500	47400	33	22	67	26	77	326	2	4	340
RPS5603	221056	326900	6010	130	100	1260	48000	39	21	73	30	80	333	0	4	360
RPS5604	221078	326886	6060	150	110	1340	50500	48	22	79	29	84	291	1	5	380
RPS5605	221100	326873	6190	140	110	660	44300	28	15	67	23	74	303	1	3	350
RPS5606	221122	326859	6110	130	110	580	46900	27	18	65	27	76	322	1	3	340
RPS5607	221144	326846	6120	140	110	770	50000	33	21	76	27	83	296	1	6	380
RPS5608	221166	326832	6120	110	90	1450	31400	20	18	129	69	72	365	0	3	310
RPS5609	221188	326819	6160	130	80	16590	51100	52	24	104	36	77	306	4	3	530
RPS5610	221210	326805	5940	110	90	6740	36700	25	20	77	35	61	370	0	3	400
RPS5611	221285	326742	5490	90	90	1460	27300	20	18	70	29	68	606	1	4	240
RPS5612	221306	326728	5190	80	80	860	28100	23	14	57	17	73	521	0	4	270
RPS5613	221327	326715	6170	110	100	1690	36100	25	23	88	35	74	435	0	3	290
RPS5614	221348	326701	6160	110	100	1900	37400	23	22	80	25	72	434	0	4	290
RPS5615	221369	326688	6310	120	100	2260	34900	20	19	85	34	74	406	0	4	300
RPS5616	221390	326674	6220	140	100	560	46400	30	20	70	25	79	334	0	4	360
RPS5617	221411	326661	6390	110	100	2080	32900	19	15	76	28	71	407	0	3	310
RPS5618	221432	326647	6220	120	110	1220	35300	23	14	81	27	72	336	2	5	290
RPS5619	221454	326634	6350	120	130	1300	39300	28	16	75	23	75	367	1	2	290
RPS5620	221475	326620	6350	120	120	1180	35900	23	10	72	24	68	330	0	3	250
RPS5621	222917	329490	14820	230	50	390	15400	2	2	34	34	60	425	1	2	120
RPS5622	222923	329502	18140	270	50	260	9200	0	3	19	32	67	449	0	2	100
RPS5623	222930	329514	10720	190	70	250	25000	3	5	27	13	45	457	0	3	100
RPS5624	222936	329526	16440	300	70	290	19500	4	1	35	33	52	364	0	4	90
RPS5625	222942	329538	15900	250	70	260	13500	3	3	28	16	54	394	0	4	100
RPS5626	222572	329845	7140	110	80	620	41900	13	6	53	25	62	505	2	6	240
RPS5627	222596	329839	9950	150	70	570	50300	5	1	33	16	54	536	1	4	160
RPS5628	222621	329833	9980	180	90	1060	60700	15	6	67	17	71	531	1	4	200
RPS5629	222645	329828	10010	180	80	410	38800	4	0	31	22	66	385	0	1	130
RPS5630	222670	329822	7790	150	110	580	43400	20	5	54	14	83	709	1	3	210
RPS5631	222694	329816	11720	230	100	450	49900	5	2	32	27	71	449	1	2	110
RPS5632	222719	329810	8170	160	110	660	59400	18	5	67	21	62	427	1	4	210
RPS5633	222743	329804	9350	170	80	420	46400	6	1	36	26	57	446	0	2	140
RPS5634	222768	329799	11970	210	70	520	34900	2	1	31	19	71	366	1	3	130
RPS5635	222792	329793	8320	130	70	650	32200	3	5	42	36	55	461	0	3	180
RPS5636	222816	329787	6740	110	90	660	40300	16	7	53	22	64	519	2	4	260
RPS5637	222841	329781	7810	120	70	350	29000	3	0	28	36	53	533	0	4	170
RPS5638	222865	329775	7390	120	100	630	46600	15	5	53	34	61	630	1	4	260
RPS5639	222890	329769	7300	120	80	430	43500	9	3	38	21	51	515	0	1	200
RPS5641	222940	329760	9200	150	70	460	39000	3	0	33	25	56	498	0	3	
RPS5642	222965	329753	8250	140	90	850	42400	15	8	64	33	70	752	2	2	
RPS5643	222990	329745	8820	140	100	1110	41600	14	11	67	31	72	951	0	4	

All Analysis by X-Ray Fluorescence

APPENDIX 10 : MAGNETIC DATA, PENARFYNYDD AREA